Texas Undergraduate Research Journal

The University of Texas at Austin | Volume 23



A CLOSER LOOK

A Defense For Muslim Minority Jurisprudence
pg. 20

Spring 2025

The University of Texas at Austin Undergraduate Research Journal is an independent student-run multidisciplinary journal of undergraduate research.

Undergraduate Research Journal

THE UNIVERSITY OF TEXAS AT AUSTIN ™

2025



Spring 2025 Volume 23

The University of Texas at Austin Undergraduate Research Journal

Copyright © 2025, The University of Texas

All rights reserved:
No part of this journal may be reproduced or utilized in any form or by any means, electronic or mechanical, including photocopying, recording or by any information storage and retrieval system without permission in writing.

This work is licensed under the Creative Commons AttributionNonCommercial-NoDerivatives 4.0 International License.

To view a copy of this license, visit creativecommons.org/licenses/by-nc-nd/4.0/ or send a letter to Creative Commons, PO Box 1866, Mountain View, CA 94042, USA.

editor.in.chief@texasurj.info
The University of Texas at Austin
2515 Speedway,
Austin, Texas 78712-1103
(512) 471-3434

Volume 23, Fall 2025
The UT Austin Undergraduate Research Journal is an independent agency at the The University of Texas at Austin.

The views of the authors do not necessarily reflect the views of the University.

Cover: Morgan Walz

ACKNOWLEDGEMENTS

The Texas Undergraduate Research Journal (URJ) would like to extend special thanks to the UT Student Government and Office of Undergraduate Research Journal for the generous continued support of our mission throughout the Journal's years of operation. Lastly, we would like to recognize the invaluable feedback of our faculty reviewers. And, most of all, we thank the authors themselves, whose inspiring research continues to change the world.

FACULTY REVIEWERS



Josh Beckham

Associate Professor of Practice
Freshman Research Initiative



Brian Sedio

Assistant Professor
Department of Integrative Biology



Samy Ayoub

Associate Professor
Middle Eastern Studies



Justin Havird

Associate Professor
Department of Integrative Biology



David Hoffman

Associate Professor
Department of Molecular Biosciences



Robert Newberry

Assistant Professor
Department of Chemistry

On behalf of the 2024–2025 editorial staff, we are honored to present the 23rd volume of the Texas Undergraduate Research Journal (URJ). Since its founding, URJ has been dedicated to promoting undergraduate excellence, encouraging students to pursue scholarship and creativity through research. Our mission to highlight undergraduate research and make it accessible across disciplines culminates in the publication of our annual journal.

In addition to the journal, URJ co-leads the Capital of Texas Undergraduate Research Conference (CTURC) and hosts free events that help undergraduates immerse themselves in the research community at the University of Texas at Austin.

The 2024–2025 academic year presented challenges, particularly with changes in funding. Nevertheless, our members and authors prevailed, creating a beautiful volume that brings URJ's purpose to life. We extend our heartfelt thanks to our members, who spent countless hours—in and out of meetings—editing manuscripts, formatting content, and dedicating many evenings to elevating undergraduate research.

Finally, we want to thank our Volume 23 authors. It has been a privilege to work with some of the brightest minds of our generation, and we could not have produced this journal without your hard work and persistence. We have no doubt that each of you has a bright future ahead—one where you will continue to improve the world and champion research for generations to come.

We at URJ hope you enjoy reading this year's outstanding work and encourage you to explore past volumes and Pioneer articles written by our editorial board to see how undergraduates are making a lasting impact.

Sincerely,
Siddhartha Shah & Rachel Muralitharan
Co-Editors-in-Chief





Siddhartha Shah
Co-Editor-in-Chief, **2024-2025**

Rachel Muralitharan
Co-Editor-in-Chief, **2024-2025**

Texas Undergraduate Research Journal Staff List 2024-2025

Co-Editors-in-Chief
Siddhartha Shah
Rachel Muralitharan

Executive Editor
Sifallah Bouyadjera

Media Director
Meghna Vergis

Financial Director
Andrew Kulkarni

Director of Communications
Naomi Ichiriu

Director of Campaigns
Sravya Gullapalli

Associate Editors
Samuel Hays
Keshv Srinivasan
Marco Keller
Yashica Sadam

Assistant Editors
Ryan Clarance
Ishan Arora
Mary Kim
Anushka Deshmukh
Dami Ogunkunle
Harshith Amaram
Abhinav Reddy
Komal Chilukuri
Aditya Venkataraman
Sanjana Arulkumaran
Santosh Gedela
Haley Goodwin
Ananya Khanna
Maidah Khan
Amay Bhatnagar
Grayson Qian
Sneha Chandak
Dhroov Pathare

Assistant Directors of Campaigns
Tanika Patil
Paarvi Chand
Swetha Venkat
Aditya Venkataraman
Saisha Salpekar

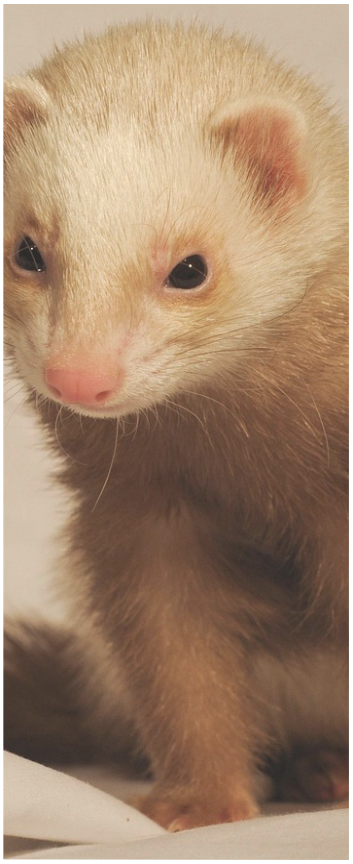
Assistant Directors of Communications
Morgan Walz
Tyler Pullum

Media and Finance
Jenna Chuan
Harsh Patel

Table of Contents

Optimizing Immunological Reagents for Use with the Domestic Ferret Model in Influenza Studies

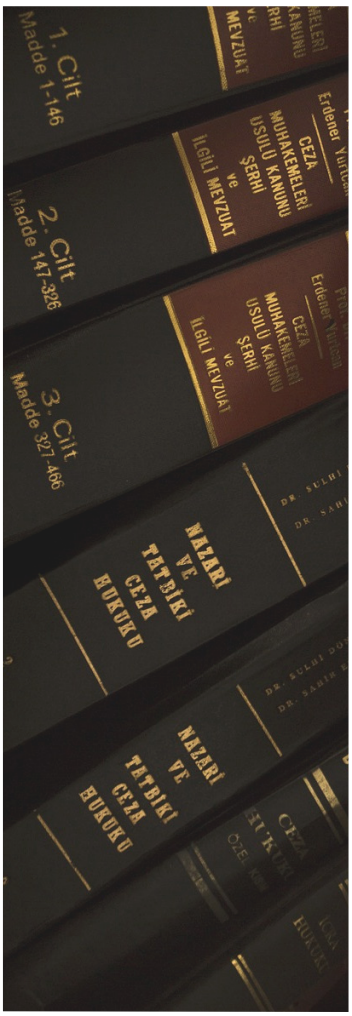
Franziska Pflaum, Luke Hebert, Allison Seeger



Immunology 8

A Defense For Muslim Minority Jurisprudence

Hasan Ansari



Law 20

An Investigation of Fungal Species in a Heavy Metal-contaminated Urban Waterway

Kathy D. Nguyen



Ecotoxicology 30

Quantifying Insect Herbivory Across Plant Diversity Gradients

Mandy Tran



Ecology 48

Synthetic Approaches to Prepare and Isolate Halogenated Anthracene Derivatives

Benjamin Rogers



Chemistry 58

Optimizing Immunological Reagents for Use with the Domestic Ferret Model in Influenza Studies

Franziska Pflaum, Luke Hebert, Allison Seeger
The University of Texas at Austin

ABSTRACT

The domestic ferret (*Mustela putorius furo*) pathophysiological response to influenza infection mimics the human response, making the ferret an ideal model to study influenza and other respiratory infections. However, the ferret genome remains incomplete and there are few ferret-specific reagents, limiting experimental methods available for comprehensive analyses. To better assess the ferret immunoglobulin (antibody) response to influenza, we developed tools to analyze plasma antibodies. Immunoglobulin G was purified from ferret plasma and the protocols for sequencing the immunoglobulins with mass spectrometry were optimized. An ammonium sulfate precipitation, an old method of crude antibody isolation, was then optimized, followed by either an affinity chromatography using Protein A or an ion exchange chromatography. Purified IgG was confirmed with SDS-PAGE and the antibody was digested with a panel of proteases to determine the best way to generate CDR-H3 peptides, the region of the antibody responsible for recognizing antigens (pathogens, like viruses and bacteria). This work advances the ferret immunological information available by uncovering the repertoire of CDR-H3 sequences expressed in ferret plasma during influenza response. Furthermore, it prepares for synthesis of ferret monoclonal antibodies found in the plasma, which can be used to determine binding patterns of ferret antibodies to influenza components, importantly informing future vaccine design.

INTRODUCTION

The immune system is made up of two interconnected systems that work together to fight foreign antigens present in our skin, tissues, organs, and bodily fluids. The first line of defense is called the innate immune system. It acts quickly to attack invading pathogens in a rapid but unspecific way. Cells and organs of the innate immune system include the skin, mucus membranes, tissue-resident defensive cells (neutrophils, monocytes, and macrophages), and signaling proteins expressed by these responding cells.[1] When the innate immune system cannot completely fight off the invasion, the adaptive immune system kicks in, and a signal is sent to the bone marrow to create immature B cells. When B cells encounter an antigen (the part of an invading pathogen recognized by the immune system) they undergo activation and differentiation, transforming into plasma cells that secrete many antibodies that help eliminate the pathogen.

The anatomy of an antibody consists of two heavy and two light chains bound together by disulfide bond to create a Y-shaped protein. The tips of the Y (otherwise known as the Fab region) have the highest affinity for antigens, and after binding can neutralize their attack.[2]

The immense depth of the adaptive immune system is dependent on a constant genetic rearrangement of numerous variable (V), diverse (D), and joining (J) genes at heavy and light chain gene loci.[3] Many B cell receptors (BCRs) are generated via V(D)J recombination and some of which, through chance, will have a specific affinity for foreign pathogens and bind to them. By binding to the pathogen, these B cells are activated and can differentiate into either plasma cells or memory cells with the help of helper T cells. The specificity of the adaptive immune system establishes a vigorous defense against both current and recurring infections. Recently, the capacity to clone plasma cells and memory cells from other mam-

mals has provided a powerful genetic tool for making more effective vaccines.[4]

The United States alone records approximately 24,000 deaths from influenza infection each season, with an economic loss of $87 billion.[5] A universal influenza vaccine would eliminate some of the mortality, morbidity, and economic loss that influenza inflicts worldwide each year. The difficulty in creating a universal flu vaccine—one that induces long term protection against all influenza strains—lies in the virus's nature to change its surface proteins responsible for binding human epithelial cells. This occurs through antigenic drift (gradual mutations in the genetic makeup) and antigenic shift (sudden changes to the genetic makeup resulting in new surface proteins, i.e. new viral subtypes). The protein on the surface of influenza that binds to host cells for entry is called hemagglutinin (HA), consisting of a constantly mutating head region and a conserved stalk region. Many vaccines are able to block this entry by binding to HA on the surface of the virus. However, influenza's high mutation rate prevents vaccines from recognizing mutated versions of HA.. This means that seasonal strains of influenza remain undetected by antibodies elicited against previous influenza vaccines. The virus continues to infect, unless the vaccine is continually reformulated to account for the mutating HA. Vaccines that elicit stem-specific antibodies are able to provide universal vaccine coverage, because influenza stem regions are generally more conserved, and cannot alter their genetic sequences via antigenic shift and drift.[6,7]

The domestic ferret (*Mustela putorius furo*) has been considered the 'golden standard' for studying adaptive immune responses to influenza because their phenotypic response to respiratory viruses closely mimics that of humans. [8,9] The ferret is susceptible to human strains of influenza, which can be transmitted via respiratory droplets to the ferret host, unlike the mouse model, which requires prior host adaptation of the human virus.[10] On a molecular level, influenza HA binds the ferret's respiratory tract epithelial cells via an alpha-2,6 glycosidic linkage, as is the case in humans, whereas HA binds mouse epithelia via an alpha-2,3 glycosidic linkage. Additionally, because the ferret is larger than the mouse, researchers can collect ferret blood after repeated exposure to influenza which better mimics the human experience since humans are exposed to influenza continuously throughout their lifetime. However, the ferret model is limited by an incomplete ferret genome and sparsity of ferret-specific reagents. Peng et al. sequenced the current draft version of the ferret genome in 2014,[11] but the immunoglobulin annotations remain incorrect or incomplete. Though immunologist Kirchenbaum and Ross recently developed a chimeric human/ferret monoclonal antibody with ferret Fc components and human Fab sequences,[12] and Wong et al. have made an initial attempt at ferret immunoglobulin gene discovery,[13] the field of ferret immunogenetics remains largely unexplored, as does ferret immunoproteomics. The Georgio Lab at UT Austin specializes in describing both the B cell repertoire (BCR-seq) and the plasma repertoire (Ig-seq) in response to human vaccination and infection which are necessary to expand this area of research, specifically the ferret Immunoglobulin G repertoire. This study provides methods to translate Ig-seq experimental protocols previously designed for human specimens to now be used with ferret specimens.

To complement ferret immunogenetics discovery work from Hebert et al. in our lab (manuscript in preparation), we optimized methods for immunoproteomics studies in the domestic ferret. The first step was purifying ferret IgG from plasma. IgG isolation was attempted using ammonium precipitation methods published decades ago as well as more modern affinity chromatography techniques. Complete characterization of ferret IgG at the amino acid level requires digestion of the protein into peptides suitable for mass spectrometry analysis. A protocol for protease digestions was optimized to cut out the CDR-H3 peptide from ferret immunoglobulins; this region can be used to describe antibody repertoires downstream. The CDR-H3 is the part of the antibody that binds antigen, i.e., has the greatest specificity for a given epitope on an influenza virus (or any invading pathogen). These protocols will allow us to pair BCR-seq and Ig-seq techniques for use in the domestic ferret model, allowing a comprehensive description of ferret humoral responses following vaccine or infection. This is especially relevant in the context of preclinical vaccine trials, most importantly as we work to develop a universal influenza vaccine.

MATERIALS AND METHODS

3.1. Sample

Ferret F5269 plasma was generously donated by the Ted Ross Lab at the University of Georgia (now at Cleveland Clinic). Ferret F2 PBMC (Peripheral Blood Mononuclear Cells) were purchased from Marshall BioResources. The PBMC are pooled from multiple ferrets of unknown gender and infection status. Human plasma was isolated from whole blood from a volunteer donor. Blood was collected after obtaining informed consent at UT Health Services.

3.2. Optimization of ammonium sulfate precipitation of immunoglobulins from ferret plasma

An ammonium sulfate precipitation of antibodies from ferret plasma was performed using four concentrations of ammonium sulfate, to determine the optimal concentration to precipitate immunoglobulins without also pulling out contaminating plasma proteins. Ferret plasma was centrifuged at 4°C for 30 minutes at 3000 g to remove large particulates. The supernatant was split equally into four tubes. Cold, saturated ammonium sulfate (4.1M (NH4)2SO4) was added dropwise to the ferret plasma at the following plasma:ammonium sulfate ratios: 1:1, 1:2, 1:3 and 2:1. Importantly, (NH4)2SO4 was added dropwise at 4°C with constant mixing and then incubated overnight at 4°C. Precipitated proteins were pelleted by centrifugation at 3000 g and 4°C for 30 minutes and each pellet was resuspended in PBS. Supernatant (containing all other plasma proteins) and pellet (containing ferret immunoglobulin) were analyzed on SDS-PAGE to identify the optimal concentration of ammonium sulfate to crudely isolate ferret immunoglobulin.

To confirm that the ferret IgG had completely precipitated, a second precipitation step was performed, as suggested in textbooks14. Using the supernatant from the first precipitation, 4.1M (NH4)2SO4 was added dropwise (1:1 ammonium sulfate:plasma) at 4°C with constant mixing during an incubation overnight at 4°C. Precipitated proteins were pelleted by centrifugation at 3000 g and 4°C for 30 minutes and the pellet was resuspended in PBS. Both the primary and secondary precipitants and supernatants were analyzed by SDS-PAGE.

To remove the ammonium sulfate from crude immunoglobulin preparation, buffers were dialyzed against their downstream applications, namely 1X PBS or 10mM Tris, pH 8.5. Crude immunoglobulin preparations were loaded into 10,000 MWCO dialysis cassettes (Thermo Scientific, 66380) and placed in 4 L of 1X PBS or 10mM Tris, pH 8.5 at 4°C with stirring for 48 hours. After 24 hours, dialysis cassettes were transferred to a fresh 4 L buffer.

3.3. Purification of ferret IgG using Protein A affinity chromatography

Ferret IgG was further purified by affinity chromatography using Protein A slurry (Thermo Fisher, 22811). To optimize a protocol for the isolation of IgG from ferret plasma, we used Protein A affinity columns to capture ferret IgG (1) directly from ferret plasma, (2) from a crude primary ammonium sulfate precipitation, or (3) from a crude secondary ammonium sulfate precipitation. Protein A slurry columns were created by adding 1.5 mL slurry to a 5 mL polypropylene column (Thermo Scientific, 29922) between two frits. Ferret plasma was diluted 1:1 in 1X PBS before added over the column, with crude ammonium sulfate precipitations having been dialyzed against 1X PBS as described above. Flow through was collected and saved (to confirm IgG was indeed captured in the Protein A resin). Columns were washed with 3 column full volumes of PBS before eluting IgG from the column with 100mM Glycine, pH 2.7. Elutions were immediately neutralized with 1M Tris-HCl, pH 8.0. IgG concentrations were measured using a NanoDrop.

3.4. Purification of crude immunoglobulin using ion exchange chromatography

To create a column for ion exchange chromatography, diethylaminoethyl (DEAE) was covalently cross linked to a sepharose matrix, which is positively charged at neutral pH. DEAE sepharose (Millipore Sigma, DCL6B100) columns were prepared by suspending the resin above a frit in a 5 mL polypropylene column (Thermo Scientific, 29922). The resin was equilibrated with 0.5N HCl followed by 0.5N NaOH. An additional 5 column volumes of 10mM Tris, pH 8.5 were then used to wash the resin. After equilibration, dialyzed solutions (crude Ig now in 10mM Tris, pH 8.5) from the primary and secondary ammonium sulfate precipitations were added to the column. Negatively charged IgG should bind the posi-

tively charged DEAE matrix. The column was washed with 10mM Tris pH 8.5. To optimize elution conditions, we eluted IgG from the column with 4 different concentrations of NaCl. IgG is eluted from the column when chlorine ions exchange places with the immunoglobulin by binding to the matrix. For human antibodies, 50 - 100mM NaCl in 10 mM Tris is used for elution[14]. Ferret IgG also seemed to elute at around these concentrations, but we optimized further by eluting with 50mM, 60mM, 70mM or 80mM NaCl. Elution solutions were concentrated using 100,000 MWCO Vivaspin Turbo 4 tubes (Sartorius, VS04T42) and the concentration measured using a NanoDrop. Each elution was run on SDS-PAGE.

3.5. SDS-PAGE

Protein samples were prepared for SDS-PAGE in 4X LDS Sample Buffer (Life Technologies, B0008) at 98°C for 5 min. SDS-PAGE was run using Bolt 4-12% Bis-Tris Plus gels (Invitrogen, NW04120BOX) bathed in 1X SDS Running Buffer at 200 V for 20 min. Gels were stained with Power Stain Solution (Thermo Scientific, 1902206) and Destain Solution (Thermo Scientific, 1902207) in a power stain machine at 25 V for 7 min.

3.6. Next generation sequencing to generate proteomic search databases for ferret plasma antibody identification

Next generation sequencing (NGS) has been used as a method to generate personalized human immunoglobulin variable heavy chain (IGHV) gene databases used for proteomic searches[15]. Recently, these methods have been adapted for use in the domestic ferret (Hebert et al., manuscript in preparation). In brief, IGHV genes were amplified from ferret cDNA synthesized from whole RNA that had been isolated from ~6.5 x 10^6 peripheral blood mononuclear cells (PBMC). IGHV gene PCR amplicons were sequenced using a 2 x 300 paired-end Illumina MiSeq platform. IgDiscover, a bioinformatics tool, was used to identify and annotate VH genes, including the framework (FR) and complementarity-determining regions (CDR)[16]. Importantly in the context of this study, IgDiscover can identify the FR3, which marks the start of the CDR-H3 region, and includes part of a variable gene (VH), a diversity gene (DH), and a joining gene (JH). Annotated IGHV genes from PBMC from ferret F5269 were compiled into a database used to conduct proteomic searches. CDR-H3 peptide sequences identified from MS analysis will later be used to query the respective IGHV database in order to identify and quantitate the antibody proteins isolated from ferret plasma.

3.7. Protease digestion optimization

Ten different digestion conditions were tested using our isolated IgG, and complete digestion confirmed on SDS-PAGE. To open our immunoglobulin proteins to make them more available for protease digestion, we first denatured, reduced, and alkylated our samples. The pH 8 of each different digestion tube was corrected to 7.5 and then an equal volume 2,2,2-trifluoroethanol (TFE) was added. IgG aliquots were then reduced by adding 5mM TCEP Bond-Breaker (Thermo Scientific, 77720) and heated to 55°C for an hour. Finally, 16.5mM iodoacetamide (IAM) was used to alkylate the samples in the dark for 30 minutes. Then each sample was diluted in 7 volumes of appropriate dilution buffer (according to the manufacturer's suggestions for each protease tested). We tested 4 different proteases alone and in combination to find the optimal digestion conditions to yield appropriate CDR-H3 peptides. The proteases tested were AspN (Promega, VA1160), ProAlanase (Promega, VA217A), human neutrophil elastase (hNE, Athens Research & Technology, 16-14-051200) and trypsin (Promega, V5280). All proteases required different concentrations of Tris buffer, except ProAlanase which is active in 0.5M HCl. Proteases were added in a 1:50 protease:substrate ratio and incubated overnight at 37°C Digestions were stopped with 1% formic acid, except ProAlanase which required heating to 92°C for 10 minutes. If a second round of digestion was performed with trypsin, then 1M Tris, pH 8.5 was used to neutralize the solutions. After neutralization, trypsin was added in a 1:50 protease:-substrate ratio and then incubated overnight at 37°C. Digestions were stopped with 1% formic acid.

RESULTS

4.1. Isolation of ferret IgG

Four different concentrations of ammonium sulfate were used to optimize isolation of crude IgG from ferret plasma. Precipitants were removed by centrifugation and immunoglobulin proteins resuspended in PBS and confirmed on SDS-PAGE. Assuming that ferret IgG is about 150 kD (as is human IgG), a ratio of 1:1 ammonium sulfate to plasma gave the clearest and strongest IgG

band (Figure 1), consistent with literature and textbook protocols for isolation of mammalian IgG.[12, 14]

Protein A specifically binds to the Fc region of human IgG and we hypothesized that it would bind the Fc region on ferret IgG as well. Because it had been reported in the literature that crude ammonium sulfate precipitation was required prior to Protein A purification, [12] we optimized both protocols in parallel. Additionally, *Antibodies: A laboratory Manual* by Ed Harlow suggests a secondary ammonium sulfate precipitation may be necessary for isolating IgG from some species, [14] so this was tested as well. We confirmed, for the first time to our knowledge, that Protein A bound ferret IgG even without a preliminary crude ammonium precipitation. Ferret IgG, like human IgG, can be isolated directly from ferret plasma with negligent protein contaminants remaining in the elution fraction. Importantly, we successfully demonstrated the removal of albumin, a major plasma protein from plasma samples.

DEAE ion exchange chromatography uses positively charged beads that can bind to negatively charged proteins in solution. Bound proteins are eluted with salt, as the salts exchange places with our proteins of interest on the beads. To test for the optimal concentration of NaCl to elute ferret IgG from a DEAE-sepharose resin, both 80mM NaCl and 60mM NaCl washes were tested following a single or double ammonium sulfate precipitation step. It was confirmed via SDS-PAGE that 60mM NaCl best eluted IgG from the DEAE matrix with fewer contaminating proteins (Figure 1).

We were able to isolate IgG from ferret plasma using both methods — crude ammonium sulfate precipitation followed by ion exchange chromatography with 60mM NaCl (Figure 1, lane 13), and Protein A affinity chromatography from plasma (Figure 1, lane 10). However, ferret IgG purification using Protein A can also be achieved without a preliminary ammonium sulfate precipitation. It is unclear why Protein A purification alone has not been tried in the past to isolate ferret Ig,[12] as a preliminary ammonium sulfate precipitation adds several days to the protocol.

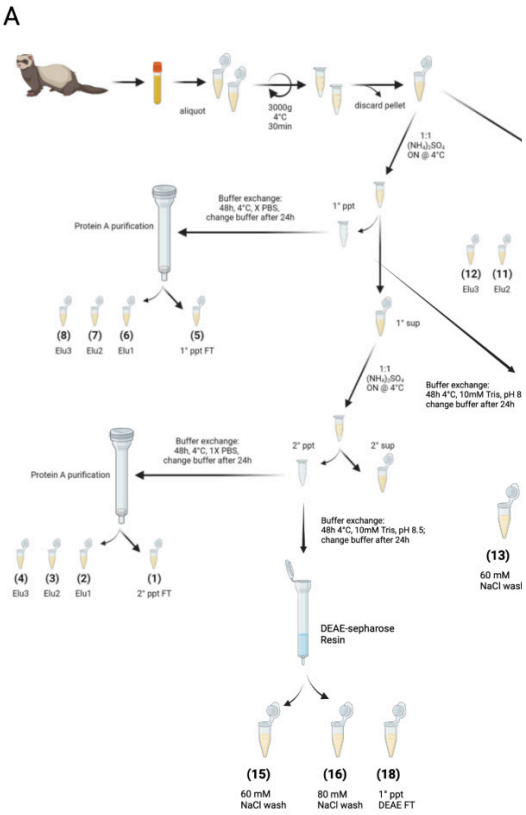
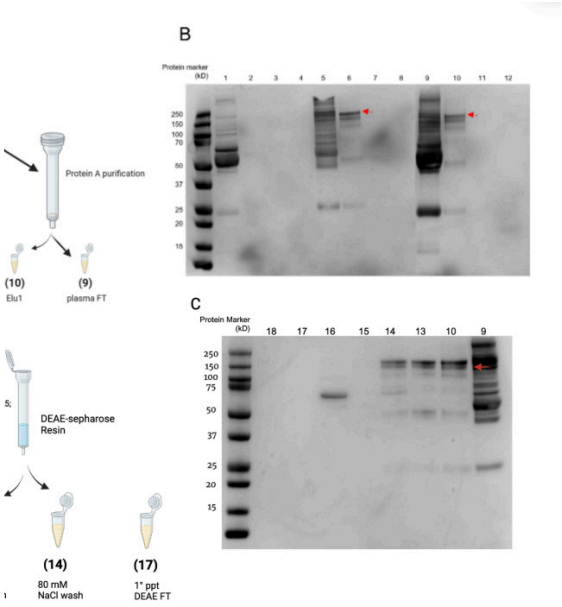


Figure 1. Isolation of IgG from ferret plasma using ammonium sulfate precipitation, Protein A affinityaf inity chromatography, and DEAE ion exchange chromatography. *(A) Process workflow for isolation of IgG from ferret plasma. Ferret plasma was centrifuged to remove particulates, then IgG isolated after two ammonium sulfate precipitation steps followed by Protein A chromatography (samples 1-4) or DEAE affinityaf inity chromatography (samples 15, 16, and 18); or a single ammonium sulfate precipitation followed by Protein A chromatography (samples 5-8), and DEAE affinityaf inity chromatography (13, 14, and 17); or purified directly from the plasma over a Protein A chromatography column (samples 9-12). (B) SDS-PAGE to illustrate protein components in each fraction after Protein A chromatography; sample numbers in parentheses in panel A correspond to sample numbers above each lane in panel B. Red arrows indicate a band at about 150 kD that we believe to be IgG. Note that this is two polyacrylamide gels that have been aligned and pasted together electronically. (C) SDS-PAGE to illustrate protein components in each elution after DEAE ion exchange chromatography; sample numbers in parentheses in panel A also correspond to sample numbers above each lane in panel C. Red arrows indicate a band at about 150*



kD that we believe to be IgG. These figures were created at BioRender.com.

4.2. In silico description of ferret IgG CDR-H3

The variable region of an immunoglobulin's heavy chain is encoded by the combination of an IGHV (Immunoglobulin G Heavy Variable), IGHD (Diverse), and IGHJ (Joint) gene. Together, this gene combination is translated into a series of alternating conserved framework regions and contrastingly hypervariable complementarity-determining regions (CDRs). Some of the framework regions identify the IGHV's evolutionary clan and family whereas the CDRs collectively determine an immunoglobulin's epitope and binding affinity. There are three CDRs on the Ig heavy chain: from N-terminal to C-terminal, CDR-H1, CDR-H2, and CDR-H3 (Figure 2). CDR-H3 is the most diverse, a hot spot for somatic hypermutation, and the center of the antibody binding site. Because the CDR-H3 sequence is so unique, we can use it to computationally distinguish antibody amino acid sequences from one another. This was done by digesting immunoglobulins isolated from human plasma with trypsin and then sequencing the resulting peptides using liquid chromatography with tandem mass spectrometry (LC-MS/MS).[15]

Peptide sequences obtained from LC-MS/MS are mapped back to personalized VH transcript sequence databases and the relative abundance of plasma antibodies containing each unique CDR-H3 describes the plasma response to a vaccine or infection, referred to as a plasma "antibody repertoire."

A critical step in this process is proteolytically excising the CDR-H3 peptide (the "fingerprint" of an antibody) in its entirety, to be identified by LC-MS/MS. Unfortunately, ferret CDR-H3 regions cannot be cleanly digested using only trypsin, as human CDR-H3s can. CDR-H3 lengths vary, but average at around 15 amino acids long[17], which is an ideal length for sequencing by mass spectrometry. Figure 2 compares the ferret amino acid CDR-H3 length (red) to human (blue) and mice (yellow). The ideal protease should not cut within the CDR-H3, so it's important to choose a protease that does not cut at an amino acid that is frequently found within CDR-H3 sequences, but does cut just outside the CDR-H3, yielding a peptide less than 25 amino acids in length that is appropriate for LC-MS/MS. Trypsin cleaves at conserved lysine (K) and arginine (R) residues at the C-terminal side, which are relatively uncommon in CDR-H3 sequences. However, unlike human IgG, it is believed that ferret IgG does not have a conserved lysine at the C-terminal end of the CDR-H3 (in the CH1 region). Therefore, other proteases are needed to cut a CDR-H3 peptide of suitable size for sequence identification via LC-MS/MS — either in addition to or in place of trypsin.

We chose to test ProAlanase, AspN, and human neutrophil elastase (hNE) to cut the CDR-H3 from ferret IgG. ProAlanase cuts at alanine (A) and proline (P) residues, AspN cuts at aspartic acid (D) and cysteine (C) residues, and hNE cuts at valine (V) and alanine residues. Because ferret constant region sequences were unavailable, we estimated the suitability of these proteases to cut the flanking CH1 using dog CH1 sequences (dog is the ferret's closest related mammal for which detailed immunoglobulin sequence information is available). Ferret framework sequences have been identified by us (unpublished) and others,[13] so we used these sequences to estimate the suitability of our proteases to cut at the N-terminal side of the CDR-H3.

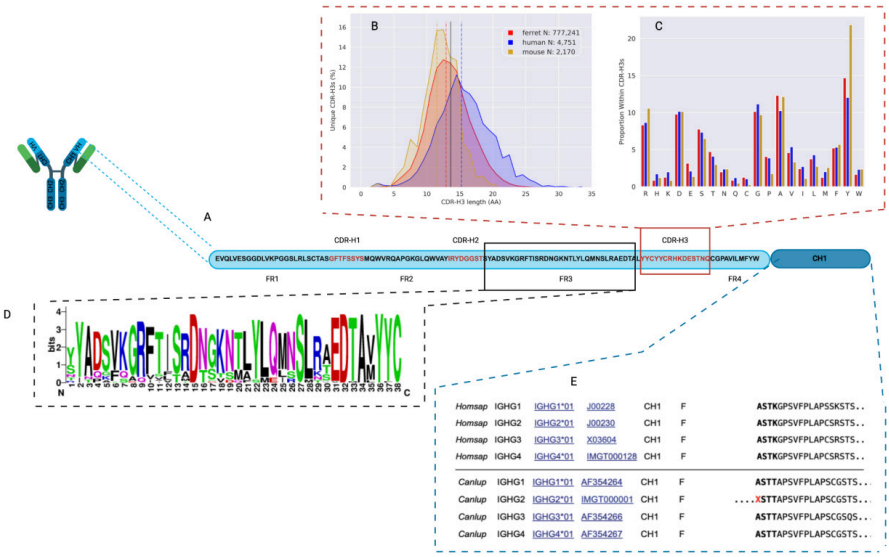


Figure 2. Characterizing the ferret IgG CDR-H3 and flanking regions. *(A) Cartoon of IgG with a close-up of the heavy chain variable region, a representative Clan III IGHV gene sequence is shown. Framework (FR) regions are shown in black text and complementarity-determining regions (CDR) sequences are shown in red text. (B) The length of ferret CDR-H3 sequences is about 12 amino acids (red) compared to human (blue) and mouse (yellow). The average dog CDR-H3 length is indicated by the grey line. (C) The frequency of amino acids used in CDR-H3 sequences in ferretsferret (red), humanshuman (blue), and micemouse (yellow). (D) To determine commonly used amino acids in ferret FR3 regions, a sequence logo was created at weblogo.berkeley.edu by aligning all FR3 in-silico translated amino acid sequences currently published for ferret. (E) To identify probable amino acid sequences at the N-terminal end of the IgG CH1 gene, CH1 sequences from dogsdog were obtained from IMGT. Constant region genes from the ferret are currently unknown, Canis lupus familiaris is the most closely related mammal to the domestic ferret for which immunoglobulin sequence information is available. This figure was created at BioRender.com.*

4.3. In silico protease digestion modeling to generate CDR-H3 peptides for identification via mass spectrometry

Our lab developed an in silico bioinformatics tool to estimate the length of a CDR-H3 peptide generated by using a single protease or combination of multiple proteases to simulate digestion of ferret IgG (unpublished). The tool utilizes immunoglobulin-encoding nucleotide data and protease specificities for its predictions. It allows us to estimate the lengths of ferret CDR-H3-containing products remaining after a theoretically complete digestion. Our nucleotide data consisted of Illumina-sequenced cDNA from ferret PBMCs; our PCR primer pool targeted IGHV genes (forward primers) and IGHJ genes (reverse primers), consequently amplifying the CDR-H3 sequences which could then be computationally translated to amino acid sequences. Representative examples of the outputs are presented as histograms in Figure 3, with the number of transcript sequences plotted on the y-axis and the amino acid distance (or length) plotted on the x-axis. Note that for this *in silico* experiment, we chose to simulate digestion of the C-terminal side's FR4 instead of the downstream CH1 sequences. The ferret IgG CH1 amino acid sequence, published in 2020 by Wong *et al.*[13], is inconsistent with the most recent version of the ferret genome (ASM1176430v1.1). Though we would ideally like to obtain both VH and isotype data from MS, we have chosen to use FR4 as the C-terminal flanking region for this simulation because we have amplified *ferret* FR4 transcript sequences in-house (unpublished). Most CDR-H3 peptides generated are of an appropriate length for identification via mass spectrometry, however cutting with only trypsin or only ProAlanase also yields peptides that would likely be too long (Figure 3, yellow boxes).

An in silico digest found that the combination of ProAlanase followed by trypsin digestion is the optimal proteo-

lytic strategy for precise cleavage at the N and C termini, generating CDR-H3 peptides shorter than 25 amino acids. Based on the in silico digestion of the ferret sample used for simulation, we would expect the majority of CDR-H3 peptides to be 16-17 amino acids long (figure 3, graph column 2 row 3). In contrast, using ProAlanase or trypsin alone would result in many longer CDR-H3 peptides that wouldn't be recognized by mass spectrometry (Figure 3, graph in column 2, row 1 and 2: yellow boxes indicate peptides that will not be recognized by MS).

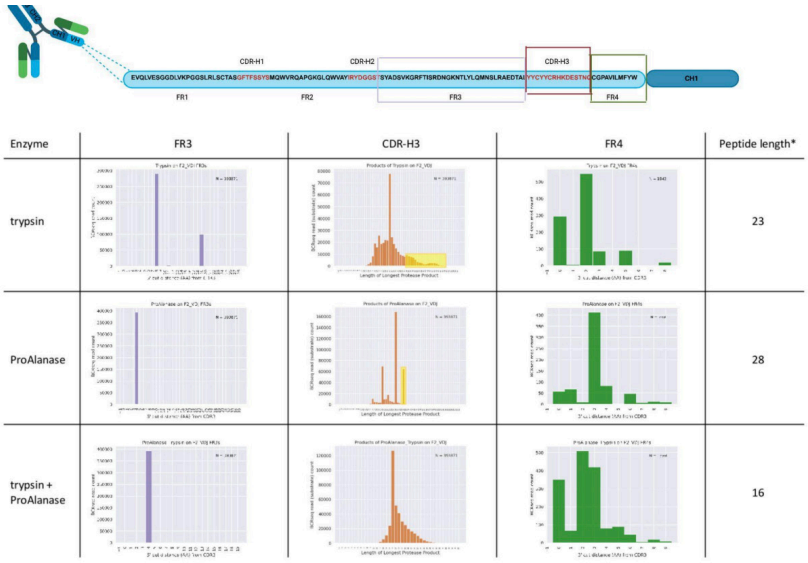


Figure 3. In silico digestion of ferret IgG with trypsin and/or ProAlanase. *A cartoon of IgG with a close-up of the heavy chain variable region, a representative Clan III IGHV gene sequence is shown in the upper left corner. Framework (FR) regions are shown in black text and complementarity-determining regions (CDR) sequences are shown in red text. The purple, red, and green boxes correspond to the FR3, CDR-H3, and FR4 histograms, respectively, shown in the table below. To amplify IGHV genes from ferret F2, RNA was isolated from PBMCs and reverse transcribed to make cDNA, which was used as a template to amplify IGHV genes. PCR products were sequenced using a 2 x 300 paired-end Illumina MiSeq platform. N = the total number of transcript sequences used for in silico digestion. FR3 and FR4 histograms show distances from the CDR-H3 (in number of amino acids) plotted on the x-axis and number of transcript sequences with cut sites at those locations plotted on the y-axis. CDR-H3 histograms have the predicted lengths of peptides containing the CDR-H3 (in number of amino acids) plotted on the x-axis and number of transcript sequences on the y-axis. Yellow boxes highlight CDR-H3 peptide lengths that will likely be too long for identification with mass spectrometry. *The most likely peptide length is listed, defined as the greatest number of CDR-H3 peptides predicted at any one length for each protease or protease pair simulated.*

4.4. Protease optimization with human IgG

Proteases cleave proteins at certain amino acids, ultimately creating smaller polypeptides that can be identified by mass spectrometry. Based on our in silico analyses and in silico digestion of ferret IgG, four different proteases (ProAlanase, trypsin, hNE, and AspN) were chosen for optimization of wet lab protocols. Purified human IgG was used to optimize digestion buffers, pH, and incubation times to achieve optimal protease activity. Optimized digestion buffers ensured that each protease held their confirmation with correctly protonated and deprotonated side chains. Each protease individually or in combination with trypsin (either simultaneously or subsequently), except for ProAlanase + trypsin, completely digested human IgG, at least as is visible on SDS-PAGE (Figure 4). ProAlanase is only active at very acidic pH while trypsin is optimally active at neutral pH, so simultaneous digestion using these two proteases was not expected to be complete. All other protease protocols completely digested human IgG, and because our in silico double digests show promise with ferret IgG, we expect complete digestion thereof with our optimized wet lab protocols.

As predicted, IgG digested with trypsin followed by ProAlanase is not visible by SDS-PAGE indicating successful cleavage of the antibody (see Figure 4C). It remains to be confirmed that the CDR-H3 peptides were digested as expected, peptide mapping back to BCR-seq V_H databases is currently underway. Digesting IgG with ProAlanase alone resulted in the appearance of two bands on our gel, indicating incomplete digestion of the antibody, emphasizing the necessity to combine ProAlanase with

trypsin. Though the trypsin digest also looks complete in the gel, we know from our in silico digestion analysis (refer to Figure 3) that CDR-H3 peptides likely exceed optimal lengths for mass spectrometry (though those peptides are probably still too small to be visible by SDS-PAGE). This gel validation roughly confirms that the in silico analysis can accurately predict wet lab digestion results. Consequently, we can proceed with confidence that we have isolated ferret CDR-H3. We also want to point out that proteases aren't always 100 percent accurate, and errors in the cleavage sites could have occurred. We need to sequence our peptides and align them with our VH genes from BCR-seq (unpublished, in progress) to confirm that we have properly cleaved all our CDR-H3, as this level of confirmation cannot be obtained from a gel.

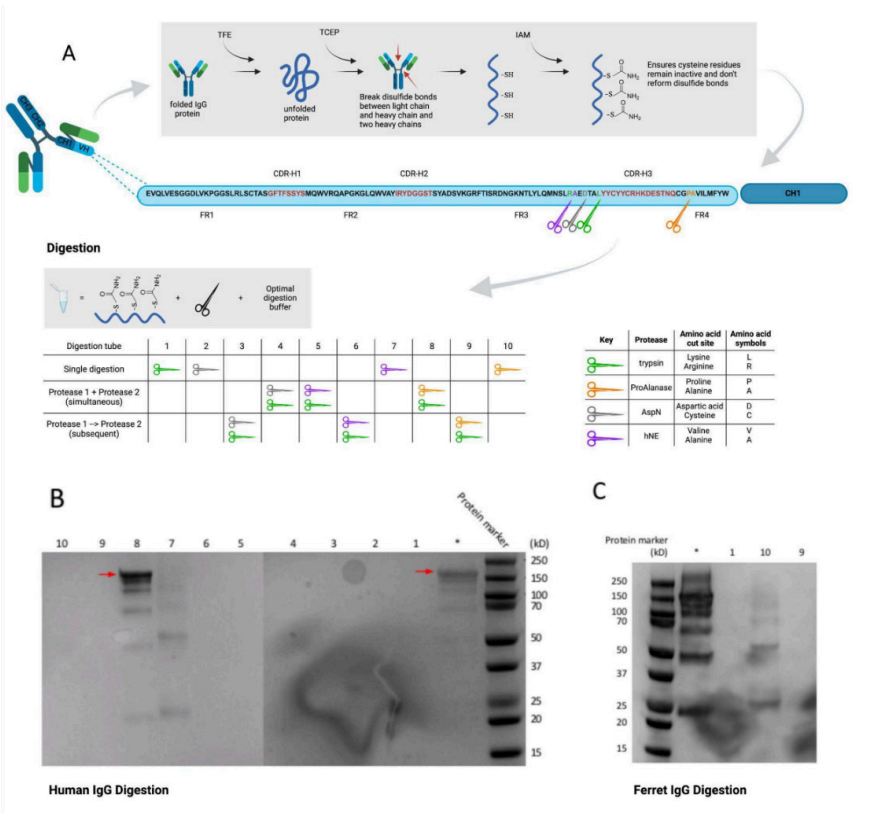


Figure 4. Protease digestion of purified IgG. (A) Workflow diagram: *Cartoon of IgG with a close-up of the heavy chain variable region, a representative Clan III IGHV gene sequence is shown. Framework (FR) regions are shown in black text and complementarity-determining regions (CDR) sequences are shown in red text. Amino acids cut with the proteases trypsin, ProAlanase, AspN, and human neutrophil elastase (hNE) are shown in green, orange, grey, or purple, respectively. The top light grey panel illustrates the process to prepare purified IgG for digestion: denaturation, reduction, and alkylation. The lower light grey panel and table describe protease digestion and the protease combinations tested in the wet lab. Column numbers correspond to lane numbers in panels B and C. (B) SDS-PAGE of* ***human*** *IgG digested with trypsin, ProAlanase, AspN, hNE, or combinations thereof. Lane numbers correspond to column numbers from Panel A. Red arrows indicate intact IgG, i.e., the digestion was not successful or complete. *Indicates uncut human IgG. Note that this is two polyacrylamide gels that have been aligned and pasted together electronically. (C) SDS-PAGE of ferret IgG cut with trypsin, ProAlanase, or combination thereof. *Indicates uncut ferret IgG. This figure was created at BioRender.com.*

DISCUSSION

In this study we adapted a technique pioneered by the Georgio Lab at UT Austin over a decade ago to describe the human antibody response in the plasma,[15] for use in the domestic ferret model, Mustela putorius furo. We optimized ferret IgG isolation and protease digestion, in preparation to ultimately sequence ferret IgG using mass spectrometry. Downstream applications include combining Ig-seq with BCR-seq and describing the plasma and cellular repertoires in the domestic ferret for the first time, to our knowledge. Little is known about ferret immunoglobulins, save a pioneering study by Wong et al.,[13] which relied on an incomplete version of the ferret genome.[11] Our lab is currently working to comprehensively describe the ferret immunoglobulin loci and the B cell repertoire in response to influenza infection (Hebert et al., unpublished).

The methods we have described here are specific to IgG, but can be adapted to purify and analyze other immunoglobulin isotypes such as IgM and IgA, especially if

using ammonium sulfate precipitation and ion exchange chromatography. These methods are cheap and easily adaptable for use with other immunoglobulin isotypes.[14] Though ammonium sulfate precipitation has been performed for decades as a preliminary or crude method to isolate human and murine immunoglobulins,[14] protocols available in textbooks and in the literature[12] have not been optimized for use with ferret plasma proteins. We followed crude immunoglobulin precipitation with either affinity chromatography using Protein A slurry or ion exchange chromatography using DEAE resin to isolate IgG fully. Here, we were particularly concerned with confirming the removal of albumin, which is the most abundant plasma protein in mammals. The molecular weight of albumin is about 70 kD and that of IgG is 150 kD, so IgG can be clearly distinguished from albumin with SDS-PAGE.

We used SDS-PAGE consistently throughout this project to monitor our optimization steps. Sodium dodecyl sulfate polyacrylamide gel electrophoresis (SDS-PAGE) is a method used to separate proteins by mass. Polyacrylamide-based discontinuous gel is sandwiched between two glass sheets with wells at the top into which a protein sample can be loaded. This cassette is placed into a box that has a positive cathode at the top and a negative anode at the bottom. The cassette is bathed in a 10% SDS running buffer. The running buffer acts like a surfactant by unfolding and enveloping the proteins with a negative charge. An electric charge is applied to the box which pushes negatively charged proteins towards the cathode. Larger proteins travel slower through the polyacrylamide matrix. A protein ladder is loaded alongside protein samples as a molecular weight marker reference.

Protein A is a 42 kD surface protein originally found in the cell wall of the bacteria *Staphylococcus aureus*. It has been shown to bind to the Fc portion of IgG antibodies in humans and other mammals. Though Protein A can be used to isolate IgG directly from human plasma, in the literature Protein A has only been used to isolate IgG from crude ammonium sulfate preparations of ferret IgG[12]. In our hands, Protein affinity chromatography alone—without the crude ammonium sulfate precipitation step prior—was sufficient to isolate IgG from ferret plasma with few contaminating proteins. Importantly, albumin is completely removed and appears only in the Protein A flow through (Figure 1B). DEAE ion exchange chromatography is an extremely simple yet effective method to isolate immunoglobulin proteins. When the pH of the starting antibody solution is raised above its pI, the antibody loses its hydrogens and becomes more negatively charged which makes it available for anion exchange chromatography; this method has been used to isolate antibodies for decades[14]. We were also able to isolate ferret IgG using ion exchange chromatography following ammonium sulfate precipitation. This method does require the initial ammonium precipitation step, but only a single precipitation step (the double precipitation did not increase our yield). Protein A affinity chromatography can be used to isolate IgG from ferret plasma in under an hour. DEAE ion exchange chromatography following ammonium sulfate precipitation also yields a clean IgG sample (Figure 1C), but takes about a week. However, DEAE ion exchange chromatography is cost efficient compared to Protein A affinity chromatography. In low resource settings or projects with smaller budgets or larger scales, the former is a suitable substitute for the latter.

The next step in adapting our Ig-seq protocol for use with the ferret is digesting whole IgG into peptides suitable for mass spectrometry analysis. Mass spectrometry (MS) is an analytical tool that measures the mass-to-charge ratio of a protein or molecule in a sample. It can be used to determine the amino acid sequences of peptides. MS is very sensitive to other macromolecules in solution, such as albumin, so purification of isolated immunoglobulin is critical before MS analysis. We use the CDR-H3 sequences to distinguish V_H genes from one another. Because the CDR-H3 is a uniquely diverse region of an antibody, it allows us to quantify plasma antibodies by the number of unique CDR-H3 peptides. Also, it is relatively short, so we can use proteases to cut out complete CDR-H3 peptides—located between the FR3 and CH1—that are not more than 25-30 amino acids long and can be identified via MS. However, unlike human CH1 sequences, ferret IgG CH1 exons do not have a tryptic site at the N-terminus. Therefore, it was necessary to optimize additional proteases for preparation of our IgG peptides for mass spectrometry. This was the first time these proteases had been in our lab for excising CDR-H3 peptides.

In silico, we determined that ProAlanase, AspN, and human neutrophil elastase would potentially cleave ferret IgG to yield the maximum number of intact CDR-H3 peptides. Experimentally, we found that trypsin and ProAlanase cut within the FR3 and FR4 while also minimizing cleavage within the CDR-H3. We optimized a subsequential digest protocol, with trypsin and then ProAlanase, first using purified human IgG as a test control and then confirming in purified ferret IgG.

Ideally, IgG isolation will be followed by isolation of hemagglutinin-specific IgG prior to protease digestion. This will allow us to describe, for the first time to our knowledge, the influenza-specific plasma antibody repertoire in the domestic ferret model. The next step will be to sequence these peptides with mass spectrometry, map these amino acid sequences to personalized V_H gene databases generated using BCR-seq (Hebert et al., unpublished), and then cluster the CDR-H3 peptides to describe the relative abundance of each cluster in the ferret plasma.

The advent of B cell repertoire sequencing has greatly advanced our understanding of the human adaptive immune response.[4,18] Advances in next generation sequencing (NGS) and the development of multiplex PCR primers allowed for an enormous growth in the number of BCR (B cell receptor) sequences available for analysis. The advantage of BCR repertoire analysis aided in closing the gap between BCR sequences in immature B cells from the bone marrow, and antigen-specific B cell receptors that develop into either plasma cells or memory cells.[16] It is now critical for the field to understand repertoire data in the context of the domestic ferret model. A deeper understanding of ferret immunogenetics and the ferret adaptive immune system is lacking. This is especially surprising as ferrets have been the model organism for studying influenza transmission and pathogenesis for nearly a century.[19] To date, few ferret-specific immunological reagents exist, prohibiting expansion of the model, though it appears to be superior to the mouse as a preclinical model for influenza.[20]

The HA reactivity of ferret immunoglobulins will give us great insight into the development of a universal influenza vaccine[21]. Paired ferret BCR-seq and Ig-seq data will allow us to identify HA-specific, paired V_H:V_L sequences present in ferret plasma. We can use these sequences to clone monoclonal antibodies (mABs). Characterizing these mAbs to determine epitope specificity and virus neutralization capacity will inform vaccine design. It's important to note that sequence alone does not govern binding properties. Additional assays will be required to detect where specifically a mAb binds HA. The HA stem mutates infrequently which means that a mAB bound to the HA stem would potentially neutralize more strains, and would ultimately be a better option for human influenza vaccines.[22] Using the ferret as a preclinical influenza vaccine model could help vaccine designers pinpoint vaccine antigens that elicit high anti-stem titers before bringing the vaccine to the clinical trial stage in humans.

ACKNOWLEDGEMENTS

This project was funded by NIAID/NIH Contract Number 75N93019C00050. 23

REFERENCES

[1]The innate and adaptive immune systems. in InformedHealth.org [Internet] (Institute for Quality and Efficiency in Health Care (IQWiG), 2020).

[2]Antibodies: Definition, Types & Function. Cleveland Clinic https://my.clevelandclinic.org/health/body/22971-antibodies.

[3]Jr, C. A. J. et al. Immunobiology. (Garland Science, 2001). Marks, C. & Deane, C. M. How repertoire data are changing antibody science. J. Biol. Chem. 295, 9823–9837 (2020).

[4]Krammer, F., García-Sastre, A. & Palese, P. Is It Possible to Develop a 'Universal' Influenza Virus Vaccine? Potential Target Antigens and Critical Aspects for a Universal Influenza Vaccine. Cold Spring Harb. Perspect. Biol. 10, a028845 (2018).

[5]CDC. How Flu Viruses Can Change. Centers for Disease Control and Prevention https://www.cdc.gov/flu/about/viruses/change.htm (2022).

[6]Andrews, S. F., Graham, B. S., Mascola, J. R. & McDermott, A. B. Is It Possible to Develop a 'Universal' Influenza Virus Vaccine? Immunogenetic Considerations Underlying B-Cell Biology in the Development of a Pan-Subtype Influenza A Vaccine Targeting the Hemagglutinin Stem. Cold Spring Harb. Perspect. Biol. 10, a029413 (2018).

[7]Enkirch, T. & Von Messling, V. Ferret models of viral pathogenesis. Virology 479–480, 259–270 (2015).

[8]Wong, J., Layton, D., Wheatley, A. K. & Kent, S. J. Improving immunological insights into the ferret model of human viral infectious disease. Influenza Other Respir. Viruses 13, 535–546 (2019).

[9]Ferrets as experimental models of influenza in humans. https://www.ecdc.europa.eu/en/news-events/ferrets-experimental-models-influenza-humans (2012).

[10]Peng, X. et al. The draft genome sequence of the ferret (Mustela putorius furo) facilitates study of human respiratory disease. Nat. Biotechnol. 32, 1250–1255 (2014). 12.

[11]Kirchenbaum, G. A. & Ross, T. M. Generation of Monoclonal Antibodies against Immunoglobulin Proteins of the Domestic Ferret (Mustela putorius furo). J. Immunol. Res. 2017, 5874572 (2017).

[12]Wong, J. et al. Sequencing B cell receptors from ferrets (Mustela putorius furo). PLOS ONE 15, e0233794 (2020).

[13]Harlow, E. & Lane, D. Antibodies: A Laboratory Manual. (Cold Spring Harbor Laboratory, 1988).

[14]Lavinder, J. J., Horton, A. P., Georgiou, G. & Ippolito, G. C. Next-generation sequencing and protein mass spectrometry for the comprehensive analysis of human cellular and serum antibody repertoires. Curr. Opin. Chem. Biol. 24, 112–120 (2015).

[15]Corcoran, M. M. et al. Production of individualized V gene databases reveals high levels of immunoglobulin genetic diversity. Nat. Commun. 7, 13642 (2016).

[16]Zemlin, M. et al. Expressed Murine and Human CDR-H3 Intervals of Equal Length Exhibit Distinct Repertoires that Differ in their Amino Acid Composition and Predicted Range of Structures. J. Mol. Biol. 334, 733–749 (2003).

[17]García-Valiente, R. et al. Understanding repertoire sequencing data through a multiscale computational model of the germinal center. Npj Syst. Biol. Appl. 9, 8 (2023).

[18]Laidlaw, P. P. EPIDEMIC INFLUENZA: A VIRUS DISEASE. The Lancet 225, 1118–1124 (1935).

[19]Basu Thakur, P., Mrotz, V. J., Maines, T. R. & Belser, J. A. Ferrets as a Mammalian Model to Study Influenza Virus-Bacteria Interactions. J. Infect. Dis. jiad408 (2023) doi:10.1093/infdis/jiad408.

[20]Collaborative Influenza Vaccine Innovation Centers (CIVICs) | NIAID: National Institute of Allergy and Infectious Diseases. https://www.niaid.nih.gov/research/civics (2023).

[21]Aartse, A. et al. Primary antibody response after influenza virus infection is first dominated by low-mutated HA-stem antibodies followed by higher-mutated HA-head antibodies. Front. Immunol. 13, 1026951 (2022).

A Defense For Muslim Minority Jurisprudence

Hasan Ansari
The University of Texas at Austin

SIGNIFICANCE

The unprecedented amount of Muslims migrating to Western countries in the past few decades has raised numerous concerns for both Muslims and Muslim scholars. This has led to the emergence of a new and contentious branch of Islamic law, known as Muslim minority jurisprudence or 'minority *fiqh*.' While minority *fiqh* has been subject to some critical analysis, this paper, 'A Defense For Muslim Minority Jurisprudence,' is purposed with the task of to providing a concise yet comprehensive support for the doctrine of minority *fiqh*. Through directly addressing the most controversial debates surrounding minority *fiqh*, this paper effectively serves both as a response to critics and an affirmation for supporters. The relevance of this doctrine is for anyone interested in the integration of Muslims into America and other non-Muslim nations through a jurisprudential framework. It is especially beneficial for fellow Western Muslims seeking to understand scholarly perspectives on adhering to their tradition in a seemingly foreign environment.

INTRODUCTION

TAs North American and European nations have seen a massive influx of Muslim migrants within the last century, Muslims have needed guidance on how to maintain their faith in a way that is flexible with their new environment. Minority *fiqh*, also known as *fiqh* al-aqalliyyat in Arabic or Muslim minority jurisprudence in English, is a new term developed in the 1990s by two prominent Muslim scholars: Shaykh Dr. Taha Jabir al-Alwani (d. 2016) and Shaykh Dr. Yusuf al-Qaradawi (d. 2022). It refers to a framework within Islamic legal theory with the goal of Muslim jurists interpreting Islam to address the unique needs and concerns of Muslims in non-Muslim countries. While this doctrine is influenced by modernism, minority *fiqh* is not[1] meant to be anything outside the bounds of Islamic orthodoxy. Minority *fiqh* is a continuation of the Islamic legal tradition in response to the newly globalized world. However, as with anything new, minority *fiqh* has been met with a great deal of criticism and debate among Islamic scholars.

In direct response to critics of minority *fiqh*, this thesis argues that minority *fiqh* is a justified and necessary branch of Islamic law. The aim is to examine and defend minority *fiqh* amidst three of the most contentious issues surrounding the new legal doctrine: the issue of emigrating Muslim territory (*dar al-Islam*), the issue of dual allegiance, and the issue of innovating Islamic tradition. The methodology behind minority *fiqh* will first be explained. Then, the three aforementioned issues will be examined, arguing in support of minority *fiqh* amidst its controversies raised by critics. Finally, the key points of the arguments will be summarized in the conclusion.

The Methodology of Minority Fiqh

One needs to understand Islamic jurisprudence before one can understand the methodology of minority *fiqh*. Commonly, the term '*shariah*' is associated with Islamic law; however, *shariah* (literally 'path to water') more accurately denotes Islam's overarching morals and ethics. In contrast, *fiqh* (literally 'understanding') pertains to the human interpretation of *shariah* into law, both in theory (*usul al-fiqh*) and in practice (f*uru al-fiqh*). The primary and divine sources of *fiqh* are the Quran and the *Sunnah*. The Quran refers to the holy text of Islam, believed to be the direct word of God, and *Sunnah* refers to the moral example and practical teachings of the Prophet Muhammad as known through *hadiths* (historical reports of the Prophet's sayings and actions).[2]

When these primary sources do not provide direct answers or require further interpretation, the secondary and human-derived process of *ijtihad* is employed. This involves qualified Islamic jurists using reason to find solutions to problems that are not immediately answered by common Islamic knowledge. It is worth highlighting that rulings based on *ijtihad* are not binding in the same way as those that are explicitly derived from the Quran and *Sunnah*. In other words, rulings that arise out of *ijtihad* do not carry an obligation or incur sin if followed or not. This is the case unless a ruling out of *ijtihad* gains universal and unanimous agreement[3] among all scholars, leading to *ijma* (juristic consensus), which makes the resulting ruling binding upon all Muslims. The opposite of *ijma* is ikhtilaf (juristic disagreement). Where there[4] is *ijtihad*, juristic disagreement naturally follows. These disagreements have led to the development of the four orthodox schools of Sunni *fiqh*: Hanafi, Maliki, Shafi, and Hanbali. It is important to note that, despite differences of opinion in *fiqh*, these four schools considered each other equally valid and jurists are not obliged to follow one school exclusively.[5]

In modern contexts, *ijtihad* is used for either legislation in Muslim countries, *fatwas* (personal advice on issues given by legal scholars), or academic writings. The application of [6] minority *fiqh* operates primarily through *fatwas*. In practice, minority *fiqh* has been institutionalized by organizations like the European Council for *Fatwa* and Research (ECFR) and the *Fiqh* Council of North America (FCNA), founded by al-Qradawi and al-Alwani respectively, which deliver *fatwas* on guiding Muslims in their respective non-Muslim lands. Minority *fiqh* still follows all of the aforementioned principles of Islamic jurisprudence, but a key difference between the methodology of minority *fiqh* and the methodology of traditional or conservative *fiqh* is that the *ijtihad* of minority *fiqh* assumes greater importance when considering these four sources of *ijtihad*: urf (cultural customs), *maslahah* (public interest), *taysir* (leniency), and *darura* (necessity). An example of a *fatwa* from the ECFR that utilizes *urf, maslahah, and taysir* [7] was a *fatwa* that allowed a European woman who converted to Islam to remain married to her non-Muslim husband. While this relationship would be considered unlawful in ordinary *fiqh*, this *fatwa* made an exception by taking European cultural norms into account, the broader public interest, and a lenient approach. That is, the relationship was permitted for the sake of keeping European women from being afraid of Islam as well as making Islam easier to practice for married women interested in the religion. Another example of a *fatwa* that utilized *taysir* as well[8] as *darura* comes from al-Qardawi in which he permitted the burial of a Muslim in a Christian cemetery if there was absolutely no way for the Muslim to be buried in a Muslim cemetery. In[9] this case, al-Qardawi made an exception by granting ease to Muslims who may have no choice in where they can bury Muslims in a non-Muslim area. As evident by these *fatwas*, jurists often use these sources of *ijtihad* interconnectedly. It is important to note that the practice of these four sources of *ijtihad* has always been accepted in Islamic law but their use has typically been limited to a mere last resort. However, the methodology of minority *fiqh* gives these sources higher importance and pushes for their further use.[10]

***The Issue of Emigrating Muslim Territory** (Dar al-Islam)*

Traditionally in Islamic political thought, the world was divided into three categories: *dar al-Islam* (Muslim nations), *dar al-ahd* (non-Muslim nations with treaties with Muslim lands), and *dar al-harb* (non-Muslim nations without such treaties). A historically prevailing view held that Muslims who found themselves in a non-Muslim nation (*dar al-harb*) would be obligated to move or migrate back to a Muslim nation (*dar al-Islam*). If one adheres to the[11] belief that it is unlawful for Muslims to reside outside Islamic territories, then this perspective would put the entire legitimacy of minority *fiqh* into question. As such, it is typical for both supporters and critics of minority *fiqh* to spend a great deal of deliberation on this issue. This section will first examine the scriptural debate on this issue, followed by a discussion on proponents against Muslims residing outside *dar al-Islam*, and then a discussion on proponents in support of allowing Muslims to reside outside *dar al-Islam*.

Those who argue that Muslims are obligated to leave non-Muslim nations often cite verse 4:97 from the Quran which states, "When the angels take the souls of those who were wronging themselves, [the angels] say, 'In what state were you?' They say, 'We were weak and oppressed in the land.' [The angels] will say, 'Was

not God's earth vast enough that you might have migrated therein?' These shall have their refuge in Hell—what an evil journey's end!"[12] However, it is also widely held by traditional interpreters of the Quran that this verse is specifically in reference to the early Meccan Muslims who did not migrate to Madinah with Muhammed and stayed loyal to the idolaters of Mecca, even fighting alongside the Meccan idolaters against the Muslims in the Battle of Badr. Further considering the fact that this verse can grammatically be read in the past tense in Arabic would also substantiate the argument that this verse can be read as a historical injunction and not just a universal injunction.[13] Additionally, many scholars will cite a *hadith* from *Sahih Bukhari*, which Muslims consider to be one of the most authentic and reliable of *hadith* compilations. The *hadith* reports that Prophet Muhammed has stated that "There is no more migration after the Conquest," and this has often been interpreted to mean that the obligation of migrating as described in 4:97 has been abrogated.[14] Some scholars such as al-Munawī (d. 1621) and al-San'ani (d. 827) have counter-argued that this abrogation is specific rather than general, applying only to the allowance for Muslims to return to Mecca, which had become a part of *dar al-Islam*. However, this perspective is undermined[15] when considering the words of Lady Aisha, the wife of Muhammad. On this very subject, she explained, "But as for today, Allah has made Islam manifest and today the servant worships his Lord wherever he wishes."[16]

Scholars examining the history of this issue frequently note that the Malikis have been the most staunchly opposed to Muslims residing in non-Muslim lands. Imam Malik (d. 795) himself, the eponym of the Maliki school, was not fond of the idea of Muslims subjecting themselves to non-Islamic law. As the Maliki Muslims faced increasing territorial losses to the Christian[17] Reconquista, their views on this matter grew stricter over time. This trend reached its zenith with the Maliki jurist, Ahmad al-Wansharisi (d. 1508), who represented the most extreme of these views. Following the fall of Islamic Spain to the Christians, al-Wansharisi demanded all Muslims leave the Christian territory immediately and any Muslim who refused to do so was effectively a heretic. The anger expressed in Al-Wansharisi's *fatwas* towards Muslims, and his even greater animosity towards Christians, whom he deemed dishonorable, reflects the bitter relations between the Iberian and North African Muslims and Christians of that era. However, it is important to recognize the great diversity that has always been present within Maliki jurisprudence. For instance, Ali al-'Adawi al-Sa'idi (d.1775) viewed Muslims residing in non-Muslim lands as sinful but not heretical. Conversely, Ibn 'Abd al-Barr (d. 1071) allowed Muslims to stay in non-Muslim lands, albeit only if their stay was temporary. While opinions[18] among Maliki jurists varied in their strictness, a general trend in the history of *fiqh* has been their disapproval of Muslims living outside *dar al-Islam*. It is worth noting that this trend for Malikis has declined. This is especially evident with the contemporary Maliki jurist, Abdullah Bin Bayyah, whose supportive views on minority *fiqh* will be elaborated on later in this section.

In the modern period, it seems that most criticisms against Muslims living in non-Muslim countries come from conservative Salafis. Salafism refers to a puritanical movement that arose in the 19th/20th century which sought to return Islam to the practices of the earliest Muslims. Shaykh al-Albani (d. 1999), a prominent figure in the Salafi movement, criticized Muslims living in non-Muslim countries, arguing that they are either ignorant of *fiqh* rulings or are unwilling to forsake the material luxuries offered by the West. Similarly, another current Salafi[19] scholar, Abu Khadeeja, has expressed criticism of Muslims residing in the West. He contends that Muslims will never be fully accepted by Westerners, as evidenced by criticism against Islam from both liberals and conservatives alike. He also highlights the prevalence of sins such as illicit sex, drugs, and violence in Western societies which make it a harmful environment for Muslims to inhabit.[20]

However, these views face several counterarguments. First, it appears that al-Albani himself was ironically the one who has ignored *fiqh* rulings. Numerous esteemed jurists in the Islamic tradition have maintained that migration from non-Muslim lands is not obligatory, a point elaborated upon in the following paragraphs. Second, the assumption that Muslim countries are free from materialism, sexual immorality, drugs, and violence is simply untrue. All of these things considered sin in the West can be found in Saudi Arabia, Pakistan, Qatar, and so forth.

Lastly, while it is true that Islam faces criticism from both Western liberals and conservatives, the concept of minority *fiqh* addresses this challenge. It aims to bridge the gap in knowledge for Muslims in minority settings so that they may be better integrated and accepted in Western societies. Muslims cannot expect to isolate themselves indefinitely, rather they need to understand how to coexist and contribute positively in diverse environments. Many contemporary and traditional experts on *fiqh* have given compelling arguments for alternative conceptions of *dar al-Islam* which favor permitting Muslims to reside in non-Muslim nations. Al-Alwani, the pioneer of minority *fiqh* and founder of the *Fiqh* Council of North America, argues that *dar al-Islam* can be any nation in which a single Muslim can freely and fully practice their religion, which would include most Western countries due to their religious freedom laws. He would define *dar al-harb* as any nation where Muslims cannot safely practice their religion, regardless of whether or not Muslims make up the majority population. This[21] view is by no means an innovation as many of the most historically renowned jurists of the Shafi and Hanbali schools, such as Imam an-Nawawi (d. 1277), Ibn Hajar (d. 1449), Ibn Qudamah (d.1223), and Ibn Taymmiyah (d. 1328), did not oblige Muslims to migrate to *dar al-Islam* from a non-Muslim land so as long they were able to practice their religion freely. Al-Alwani also uses[22] the renowned traditional exegesis of Fakr al-Din al-Razi (d. 925) to offer another territorial division. This view divides the world into *dar al-Islam* and *dar al-dawah* (land of invitation). In other words, rather than thinking of the world as consisting of those who are Muslim and those who are not, Muslims can instead think of the world as those who are already Muslim and those who can be invited to Islam. This distinction would alleviate the obligation of a Muslim to live in a Muslim nation since they have the responsibility to invite others to Islam and universalize the religion. A leading Shafi jurist shared this sentiment on Muslims spreading dawah, Shams[23] al-Din al-Ramli (d. 1597), who went as far as to forbid the Aragon Muslims from leaving the Christian Kingdom as he argued that their presence was the only thing that might allow Islam to spread there.[24]

Contemporary European scholars such as Tariq Ramadan, Abdullah Bin Bayyah, and al-Qaradawi have also shared similar views to al-Alwani. Tariq Ramadan employs the term *dar al-shahadah* (land of the testimony of faith) which is similar to al-Alwani's definition of *dar al-Islam* in that it encompasses any land in which a Muslim can adhere to his or her faith. Although, Ramadan takes it a step further than al-Alwani in that he argues that virtually the entire world would fall under *dar al-shahada*. Abdullah Bin Bayyah believes that there is absolutely no reason to adhere to these concepts at all as they are not grounded in scripture or scholarly consensus, but nonetheless offers the idea that Muslims in the West are in *dar al-aman* (land of trust) as these countries offer Muslims security, religious freedom, and the right to spread Islam. In a similar manner, al-Qaradawi gives the argument that even if Muslims were to[25] adhere to the traditional conception of *dar al-Islam*, *dar al-harb*, and *dar al-ahd*, the vast majority of nations would fall under *dar al-ahd* anyway in which Muslims are not obliged to emigrate from. Qaradawi's view is corroborated by tradition as well since the Hanafi school of[26] law considered *dar al-ahd* to merely be another part of *dar al-Islam*, meaning they too held that Muslims were permitted to live as minorities in non-Muslim nations. All of these views,[27] traditional and contemporary, substantiate the argument that Muslims being obliged to only live in Muslim countries was never a unanimous ruling. The notion that it is permissible for Muslims to reside in non-Muslim countries is not new and has only become more vital for Muslims in this globalized world.

The Issue of Dual Allegiance

Minority *fiqh* has been criticized for opening up the issue of dual allegiance for Muslims, namely their allegiance to the laws of Islam and the laws of their host nation. As contemporary jurist, Khalid Abou el Fadl, posits the issue, "To what extent are Muslims residing in non-Muslim territory bound by Islamic law, and how does that affect their obligations to their country of residence?" Although jurists have articulated different ways in which Muslims can abide[28] by both legal systems, the crux of this issue arises when the two systems are at odds with each other. As al-Alwanani summarizes, those who argue against Muslim involvement in Western politics do so on the basis that Muslims are allied with individuals who oppose Muslim interests and promote the acceptance of a political status quo that devalues the religion. This[29] dis-

course also manifests through the controversy of allowing Muslims to serve in non-Muslim militaries. This section will first go over the extent to which Muslim minorities must be loyal to[30] Islam, then it will hold a discussion in support of Muslim minorities being politically active in their host nation, and lastly, it will give a discussion on Muslim minorities in military service.

Virtually all Islamic jurists agree that Muslims are bound not only to each other through their sacred bond of brotherhood but also to divine *shariah* law. Even though this assertion is unanimously agreed upon, its ambiguity lends itself to be open to further interpretation as to what extent Muslims have responsibilities to each other and to what extent *shariah* law is applicable outside Muslim nations. For example, despite their disapproval of Muslim minorities being in non-Muslim countries, the Maliki is still argued that Muslim minorities had legal rights to protection by surrounding Muslim states. Likewise, Shafi and Hanbali jurists argued that Muslim states have responsibilities towards non-Muslim states if there is a Muslim population present in that state. These responsibilities included protecting the property rights of Muslims as well as prosecutorial duties since they held that Muslims who committed crimes were liable in *shariah* courts, no matter their location. The Hanafis were unique in that they held that legal protection and proceedings are based on territory, not religion, and therefore *shariah* courts have no jurisdiction over non-Muslim lands.[31]

It would be helpful for this discussion to examine the distinction between the legal and moral aspects of *shariah*. Bin Bayyah explains that the pillars of Islam are universally binding but the rules of governance (*ahkam al-sultaniyyah*) are not. He argues through social contract philosophy that Muslim immigrants, no different than someone natively born in a secular nation, have a duty to abide by the laws of that nation in exchange for the security and benefits of that nation. Bin Bayyah compares this approach to Islam to the approach of Prophet Muhammed when he first migrated to Mecca, making no claims to governmental authority and abiding by the law of the land while maintaining his own faith. Relatedly, Dr. Mohammed Hashim Kamali[32] explains that *shariah* can be broadly divided into two categories: *muamalat* and *ibadat*. These refer to interpersonal civil obligations and religious obligations respectively. The matters of *muamalat* (which included things like the exchange of goods, matrimonial law, and civil litigation) were under the jurisdiction of the government, whereas matters of *ibadat* (which included things like prayer, fasting, and alms-givings) were still obligatory upon Muslims but outside governmental jurisdiction.[33] For minority *fiqh*, it seems best to follow the Hanafi school's line of reasoning which would argue that Muslims are not necessarily bound to all of the legal aspects of *shariah* depending on their location. Muslims in secular nations ought to focus on using *fiqh* for maintaining their essential Muslim identity rather than applying governmental *fiqh* which would not only be unnecessary but would go against the public interests of Muslims by causing social disruption.

As Muslims have no obligation to turn Western countries into *shariah* states, proponents of minority *fiqh* maintain that Muslims can (and should) be active in their host nation's politics. While critics may argue that it is like treason for a Muslim to participate in the politics of non-Muslims, other scholars have argued that it is not only permissible but also within the spirit of Islam to do so. In regards to the issue of Muslims voting in a non-Muslim state, The ECFR outlines three points. First, the ECFR divides loyalty for Muslims into two parts: loyalty to the tenets of faith in Islam and loyalty to worldly matters, where social contracts with non-Muslims are permissible. Secondly, the ECFR cites several examples of Prophet Muhammad politically aiding non-Muslims, such as defending Mecca in the Fujjar conflict and aiding oppressed Meccans (regardless of their religion) through the Fudul alliance. And thirdly, the ECFR references Muhammed's Constitution of Madinah which established a religiously pluralistic society. From this, the ECFR not only permits Muslims to be politically active but actually encourages them to enjoin in the development of their wider society. Bin Bayyah is in agreement that Muslims exerting political influence in a positive[34] way would be beneficial for everyone, Muslims and non-Muslims alike. Islamic ethics and values are meant to be universal, not exclusive. As Ramadan stipulates, Islamic morals may originate from scriptural sources, but they can be translated into secular values. This is not to undermine Islam as a religion but rather to better share good morals in

a secular state which is still very much in the spirit of Islam. Indeed, Islam's messages of love, justice, and altruism are values that everyone favors and Muslims should strive to implement these values into their society. A similar view is held by a prominent jurist of the 14th century, Ibn Qayyim[35] al-Jawziyya, who argued that even if something is not specifically from Islamic law but is used to deliver the path of justice, it should still be followed by Muslims because, in actuality, the essence of *shariah* and the path of justice are inseparable.[36]

Perhaps the most pressing topic within this issue is the topic of military service. Especially since America's war on terror, a great number of Muslims have questioned if military service for non-Muslim nations is truly acceptable if it means being involved in the killing of other Muslims. According to Kahlid Abou el Fadl, traditional Hanafi jurists held that Muslim minorities are to "maintain a rule of strict neutrality, even in situations where the host state is engaged in war with a Muslim state. Muslims may, however, join in the defense of their host state if it is attacked by another non-Muslim country." Hyder Gulam, the honorary solicitor for[37] the Australian National Imam Council (ANIC), also argued that it should be permissible for Muslims to serve in non-Muslim militaries because within the Prophet Muhammed's lifetime, Muslims fought under the Christian Ethiopian king in exchange for the king's protection. But beyond[38] neutrality or fighting non-Muslims, the question would still remain of whether it is acceptable for Muslims to actively participate in a war against their fellow Muslims. This concern has reached far beyond American Muslims as Luke Wessel, an Islamic scholar and Australian Infantry officer, notes that the low Muslim participation in Australia's defense force can have long-term negative effects. Wessel urges Australian Muslim leaders to address this concern if they do not wish for the reputation of Australian Muslims to be jeopardized. Indeed,[39] while it may be easy for a Muslim jurist to forbid fighting one's own brothers, this prohibition may only lead to more harm for Muslims by making Western powers question the loyalty of their Muslim populace. This has already been a huge issue in America due to the Patriot Act, which has wrongfully detained roughly 1,200 individuals who were suspected to be terrorists. It was precisely[40] because of this fear of greater harm that al-Qaradawi permitted American Muslims to fight against Afghanistan in a controversial *fatwa* in 2001. Although, in 2003, al-Qaradawi issued another *fatwa* encouraging American Muslim soldiers to request leave or temporary exemption. However, if they are still forced to fight their fellow Muslims then an effort should be made to minimize direct confrontation as much as possible. Critics of this *fatwa*, like the conservative[41] Salafi scholar Salah al-Sawi, have attacked this *fatwa* on the grounds that it is a wrongful justification for the attack on Afghanis. However, as Dr. Basheer Nafi explains, these criticisms fail to understand the nuances and purposes behind this *fatwa*. Al-Qardawi's *fatwa* was not an edict in support of U.S. foreign policy or a condemnation. Rather, al-Qaradawi issued this *fatwa* as a way of giving aid to the needs of Muslims struggling to figure out how to normalize their lives in a difficult situation.[42] Whether a Muslim individual should or should not serve in a non-Muslim military will need to be judged on a case-by-case basis, but at the very least, it should not be declared to be forbidden so as to prevent greater harm to Muslims in Western nations.

The Issue of Innovating the Tradition

Beyond just examining minority *fiqh* in theory, the applied practice of minority *fiqh* has garnered serious criticism, especially through the charge that this legal doctrine has made way for *bid'ah* (an innovation or alteration in the religion). For example, the traditionalist scholar Said Ramadan Al-Bouti condemns minority *fiqh* based on his worldview that Islamic law should remain constant regardless of socio-political circumstances. He criticizes al-Alwani and the ECFR for using *ijtihad* to satisfy personal desires by permitting what is traditionally forbidden. While it is undeniable that *bid'ah* is a grave sin in Islamic law, scholars have[43] always debated as to what exactly constitutes something to be *bid'ah*. Many scholars hold the opinion that *bid'ah* can exist as either praiseworthy *bid'ah* or blameworthy *bid'ah*. Imam al-Shafi (d. 820), the eponym of the Shafi school, explained that any new practice that is in opposition to the Quran and *Sunnah* is a blameworthy *bid'ah*, and any new practice in line with the Quran and *Sunnah* is a praiseworthy *bid'ah*. However, some Muslim jurists hold very[44] conservative views on *bid'ah*. Some jurists even went as far as to forbid television, photography, and kitchen utensils, merely on the grounds that these things were not utilized

by the Prophet Muhammed and the earliest generation of Muslims. Though as Dr. Mohammed Hashim Kamali explains, these extreme conservative views from 19th and 20th-century jurists are the product of Muslims coping with Western cultural and territorial colonialism.[45] Nevertheless, these conservative criticisms still persist and they have since latched onto the doctrine of minority *fiqh*. One of the most common manifestations of said conservative criticisms has been through the controversy of proponents of minority *fiqh* issuing *fatwas* which permit interest-based mortgages. This section will give a brief overview of the topic of permitting interest-based mortgages and will then explain why minority *fiqh* cannot be considered an innovation of any sort.

In traditional Islamic law, any form of interest was strictly prohibited and was considered a grave sin. However, since Muslims have been subject to non-Muslim economies, in which the use of interest is nearly inescapable, many—especially those struggling to buy homes without an interest-based loan—have sought guidance on this matter. Australia's Darulfatwa Islamic High Council ruled that it is unlawful for Australian Muslims to take out a loan to buy a house on the grounds that usury is traditionally forbidden in Islam. This ruling gained a lot of attention and left many Australian Muslims unsatisfied, especially since this ruling did not elaborate past a literalist reading of scripture and offered no other alternatives for Australians struggling to buy a home. Similar strict positions have been shared by other Islamic institutions such as the[46] Academy of Muslim World League, the Second Conference of Islamic Banks, and the Organization Islamic Conference. Much more favorable towards Muslim minorities, The European Council for *Fatwa* and Research (ECFR) and the Sharîʿa Scholars Association of North America (SSANA) ruled that if there are no alternatives available then it is permissible to take an interest-based loan for a mortgage on the grounds that housing is a necessity (*darura*). This view is corroborated by Imam Abu Hanifa (d. 767), the eponym of the Hanafi school, who stated that "Muslims are not responsible for changing economic and political rules in non-Muslim countries, and their subsequent economic vulnerability which contradicts the objectives of Sharîʿa." Additionally, *fiqh* commentator Adil Salahi reinforces this ruling by[47] mentioning that the ownership of property is considered one of the essential values of Islamic law (alongside life, religion, intellect, and family). Lastly, al-Alwani argues that minority *fiqh* is[48] not utilizing *darura* simply to change the ruling on interest, but rather it should be understood that the traditional understanding of interest in Islam is not applicable to the way interest is used in Western economies. Al-Alwani argues that interest as it is used in the West is used as a justified countermeasure for inflation in an economy in which the value of money is constantly changing, and not the exploitation of a borrower as forbidden by Islam.[49]

Indeed, this allowance for Muslims to pay interest is a radical departure from the traditional norm. However, to use a departure from the norm to constitute *bid'ah* would be a failure to have a holistic understanding of Islamic law and ethics. Islamic law has always been susceptible to flexibility and change. Al-Alwani supports this notion by citing the *hadith* in which the Prophet Muhammed said, "I used to forbid you from visiting graves, but now visit them; and I used to forbid you to keep sacrificial meet for more than three days, but now keep whatever you see fit; and I used to forbid you to drink nabīdh except from waterskins, but now drink it from all kinds of vessels, but do not drink any intoxicant." He goes on to explain that since the Prophet's time, *fatwas* have always been based on the surrounding circumstances and needs of Muslims. For al-Alwani, minority *fiqh* is not a means to permit what is ordinarily unlawful simply for the sake of it, but rather to continue to implement *fiqh* in such a way that applies to the current circumstances of Muslims, just as it always has been done. The[50] contemporary jurist Muhammad al-Mukhtar al-Shinqiti directly states that minority *fiqh* is not a *bid'ah*. He mentions that the earliest books of jurisprudence have addressed these same issues of Muslims living as minorities in non-Muslim lands. The only thing innovative about minority *fiqh* is its name but "there is nothing wrong in changing terms."[51]

Al-Alwani also defends minority *fiqh* by citing the Quranic injunctions which call for Muslims to be representative of the best nation for mankind. Any sort of humiliation or negative social clash with others would go against this Quranic principle. Minority *fiqh* is a means to[52] uphold this Quranic principle, taking advantage of the flexibility of *fiqh* for the sake of the greater good of

Muslims. Al-Alwani believes that minority *fiqh* serves to make Islam more accessible to the wider world and gives Muslims the power to interact with non-Muslims so that Islam can further spread. Recall that Imam al-Shafi considered innovations in line with the[53] Quran and *Sunnah* to be a good *bid'ah*. Support for minority *fiqh* would be well in the interests of all Muslims worldwide.

CONCLUSION

Minority *fiqh* is a legal doctrine that utilizes the flexible nature of *fiqh* to give guidance to Muslims in non-Muslim environments. While this branch of *fiqh* gained traction only within the last couple of decades, the idea of utilizing *fiqh* to address the needs of Muslims in unique situations has been a concept for over a thousand years. The modern application of minority *fiqh* has been mostly through *fatwas* given by al-Alwani and al-Qaradawi, as well as their respective councils: the ECFR and the FCNA. Their approach to *fiqh* is characterized by their elevated considerations of cultural customs (*urf*), public interest (*maslahah*), leniency (*taysir*), and necessity (*darura*). Utilizing these sources of *ijtihad* to a greater extent allows jurists to give much more dynamic and practical solutions to the concerns of Muslim minorities. Yet, this approach has not been exempt from criticism, mostly from more conservative-minded Muslims. The three most contentious debates surrounding minority *fiqh* are on the issues of emigrating from Muslim territory, dual allegiance, and innovating the tradition.

The issue of emigration was addressed by proving two key points: firstly, there is a lack of scriptural basis for the argument that it is unlawful for Muslims to reside outside *dar al-Islam*; secondly, a great number of jurists throughout history have held that Muslims are permitted to reside in any nation so as long as they can adhere to their faith there. Indeed, it is not the land that makes a Muslim but their deeds. The issue of dual allegiance was addressed by explaining that Islamic scholars make a distinction between obligations in religious affairs and obligations in civil affairs, in which the latter falls under the social contracts of the governments which they reside under. Political participation for Muslims, even for non-Muslim governments, ought to be encouraged since it gives an opportunity for Muslims to spread altruism and justice. As for military service, while it may not be morally encouraged, it still ought to be made legally permissible on the grounds that forbidding Muslims from serving in the military could cause much greater harm to Muslims by putting their loyalty into question. Lastly, the accusations of minority *fiqh* being an innovation as well as the controversy of permitting usury were addressed by explaining that *fiqh* has always been flexible based on surrounding circumstances. The adaptation of *fiqh* to meet the necessities of contemporary Muslims, as seen in the case of interest-based mortgages, is in line with the spirit of Islam, which takes into account the realistic conditions and circumstances of its followers. Not only has minority *fiqh* always existed in the conceptual sense, but currently it stands to aid Islam by giving it a much wider positive image and practice which is encouraged by the Quran and therefore cannot be considered a blameworthy *bid'ah*.

As it has been demonstrated, the arguments on viewing minority *fiqh* as anything less than a legitimate and needed branch of *fiqh* are inconclusive. It is imperative that this legal doctrine be accepted if the *fiqh* tradition is to survive in this rapidly changing world. Minority *fiqh* allows Muslims to adapt to a pluralistic and globalized world while still respecting the core principles of Islam. Minority *fiqh* stands as a testament to the dynamism of Islamic jurisprudence, ensuring that Muslims can adhere to their faith regardless of their time and place.

REFERENCES

[1] Fishman Shammai Hudson Institute and Center on Islamic Democracy and the Future of the Muslim World. 2006. Fiqh Al-Aqalliyyat : A Legal Theory for Muslim Minorities. Washington DC: Hudson Institute. 3

[2] Kamali, Mohammad H. 2008. Shari'ah Law: An Introduction (Foundations of Islam). N.p.: Oneworld Publications. 41

[3] Ibid 42.

[4] Ibid 101.

[5] Ibid 68.

[6] Ibid 171.

[7] Fishman, "Fiqh Al-Aqalliyyat," 8.

[8] Ibid 12.

[9] Ibid 10.

[10] Ibid 9.

[11] Ibid 4-5.

[12] Nasr, Seyyed Hossein, Caner K. Dagli, Maria Massi Dakake, Joseph E.B. Lumbard, and Mohammed Rustom, eds. The Study Quran. New York: HarperOne, 2015, 237-238.

[13] Ibid 238.

[14] al-'Awayishah, Husayn. 2006. A Conclusive Study on the Issue of Hijrah. N.p.: Al-Ibaanah Book Publishing. 82.

[15] Ibid 86-88.

[16] Ibid 83.

[17] Khaled Abou El Fadl. "Legal Debates on Muslim Minorities: Between Rejection and Accommodation." The Journal of Religious Ethics 22, no. 1 (1994): 133-134.

[18] Ibid 137-138.

[19] bin Abdul-Aziz Al ash-Sheikh, Saleh. 2022. Clarifying the Obligation of Migration From the Lands of Disbelief To the Lands of Islām. N.p.: Kalamullah. 42.

[20] Abdul, Abu K. 2021. "A question about Hijrah from the Non-Muslim Countries to the Lands of Islam And the reality of life in the West for Muslims once you remove the rose-tinted glasses...." Abu Khadeejah. https://abukhadeejah.com/question-about-hijrah-from-the-non-muslim-lands-to-the-lands-of-islam/

[21] Hellyer, H. A.2009. Muslims of Europe: The 'other' Europeans. N.p.: Edinburgh University Press. 86.

[22] al-'Awayishah, "the Issue of Hijrah." 78.

[23] Fishman, "Fiqh Al-Aqalliyyat," 4-5

[24] Khaled Abou El Fadl. "Legal Debates on Muslim Minorities: Between Rejection and Accommodation." The Journal of Religious Ethics 22, no. 1 (1994): 141.

[25] Hellyer, Muslims of Europe, 86.

[26] Fishman, "Fiqh Al-Aqalliyyat," 7.

[27] Shaybānī, Muhammad ibn a. 1966. The Islamic Law of Nations: Shaybānī's Siyar. Edited by Majid Khadduri. Translated by Majid Khadduri. Johns Hopkins Press. 12.

[28] Fadl, "Legal Debates" 146.

[29] Verskin, Alan. 2013. Oppressed in the Land? Fatwas on Muslims Living Under Non-Muslim Rule from the Middle Ages to the Present. Markus Wiener Publishers. 139-143.

[30] Fishman, "Fiqh Al-Aqalliyyat," 13-14.

[31] Fadl, "Legal Debates," 143-145.

[32] Hellyer, Muslims of Europe, 88.

[33] Kamali, Shari'ah Law, 17.

[34] Hellyer, Muslims of Europe, 91.

[35] Ibid 91-93.

[36] Kamali, Shari'ah Law, 31-32.

[37] Fadl, "Legal Debates," 149-150.

[38] Whyte, Shaheen. 2017. "Whither Minority Jurisprudence? The Case Of Fiqh Al-Aqalliyat In Australia." Australian Journal of Islamic Studies 2, no. 3 (October): 64.

[39] Ibid 65.

[40] Guttentag, Lucas. "Immigrants' Rights in the Aftermath of 9/11: Detention, Discrimination and Secrecy." In Defense of the Alien 25 (2002): 5.

[41] Whyte, "Whither Minority Jurisprudence," 64.

[42] Nafi, Basheer M. "Fatwā and War: On the Allegiance of the American Muslim Soldiers in the Aftermath of September 11." Islamic Law and Society 11, no. 1 (2004): 114.

[43] Verskin, Oppressed in the Land, 145.

[44] Goldziher, Ignac. 1971. Muslim Studies. Translated by Barber R. C. and Stern M. S. Vol. 2. N.p.: State University of New York Press Albany, 36–37.

[45] Kamali, Mohammad Hashim. "Issues in the Understanding of Jihād and Ijtihād." Islamic Studies 41, no. 4 (2002): 626.

[46] Whyte, "Whither Minority Jurisprudence," 63.

[47] Taha, Dina M.. Muslim minorities in the west: between fiqh of minorities and integration. 2012. American University in Cairo, Master's Thesis. AUC Knowledge Fountain. 45.

[48] Whyte, "Whither Minority Jurisprudence," 63.

[49] Taha, "Muslim minorities in the west," 47-48.

[50] Yakar, Emine Enise; Yakar, Sumeyra, "The Critical Analysis of Taha Jabir al-Alwani's Concept of Fiqh al-Aqalliyyāt", Hitit İlahiyat Dergisi, (Haziran/ June 2021) 20/1: 387.

[51] Tauseef Ahmad Parray (2012): "The Legal Methodology of 'Fiqh al-Aqalliyyat' and its Critics: An Analytical Study." Journal of Muslim Minority Affairs, 32:1, 102.

[52] Yakar; Yakar, "The Critical Analysis," 396.

[53] Fishman, "Fiqh Al-Aqalliyyat," 13-14.

Abdul, Abu K. 2021. "A question about Hijrah from the Non-Muslim Countries to the Lands of Islam —And the reality of life in the West for Muslims once you remove the rose-tinted glasses...." Abu Khadeejah. https://abukhadeejah.com/question-about-hijrah-from-the-non-muslim-lands-to-the-lands-of-islam/.

al-'Awayishah, Husayn. 2006. A Conclusive Study on the Issue of Hijrah. N.p.: Al-Ibaanah Book Publishing.

bin Abdul-Aziz Al ash-Sheikh, Saleh. 2022. Clarifying the Obligation of Migration From the Lands of Disbelief To the Lands of Islām. N.p.: Kalamullah.

Goldziher, Ignac. 1971. Muslim Studies. Translated by Barber R. C. and Stern M. S. Vol. 2. N.p.: State University of New York Press Albany.

Guttentag, Lucas. "Immigrants' Rights in the Aftermath of 9/11: Detention, Discrimination and Secrecy." In Defense of the Alien 25 (2002): 3–11.

Hellyer, H. A. 2009. Muslims of Europe: The 'other' Europeans. N.p.: Edinburgh University Press.

Kamali, Mohammad Hashim. "Issues in the Understanding of Jihād and Ijtihād." Islamic Studies 41, no. 4 (2002): 617–34.

Kamali, Mohammad H. 2008. Shari'ah Law: An Introduction (Foundations of Islam). N.p.: Oneworld Publications.

Khaled Abou El Fadl. "Legal Debates on Muslim Minorities: Between Rejection and Accommodation." The Journal of Religious Ethics 22, no. 1 (1994): 127–62.

Nafi, Basheer M. "Fatwā and War: On the Allegiance of the American Muslim Soldiers in the Aftermath of September 11." Islamic Law and Society 11, no. 1 (2004): 78–116.

Nasr, Seyyed H., Caner K. Dagli, Maria M. Dakake, Joseph E. Lumbard, and Mohammed Rustom, eds. 2015. The Study Quran: A New Translation and Commentary. N.p.: HarperCollins.

Shaybānī, Muhammad ibn a. 1966. The Islamic Law of Nations: Shaybānī's Siyar. Edited by Majid Khadduri. Translated by Majid Khadduri. N.p.: Johns Hopkins Press. Taha, Dina M.. Muslim minorities in the west: between fiqh of minorities and integration. 2012.American University in Cairo, Master's Thesis. AUC Knowledge Fountain.

Tauseef Ahmad Parray (2012): "The Legal Methodology of 'Fiqh al-Aqalliyyat' and its Critics: An Analytical Study." Journal of Muslim Minority Affairs, 32:1, 88-107.

Verskin, Alan. 2013. Oppressed in the Land? Fatwas on Muslims Living Under Non-Muslim Rule from the Middle Ages to the Present. N.p.: Markus Wiener Publishers.

Whyte, Shaheen. 2017. "Whither Minority Jurisprudence? The Case Of Fiqh Al-Aqalliyat In Australia." Australian Journal of Islamic Studies 2, no. 3 (October): 55-75. 10.55831/ajis.v2i3.59.

Yakar, Emine Enise; Yakar, Sumeyra, "The Critical Analysis of Taha Jabir al-Alwani's Concept of Fiqh al-Aqalliyyāt", Hitit İlahiyat Dergisi, (Haziran/ June 2021) 20/1: 377-404

An Investigation Of Fungal Species In A Heavy Metal Contaminated Urban Waterway

Kathy D. Nguyen
The University of Texas at Austin

ABSTRACT

Biosorption is a low cost and environmentally friendly form of bioremediation. It has been found to be effective for removing heavy metals from both soil and water. This study focused on the fungal biosorption of specific heavy metals (Cd, Cr, Cu, As, Pb, and Zn) that are common environmental pollutants, as a means to bioremediate pollutants that can be consequences of rapid urbanization and industrialization. Fungal species were collected from contaminated sites along Waller Creek and their ability to biosorb heavy metals was investigated using ICPMS. Results found that *Penicillium spp.* from Waller Creek site CS was able to best biosorb Zn (110 µg Zn/g fungal dry mass), while also performing well with Cr and Pb (4.6 and 4.0 µg/g, respectively) and having detectable levels of As and Cd (0.3 and 0.2 µg/g, respectively). Ag and Cu were only detected in single replicates, so they are not reliable data points. Further investigation for other fungal species might be able to provide a deeper understanding on how different fungal characteristics like hyphae type, sporulation, and growth environment affect their heavy metals bioremediation process. Additional replications with varying concentration of heavy metals standard or performing more repeated runs on the ICPMS are suggested to reduce uncertainties in the data.

INTRODUCTION

Urban Ecosystems

Urbanization, although a sign of development and growth, can also bring forth many environmental and health implications. Not only can it fuel socioeconomic inequalities,[1] urbanization can also transform the landscape in a number of ways by introducing more impervious surface cover, altering both the natural stream habitat and the hydrology and geomorphology of urban greenspaces.[2] Aside from impervious surface cover, other consequences include an increased discharge of waste and pollutants from urban activities, which also contribute to environment degradation.[3]

The resulting runoff, more specifically through either sewage or industrial, domestic, hazardous, municipal, medical, or manufacturing waste,[4] can lead to an increased loading of nutrients, metals, pesticides, and other contaminants to urban waterways.[2]

Over time, these different forms of pollution can therefore develop into a decline in the richness of algal, invertebrate, and fish communities' health.[2] Since the health of these communities are vital factors within stream health and the ecosystem as a whole, urbanization ultimately can be seen as the cause of this chain of events.

Waller Creek, located in central Travis County, is a fully urbanized creek whose entire length runs through the city of Austin, including the eastern side of the UT Austin campus. Due to its positioning which cuts through the inner city, an academic medical center, a large stadium, and more, Waller Creek has been subjected to many changes throughout its history, including but not limited to having its route modified through forceful removal of trees and building of impervious covers and sidewalks to make room for new infrastructures and expansion of the

UT Austin campus. Despite active restoration efforts, this urban watershed still encounters severe flooding, sewer leakage, and elevated levels of various pollutants, which are essential to both aquatic and human health and should be addressed.

Heavy Metals Pollution

Heavy metals are well known environmental pollutants due to their toxicity, persistence, and bioaccumulative nature, and can often be found along water sources or soil.[5] Prior research has found that heavy metal pollutants most common in the environment include Cr, Mn, Ni, Cu, Zn, Cd, and Pb.[6] Because heavy metals are so persistent in the environment, they can contaminate the food chains and cause different health problems to humans as well as fishes, invertebrates, and other organisms within urban waterways. Additionally, it has been found that chronic exposure to heavy metals in the environment poses a serious threat to living organisms.[5] Aside from effects on humans, in regards to plants and green spaces, heavy metals above a certain threshold can also affect the microbiological balance of soils and reduce their fertility,[5] therefore can directly influence the quality of trees and their abilities to conduct photosynthesis and normal respiration.

Several locations along Waller Creek on the UT Austin campus have been found to have elevated levels of some heavy metals, which is cause for concern about possible effects on students and individuals residing near these creek sites. More specifically, when this project was being planned in Spring of 2022, elevated Pb levels had been observed. Since then, although the Pb has reduced to normal levels, the Heavy Metals team within the Urban Ecosystems research stream has found elevated levels of Cd and Ag at their four regular campus sampling sites in their most recent samples collected in March and April of 2023, which suggests an upward trend that should be monitored closely. The level of Cd detected has exceeded the Environmental Protection Agency (EPA) recommended criterion continuous concentration (CCC) threshold of 0.72 ppb, while the level of Ag is also close to exceeding the CCC threshold of 3.2 ppb.[7]
Therefore, active effort is needed to investigate ways to remediate this problem.

Fungi and Mycoremediation

In combating different forms of pollution, past researchers have investigated algae, bacteria, and plants bioremediation. The natural ecological relationships between algae and bacteria have been investigated in the removal and conservation of wastewater nutrients through creating a symbiotic system. Additionally, a genus of algae, *Chlorella spp.*, and bacteria, *Pseudomonas spp.*, have been found to be able to form a symbiosis that can bioremediate heavy metals.[9] In this research, fungal remediation of heavy metals is investigated, by determining which species of fungi present in Waller Creek may be capable of tolerating heavy metals.

Mycoremediation is a term used to describe the bioremediating effects performed by fungi. Because fungi produce a variety of metabolites while their sporulation characteristics allow for easy propagation and distribution, they are known to be good bioremediators.[10] They can modify their structure, appearance, and genetic makeup[11, 12] to allow for tolerance of pollutants like heavy metals. Fungi can remediate by retaining pollutants by either active bioaccumulation[13] or passive biosorption. Fungi can to perform biosorption efficiently because of their high surface area, due to the filamentous nature of their mycelium.[10] Biosorption is a physical process that is achieved through ion exchange, surface complexation, and precipitation, which includes passive uptakes of pollutants and can be present in both living and dead fungal cells.[14] More specifically, cells can bioaccumulate heavy metals pollutants until a certain point when the cells cannot handle the toxicity anymore and turn into dead biomass. This works in cells regardless of their living state, because toxicants are transported across the cell membrane into cells through the cell metabolic cycle and accumulate intracellularly until the level of pollutant exceeds a threshold where the organism's metabolism is interrupted, leading to cell death.[14] The biosorption process involves a solid phase biosorbent, the material doing the biosorption, and a liquid phase solvent containing heavy metal ions (sorbate) to be sorbed.[14] Because of the initial difference in concentration of heavy metals present inside and outside of the biosorbent, in this case the fungal cell, metal ions are driven to move along the concentration gradient into the cell until an equilibrium is reached, at which point the ions

become adsorbed onto the surface of the biomass. enriching the biosorbent with metals.[14] The mechanisms for this process are generally based on the physicochemical interactions between the metal sorbate and functional groups present on the cell surface, whereas the biosorbent properties of biomaterials are dependent upon the make-up of their cell walls.[14] The carboxylate, hydroxyl, amine, and phosphoryl functional groups present within the polysaccharides, lipids, and proteins that make up the cell wall interact with metal ions and result in electrostatic interactions, ion exchange, and metal-ion chelation or complexation.[14]

Biosorption includes both the adsorption and absorption of heavy metals by fungal species, where adsorption involves the adhesion of heavy metals onto the fungal hyphae and absorption involves the fungi actively soaking up the heavy metals found in its surrounding environment by mass transfers through the fungal chitin and cell wall. Previous studies exploring mycoremediation have determined adsorption, which involves the process of ion-exchange to allow for adhesion, as the primary bioremediation mechanism for fungi.[10] Because the binding process in biosorbent is independent of metabolism, this reaction is reversible and allows for the cell to desorb in order to be regenerated and reused to biosorb more heavy metals pollutants.[14]

Mycoremediation is especially valuable because of fungi's high metal sequestration ability. Chitin in the fungal cell walls consists of many functional groups capable of binding metal ions, although the specific ratios depend on the individual fungal species.[14] The additional strength introduced by the thick chitin wall also allows for the fungi to take up more pollutants while still retaining structure integrity. Finally, another advantage is that fungi can be easily grown on multiple different media (e.g., Potato Dextrose, Czapek Dox, Sabouraud Dextrose, Corn Meal agar, and more) and can be incubated at around room temperature with high yield rates and short growth times. Essential factors that can influence the effectiveness of fungal adsorption of heavy metals include pH, metal-ion to biomass ratio, cell-wall fraction, presence of ligands, and temperature variation.[10]

Many species of fungi have been found to be able to perform bioremediation of heavy metals extremely well, especially the *Aspergillus* genus, more specifically, *Aspergilllus piperis*, which has been proven to be capable of remediating Pb experimentally.[10] Additionally, *Aspergillus terreus, Trichoderma longibrachiatum, Aspergillus niger*, and *Aspergillus flavus* are successfully biosorbent of heavy metals within water,[15] while *Penicilium chrysosporium* is able to accumulate Cr and Ni.[16] *Aspergillus versicolor* was found to have the ability to bioaccumulate over 7 mg of cadmium per 1 g of mycelium, followed by 5.878, 5.243, and 5.075, 4.557 by *Paecilomyces sp., Aspergilus fumigatus, Microsporum sp.* and *Terichoderma sp.,* respectively.[13] Symbiotic systems of fungi and bacteria have also been investigated, which show an intricate feedback system between microbial metabolisms and metal mobility and therefore were able to create synergistic bacteria-fungal pairs that can be more tolerant to Cadmium pollution than either organism on their own.[12]

These various species of fungi create countless possibilities for the development of natural alternatives to combat heavy metals pollution within urban water sources instead of expensive chemical sterilization processes. The identification of fungal species present along heavy metals contaminated sites in urban waterways can contribute to the understanding of which genus of fungi are more likely to be able to tolerate a high amount of heavy metals. In understanding which species are more effective in remediating which types of heavy metals, methods to introduce these species into the environment through waterway systems can be designed.

Because of their natural characteristics and the fact that the fungi species used within this research were all taken from the local Waller Creek, the use of microorganisms like these in decontaminating the environment through biosorption can be considered a good option for bioremediation throughout the Austin's urban core.[16]

Hypothesis

Since many species of fungi have been previously found to be able to bioremediate heavy metals, it is hypothesized that species of fungal spores found at sites along Waller Creek where there is a high amount of heavy metals pollution should also be able to perform biosorption successfully.

METHODOLOGY

Experimental Approach Summary

Water samples from sites with a high amount of heavy metals contamination will be collected and filtered to collect fungal spores. Spores will be cultured on Potato Dextrose Agar (PDA) media, incubated in a dark environment at room temperature. After cultures have matured, the mycelium and spores will be observed under the microscope to perform species identification. Identified species will then be re-cultured on PDA to ensure they are individual species, and then cultured on heavy metals spiked PDA. Their spores would then be dried and ashed to remove biomass, leaving behind any biosorbed heavy metals. The resulting ashes will be dissolved in HNO3 and analyzed using ICPMS.

Sample Collection

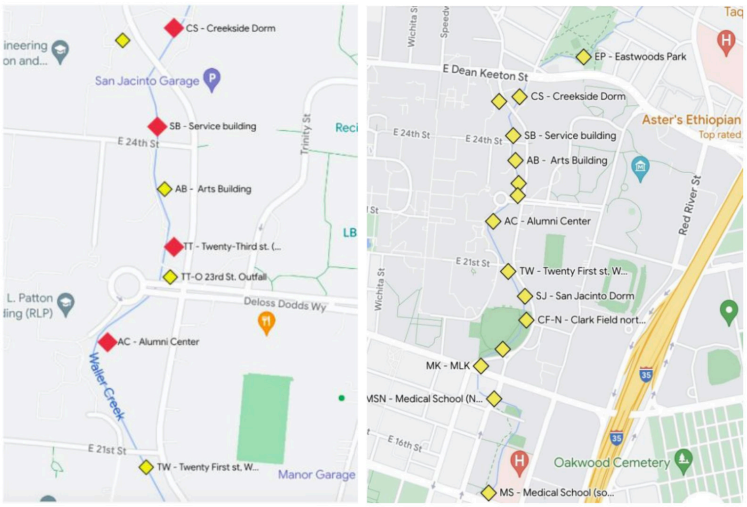


Figure 1: *Sampling sites on Waller Creek, with locations marked in red diamonds (left) and a more general map of the area (right).*

Samples were collected at four sites along Waller Creek: AC (Alumni Center), CS (Creekside Dorm), SB (Service Building), and TT (Twenty-Third St.) as shown in Figure 1. These four sites have been previously determined by the Heavy Metals research team within Urban Ecosystems FRI stream to have elevated concentrations of heavy metals pollution, especially Pb, during the spring of 2022.

Water sample collection was performed using 500 mL amber bottles rinsed with 10% (v/v) HCl acid. Each bottle was rinsed with sample water three times before a final sample was taken, by collecting a small amount of water upstream, then capping and shaking the bottle before disposing of the rinse downstream. Bottles were then submerged under water facing upstream against the direction of water flow for sample collection. The samples were collected near soil and tree roots on the creek bank where there is a steady and gentle flow of water to allow for more variation in fungal spores. The samples were stored in a refrigerator until filtration and spore elution.

Sample Processing and Separation of Spores

Sample processing and elution techniques involve protocols based on the work of Grabinska-Loniewska et al.[17] A solution of 0.28% pyrophosphate was prepared by dissolving 0.28 g solid sodium pyrophosphate in ~10 mL of DI water, before bringing it to a final volume of 100.00 mL with DI water. Each sample was filtered through a 0.22 µm Millipore paper membrane (Sigma Aldrich, 25mm in diameter) placed in a Buchner funnel connected to a vacuum manifold using a funnel adaptor. A plastic volumetric pipette with a pipette pump was used to transfer each sample onto the filter paper in 10 mL increments until liquid could no longer pass through the membrane, and the final amounts of water sample passed through the membrane was recorded. Each filter membrane, with retained biomass was transferred using a clean pair of tweezers washed with DI water and cleaned with 70% ethanol solution into a 0.28% sodium pyrophosphate solution. Each filter was submerged in either a 50 mL beaker containing 30 – 40 mL of 0.28% sodium pyrophosphate or a 15 mL plastic centrifuge tube containing 10 mL of 0.28% sodium pyrophosphate and placed on a shaker at 80 rpm for 30 – 90 minutes to elute fungal spores. After that, the sodium pyrophosphate bio-

mass suspension was disrupted in an ultrasound disintegrator UD 20 with vibration amplitude A=20 μm for 40 seconds. Each suspension was then transferred onto the surface of an agar plate to start the culturing process.

Media Preparation and Initial Culturing Process

Potato Dextrose Agar (PDA) media was prepared by dissolving 24 g of broth PDA powder (Difco) and 15 g agar powder into 1 L of DI water in a 1 L glass bottle. This bottle was then placed on a stirring plate with medium heat, and a magnetic stir bar was used to mix the media. Media bottles were autoclaved at 121°C for ~1 hour using the autoclave's liquid cycle. 1 mL of Chloramphenicol (25 mg/mL) was added per 1L of PDA media using a p1000 micropipette, either before or after autoclaving as Chloramphenicol is heat stable. PDA plates were made under a biohood and the work surface was sprayed with 70% ethanol for sterilization purposes. To make PDA agar plates, ~ 25 mL of autoclaved PDA media was transferred to each empty plastic petri dish (100 mm diameter, 15 mm thick) using a plastic volumetric pipette with a pump. After the media solidified, either 100 or 200 μL of biomass elution in 0.28% sodium pyrophosphate solution was transferred onto the center of each agar plate using a 200 μL micropipette and sterilized tips. Control plates with only PDA and Chloramphenicol were made to check sterilization of the culturing process and conditions. Finally, plates were wrapped with parafilm and labeled based on sample collection sites. These fungal cultures were incubated at room temperature in a dark environment within a desk drawer for 7 – 21 days, and growth was recorded every 1 to 4 days. Out of these cultures, fungal colonies which occupied a large surface area of each plate or have not been dried up yet were chosen to be re-cultured onto more agar plates for replicates.

Re-culturing and Transferring of Replicates

Because the initial fungal plates were cultured from a general biomass elution, these plates contained a variety of fungal colonies of different species and at times some bacterial contamination. When choosing fungal colonies for re-culturing to make replicates, only colonies that were larger than ~30 mm in diameter, and that allowed for an agar square to be cut out without including any bacterial colonies or contamination due to other fungal species' spores were chosen. The purpose of this elimination process is to result in pure fungi cultures with only one type of fungal species per petri dish. The re-culturing of fungi colonies was performed under the biohood with the work surface being sprayed with 70% ethanol for sterilization. A scalpel washed with DI water, then sprayed with 70% ethanol and dipped into a glass bead sterilizer at 265°C for 10 – 30 seconds was used to cut out 5 – 8 mm side length cubes of fungi cultures from agar plates. Agar squares were placed face-down on the center of fresh PDA plates, prepared as described previously, and then each plate was sealed with parafilm and incubated again for 1 – 3 weeks until fungi colonies filled the entire plate surface. Cultures were monitored every 1 – 4 days.

Identification of Fungi

Only replicates/ re-cultures showing pure fungi samples with one species per agar plate were used for species identification and heavy metals bioremediation analyses. Fungal species were identified both through physical properties like the overall shapes, colors, and textures of the mycelium and hyphae characteristics like branching, fruiting bodies, filaments, and whether they are septate or non-septate. Fungal identification keys, online fungal databases, and previous research articles containing fungal species were used to identify species.[17,18,19, 20, 21, 22, 23, 24, 25, 26, 27]

A scalpel was sterilized by first washing with DI water, then sprayed with ethanol and dipped into a glass bead sterilizer at 265°C for 10 – 30 seconds, and then used to pick up small amounts of fungal spores off the surface of agar plates to prepare glass microscope slides for identification purposes. Spores were transferred onto the center of each microscopic slide and covered with a plastic cover slip. Fungal spores were viewed under the microscope at 40× and 100× total magnifications. Pictures of each type of fungi species spores were taken by aligning a phone camera with either one of the eyepieces for documentation, and agar plates were wrapped again with parafilm for storage.

Heavy Metals Standard Dilutions in Media Cultures

When working with heavy metals, all glassware was rinsed with nitric acid to remove all trace metal ions that can bind to glass surfaces. To perform acid rinsing,

pipette tips were submerged in 50% (v/v) HNO_3 for 1 – 2 hours, then rinsed with DI water twice while finishing off with a final rinse of nanopure water, before drying for 24 hours. For the source of heavy metals, a 25-element environmental calibration stock solution in 5% (v/v) HNO_3 was used (IV-Stock-50, Inorganic Ventures). Of the 25 elements contained in this solution, this stock contains 10 µg/ mL concentration (10000 ppb) of each of the seven heavy metals of environmental pollution interest (Ag, As, Cd, Cr, Cu, Pb, and Zn). A calibration curve was made by diluting this heavy metals standard to different concentrations using volumetric pipettes. To make a series of heavy metal spiked PDA agar plates, a 50 ppb dilution was prepared by transferring 50 µL of the stock into a 10 mL volumetric flask, then filling to the line with 5% (v/v) HNO_3. PDA agar plates were prepared as described previously; however, Chloramphenicol was not added to these plates. Instead, after transferring exactly 25 mL of PDA onto new petri dishes, 1 mL of the 50 ppb heavy metal stock solution was added to the dish, then stirred into the PDA agar media using a sterilized scalpel before the media solidified. These heavy metal-spiked PDA plates were then used to re culture all the pure fungal species replicates.

Ashing Samples

When fungal colonies have covered the entire agar surface, plates were ready to be processed for ICPMS analysis. A small section of fungi was scraped off first for microscopic observation, while the rest of the fungi were scraped onto pre-combusted glass fiber filter paper with a sterilized scalpel. Because each agar plate was covered with a large number of fungal spores, three filter papers were needed to accommodate all of the fungi from a single plate. Each filter was placed inside a crucible and placed in a drying oven at 65˚C for 72 hours to evaporate all the water from the fungi. The initial mass of wet samples were recorded and measured again once every 24 hours. At the 72 hours mark, when the samples were completely dry, the dried fungal samples on filters were ashed by placing the filter-containing crucibles in a furnace at 500˚C for an hour to combust all organic matter, leaving only trace amounts of heavy metals behind. The ashed filters were reweighed and then submerged in 10 mL centrifuge tubes of 5% (v/v) trace metal grade HNO3. After samples were vortexed for a minute each, they were centrifuged at 2000 rpm for 6 minutes in 24˚C to pellet out the filters. Finally, the supernatant (8.5 mL) were transferred to new clean centrifuge tubes via a 10 mL glass syringe with a 0.2 µm nylon filter to remove particulates before being diluted 5× and 100× for the detection of As, Ag, Cd, Cr and Cu, Pb, Zn metals respectively. The nylon filters were changed after filtering materials from different agar plates to avoid cross contamination.

Inductively-Coupled Plasma Mass Spectrometry

The method of choice for detecting heavy metals is inductively-coupled plasma mass spectrometry (ICPMS), which is able to detect meals at very low concentrations. An inductively coupled plasma is used to ionize samples prior to performing mass analysis. The ICP uses Argon (Ar) gas, heated by an inductive coil to the point of forming a plasma.[28] A liquid sample introduced into this high-temperature plasma will be atomized into its constituent elements, and then ionized.[29] These ions will be extracted through the interface region and into electrostatic lenses, called ion optics,[30] which will guide the ions into the MS part of the analyzer. Mass spectrometry separates the ions by mass through its magnetic sector, using the mass-to-charge ratio of each element.[29]The ICPMS measures intensity values derived from the electrical signals of the detector, and so calibration curves need to be made using known concentrations of specific metals of interest, so that these intensities can be converted into concentrations in unknown samples.

Calibration curves for each metal were made by diluting the heavy metals standard from the original 10000 ppb into 0.05, 1, 5, 8, and 10 ppb. A calibration curve was graphed for each individual metal with the intensity values measured in relation to each known concentration, and the equations of the lines of best fit for each calibration curve could then be used to determine the concentration of metal in each fungal sample. When diluting samples, two replicates were performed to ensure accuracy. 5% trace metal grade HNO_3 was used as a blank for these runs, and contamination between samples were minimized not only by a 5% trace metal grade HNO_3 wash every 6 samples, but also by running the ICPMS from most diluted samples to least.

RESULTS

Fungal Growth and Variety

		AC	TT	SB	CS
Non-processed	1st trial (10/27)	0	2	0	1
	2nd trial (12/2)	3	2	4	5
Processed	1st trial (12/3)	3	5	4	6
	2nd trial (1/25)	4	2	1	5
	3rd trial (2/10)	5	4	6	2

Table 1: *Number of fungal species identified at four sample sites along Waller Creek known to have measurable heavy metals contamination.*

aspergillus spp.	*penicillium spp.*	others
aspergillus fumigatus	*penicillium commune*	*alternaria alternata*
aspergillus niger	*penicillium crustosum*	*cladosporium cladosporioides*
aspergillus sydowii	*penicillium expansum*	*paecilomyceas variotti*
Aspergillus flavus	*penicillium ruben*	*trichoderma spp.*

Table 2: *Fungal species identified from cultures of sites AC, TT, SB, CS.*

Table 1 shows a comparison of fungal richness – the number of different species of fungus identified, over the course of five different culturing batches, which involved slightly different sample processing and culturing techniques. Non-processed samples were cultured by spreading several dots of creek water sample evenly spaced across a petri dish and one in the center so that the total amount of sample used for culturing is 1 mL, while processed sample first trial involves spreading of only 200 µL across 3 dots in a straight line. Processed sample second and third trials involve only using 100 µL of sample and placing it directly in the center of the dish, as it has been discovered over previous trials that the amount of sample used did not affect fungal growth speed, while also making it harder to monitor the spread of spores. Table 2 shows a general listing of fungal species identified over these four heavy metals contaminated sites along Waller Creek.

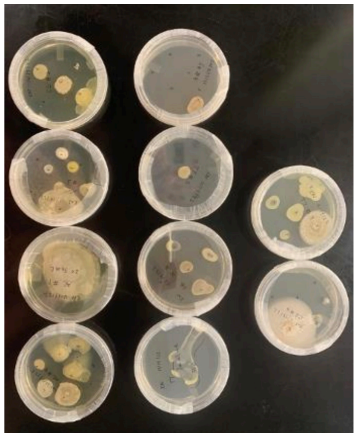


Figure 2: *Growth for unprocessed sample collected on 10/27/2022 and cultured on 11/14/2022*

Figure 2 shows the first batch of fungal cultures from unprocessed samples on PDA and Chloramphenicol, where it is evident that fungal spore growth was limited by multiple bacterial colonies.

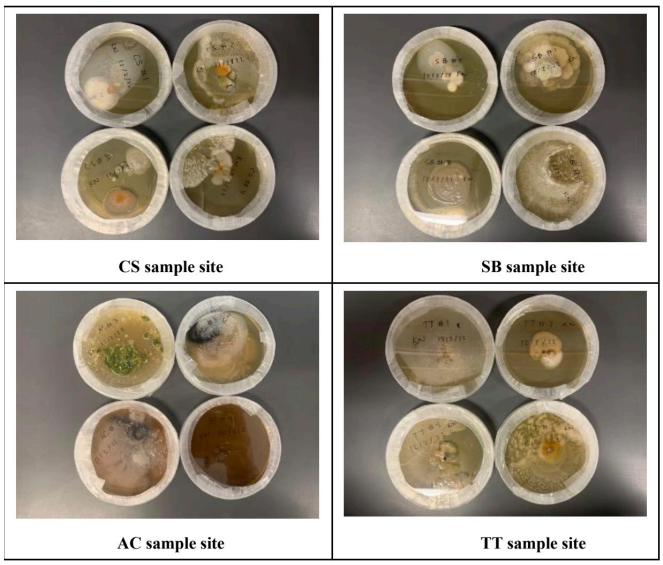


Figure 3: *Unprocessed sample collected on 12/1/2022 and cultured on 12/2/2022*

In Figure 3, the second batch of cultures from unprocessed samples were separated by sample sites, where it can be seen that orange and yellow jelly-like bacterial colonies sometimes are located right inside or on top of a fungal colony. Fungal colonies can be distinguished from bacterial colonies through their fuzzy or powdery nature, due to fungal spores. A dish with many bacterial cultures can interfere with fungal growth by either taking up

some of the growth area or limiting or decreasing fungal growth rate. This is especially clear in Figure 3 on the CS #4 plate located at the bottom right corner, where the natural circular spread of fungal spores was blocked by the presence of bacteria in the center of the plate, causing the white fuzzy spores to only exist on one half of the agar plate.

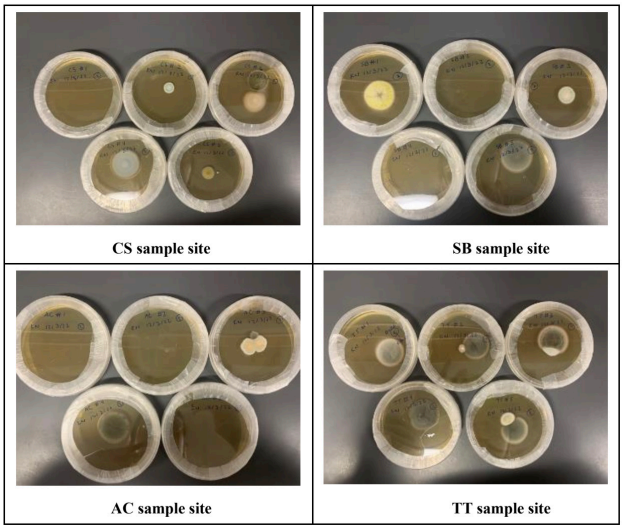


Figure 4: *Processed sample collected on 12/1/2022 and cultured on 12/3/2022, photographed on 12/12/2022*

It was observed that processed samples fared better than unprocessed samples in terms of fungal yield, variety of species, and reduced bacterial contamination. Processed samples were plated using cultures made from sodium pyrophosphate suspensions, as seen in Figure 4, which shows the first batch of samples processed on 12/3/2022, around ten days after culturing. In this third culturing trial, all four images representing four different sites exhibit clear and normal circular growth. We see variety in species of fungi present within the CS site and a consistent species was detected at the TT sampling site. Cultures from AC and SB sites also exhibit uncontaminated and proficient growth at the early stages.

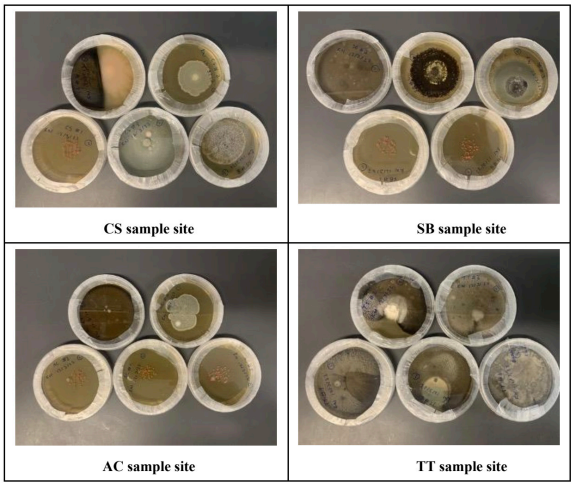


Figure 5: *Processed sample collected on 12/1/2022 and cultured on 12/3/2022, photographed on 1/9/2023*

Unfortunately, one of the main limitations of this study was the multiple periods during the fungi incubation process where culture conditions could not be monitored as frequently, which occurred over Thanksgiving, winter, and spring breaks. Due to this, the promising cultures seen in Figure 4 used up all the nutrients present within the media and either dried or died before they could be processed. The conditions of dried fungal colonies can be seen in Figure 5, where dried colonies were not able to retain their original colors and properties, and also made it more difficult to be examined under the microscope.

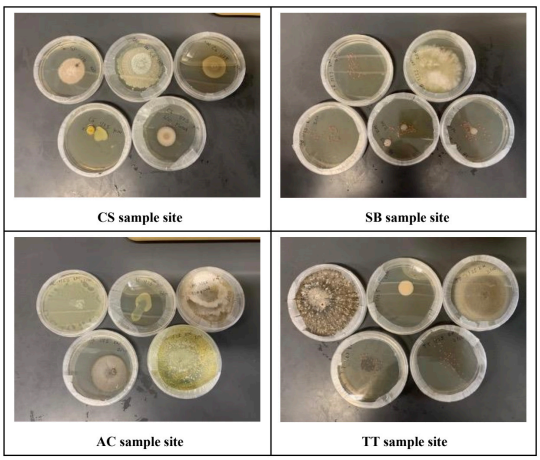


Figure 6: *Processed sample collected on 1/25/2023 and cultured on 2/10/2023, photographed on 3/1/2023*

For this reason, another batch of fungi cultured from processed samples collected on 1/25/2023 were

made on 2/10 (Figure 6). This fourth batch (Figure 6) of cultures experienced slightly less species variation than the previous batch seen through Figure 5, although the colonies that were able to grow stayed consistent between sites, as *Aspergillus spp.* was seen in AC site cultures, and *Penicillium spp.* was still seen in CS site cultures.

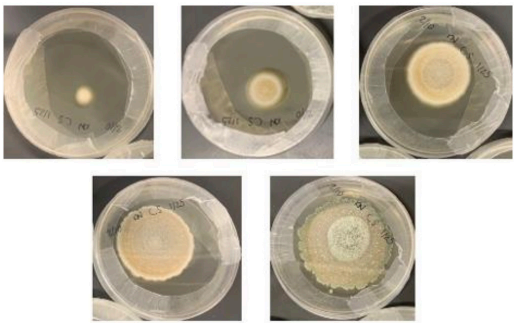


Figure 7: *Growth of Penicillium spp. started on 2/10, taken on 2/14, 2/16, 2/20, 2/23, 3/1, from left to right and top to bottom, respectively. A detailed view/growth rate monitor of fungal species identified from CS site from Figure 6, since this is the only species that survived the spiked metal PDA media. This figure, however, shows the natural growth of this species without any metals being introduced yet.*

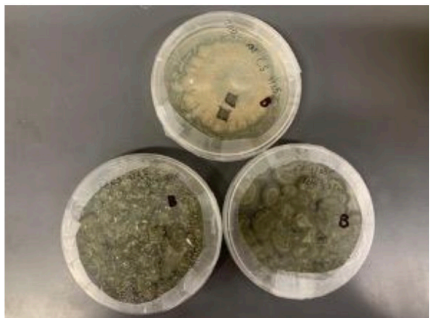


Figure 8: *Two replicates of Penicillium spp. from Figure 7 re-cultured in PDA without antibiotics and without spiked metals.*

One or two fungal species which exhibited the most persistent growth and were large enough (~ 3 cm in diameter) were selected from each site to be re-cultured for replicates. An example is Figure 7, a circular colony without bacterial contamination that fills a majority of the petri dish surface. Figure 8 is an example of re-culturing of the fungi shown in Figure 7, showing pictures of two replicates based on one species. After replicates have grown and covered the entirety of the agar surface, from those replicates, agar squares containing spores were re-cultured one more time, this time in PDA spiked with 50 ppb heavy metals standard in HNO_3.

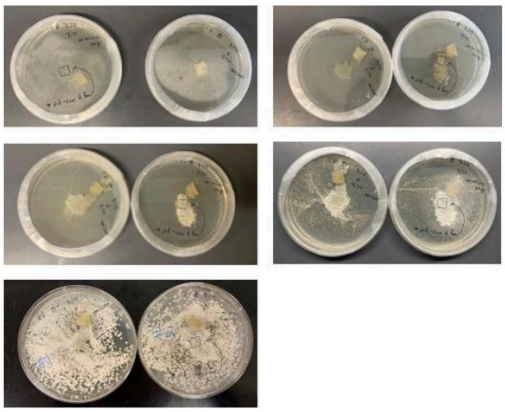


Figure 9: *Cultures of Penicillium spp. On heavy metals (50 ppb) spiked PDA from CC site, started on 4/10, taken on 4/11, 4/12, 4/13, 4/14, 4/17, from left to right and top to bottom, respectively*

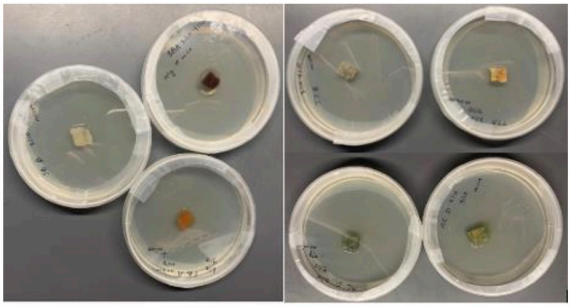


Figure 10: *Growth of fungi on heavy metals (50 ppb) spiked PDA from AC, SB, and TT sites started on 4/10 and taken a week after.*

Penicillium spp. from CS site was observed to grow well in media spiked with 50 ppb metals (Figure 9); however, other fungi colonies which belong to the three other sampling sites exhibited only some condensation but no growth on the heavy metal media (Figure 10).

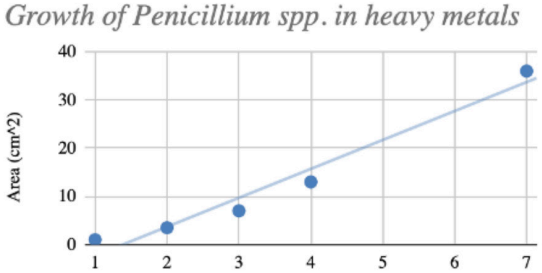


Figure 11: *Graph showing the estimated growth of Penicillium spp. from CS site in PDA spiked with 50 ppb heavy metals standard, made from the images in Figure 7*

The growth rate of the culture shown in Figure 7 is represented by surface area, and then plotted in Figure 11, where the total increase in surface area is graphed against time in days, showing a continuous and gradual growth rate.

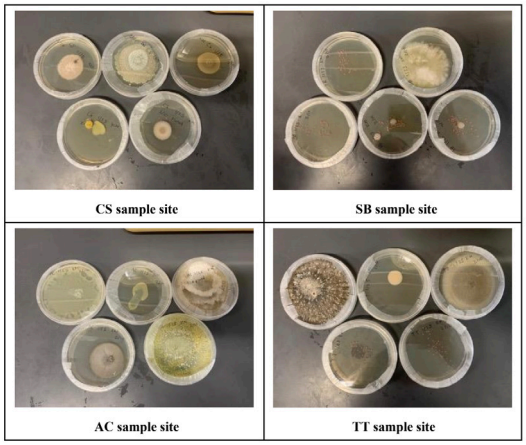


Figure 12: *Microscopic observations of Penicillium spp. from CS site on PDA with heavy metals cultures, showing an aerial hyphae connected by vegetative hyphae, followed by finger-like branching at the ends of aerial hyphae and chains of fungal spores called Conidia at the tip*

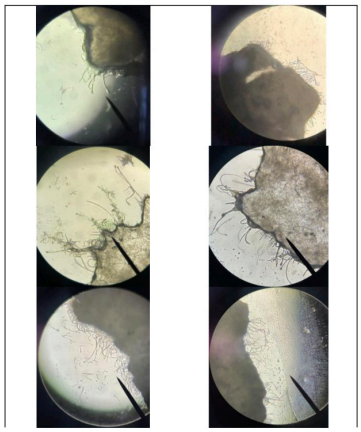


Figure 13: *Microscopic observations of Penicillium spp. from CS site on PDA with heavy metals cultures, showing an aerial hyphae connected by vegetative hyphae, followed by finger-like branching at the ends of aerial hyphae and chains of fungal spores called Conidia at the tip*

Figures 12 and 13 show microscopic observations of the *Penicillium spp.* fungus shown in Figure 7 – 9, which contain aerial hyphae connected by vegetative hyphae, followed by finger-like branching at the ends of aerial hyphae and chains of fungal spores called conidia at the tip. Due to colony characteristics like blue spores and clear round projections organized in a ring shape outside of the center, the species was determined to belong to Penicillium spp, which can be found in decaying matter or compost.



Figure 14: *Microscopic observations of Trichoderma spp, bright green colony (cannot be seen here but can be seen in Figures 6 and 10, with repetitively branched conidiophore structure)*

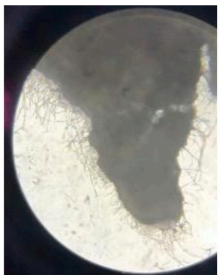


Figure 15: *Microscopic observations of Alternaria spp. known for their production of melanin, black in color, with elongated spores forming long chains)*

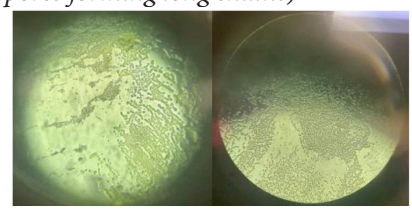


Figure 16: *Microscopic observations of Aspergillus spp. spore suspension (round conidia forming long chains, yellow-green colonies, large branches of conidiophores which cannot be seen here as this slide only consists of conidia shapes)*

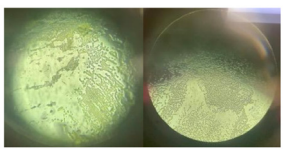


Figure 17: *Microscopic observations of Paecilomyces spp (septate hyphae, irregularly branched conidiophores, cylindrical phialides and conidia, colonies with wooly or powdery texture).*

Figures 14 – 17 show microscopic observations of

other fungal species *Trichoderma spp.* (bright green colony with repetitively branched conidiophore structure, can be found in plant roots or rotting wood), *Alternaria spp* (known for their production of melanin, with elongated spores forming long chains)., *Aspergillus spp.* (round conidia forming long chains, yellow-green colonies, large branches of conidiophores), *Paecilomyces spp.* (septate hyphae, irregularly branched conidiophores, cylindrical phialides and conidia, wooly or powdery texture) respectively, which did not successfully survive on the 50 ppb heavy metals-spiked PDA. As a trend that was observed, *Aspergillus spp.* was more common at the AC sampling site, while *Penicillium spp.* was more common at the CS sampling site. *Aspergillus fumigatus,* typically found in soil and organic matter, was common at all four sampling sites.

Ashing and ICPMS

Crucible #	Fungi Plate #	Filter weight (g)	Crucible weight (g)
9	1 (A)	0.074	14.1370
42	1 (A)	0.0725	15.4870
11	1 (A)	0.0725	15.1320
8	2 (B)	0.0725	15.0545
1	2 (B)	0.0725	14.5235
p (or d)	2 (B)	0.072	9.68

Table 3: *Initial crucible information*

The initial mass of each pre-combusted glass fiber filter and its sample can be found in Table 3. Because there were two cultures of *Penicillium spp.* grown on 50 ppb metals PDA, one petri dish was labeled as "1" or "A" and the second was labeled as "2" or "B".

Table 4: *Mass data during oven drying*

Crucible #	Fungi filter + Crucible (g)	Fungi + filter (g)	Fungi (g)	Fungi filter + Crucible (g)	Fungi + filter (g)	Fungi (g)
	Day 0, initial wet fungi data			Day 1 after 24 hours oven drying		
9	15.222	1.085	1.011	14.2875	0.1505	0.0765
42	17.121	1.634	1.5615	15.6485	0.1615	0.089
11	16.5015	1.3695	1.297	15.2770	0.145	0.0725
8	16.3730	1.3185	1.246	15.2015	0.147	0.0745
1	15.6575	1.134	1.0615	14.6720	0.1485	0.076
p (or d)	10.8465	1.1665	1.0945	9.8210	0.141	0.069
	Day 2 after 48 hours oven drying			Day 3 after 72 hours oven drying		
9	14.2855	0.1485	0.0745	14.286	0.149	0.075
42	15.6475	0.1605	0.088	15.6475	0.1605	0.088
11	15.275	0.143	0.0705	15.2750	0.143	0.0705
8	15.201	0.1465	0.074	15.201	0.1465	0.074
1	14.671	0.1475	0.075	14.671	0.1475	0.075
p (or d)	9.8195	0.1395	0.0675	9.821	0.141	0.069

Table 4 shows the mass of each filter after having been dried in the oven to remove any excess water for 0, 24, 48, and 72 hours respectively. It was observed that Days 2 and 3 showed little to no change in mass of each filter, meaning the filters only took around 48 hours to dry off completely instead of the expected 72 hours. This is not surprising as our protocol is typically used for algae, which is much more moist than fungus.

Crucible #	Combusted filter + Crucible (g)	AshMetal + filter (g)	AshMetal weight (g)
9	14.212	0.075	0.001
42	15.563	0.076	0.0035
11	15.206	0.074	0.0015
8	15.1285	0.074	0.0015
1	14.5975	0.074	0.0015
p (or d)	9.7545	0.0745	0.0025

Table 5: *Weight retained in each crucible and filter after ashing*

Table 5 shows the mass of combusted filters and metal after being in the 500˚C furnace for an hour. Because dry fungal spores were scraped directly onto filters, not all of them were able to stay adhered to the filter surface during the combustion process, leading to the crucibles being stained black with metal at the bottom. 5% trace metal grade HNO_3 was poured into each crucible, and a spatula had to be used to scrape off these metal stains to perform dilutions.

	Cr	Cu-63	Zn-66	As-75	Ag-107	Cd-111	Pb-208
Concentration (ppb)	Intensity						
0.05	46313.0	2063265.2	1445989.3	8075.8	64227.1	8356.9	1615792.0
1	105265.0	2997544.3	1513701.3	84309.3	707928.0	115573.7	3294933.3
5	373926.0	4105870.5	1991781.3	420704.0	3826197.3	588298.7	9465599.8
8	561058.0	4868198.0	2084736.0	661570.7	5867992.3	944120.3	13703030.7
10	680883.1	5584391	2189653.3	820138.7	7245940.7	1176731.7	16675369.2

Table 6: *ICPMS measurements of intensity for calibration curve dilutions*

Table 6 shows the data obtained from the ICPMS runs for the calibration curve dilutions.

Silver (Ag) Detection

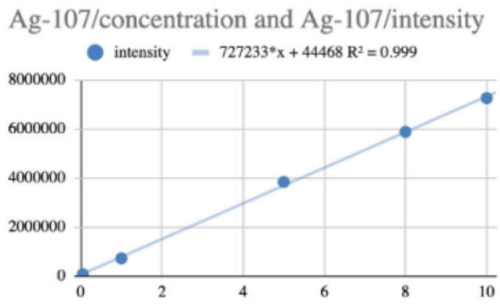


Figure 18: *Silver calibration curve*

Petri dish	Crucible	Replicate	Dilution	Intensity	Conc. (ppb)	Actual conc. (ppb)	Average conc. (ppb)	Metal/fungus (ng/g)
A	9	1	5×	42795.7	-0.00229954	-0.0114977	Below detection limit	ND (Not detected)
A	9	2	5×	42205.9	-0.00311056	-0.0155528		
A	42	1	5×	47805.6	0.00458945	0.0229473	0.0294431	3.346
A	42	2	5×	49695.2	0.00718779	0.0359390		
A	11	1	5×	44279.6	-0.000259064	-0.00129532	Below detection limit	ND
A	11	2	5×	42073.3	-0.00329289	-0.0164645		
B	8	1	5×	36951.4	-0.0103359	-0.0516794	Below detection limit	ND
B	8	2	5×	36909.2	-0.0103939	-0.0519696		
B	1	1	5×	35699.2	-0.0120578	-0.0602888	Below detection limit	ND
B	1	2	5×	35633.6	-0.0121480	-0.0607398		
B	P	1	5×	37050.8	-0.0101992	-0.0509960	Below detection limit	ND
B	P	2	5×	37919.2	-0.00900509	-0.0450255		

Table 7: *Silver concentration, where "Conc." is the amount of Ag detected in each filter sample after taking into account the 5× dilution factors, "Actual conc." corrects for the concentration of Ag before dilution factors, "Average conc." averages each pair of replicates, and Metal/Fungus corrects for the mass of dried fungus on that filter so that values can be directly compared between samples.*

The calibration curve used for Ag detection is shown in Figure 18, represented by the equation Intensity = 727233x[Ag] + 44468. This curve had an R^2 value of 0.999. The equation of the line of best fit to the calibration curve can be used to convert the ICPMS Ag signal from each sample into a concentration in ppb of Ag (Table 7). After correcting for the dilution of each sample, the two diluted replicates for each filter were averaged. The ash from each filter was dissolved in 10 mL nitric acid before being divided into two replicates, and we can use this volume to convert the average [Ag] ppm into the mass of silver found on each filter. This can be divided by the dry mass of fungus that had been ashed on that filter to calculate the mass of Silver per mass of dry fungal mass. Five of the six samples were below the limit of detection of Silver, and the sixth sample detected showed 3.346 ng Ag per gram of dried fungus.

Arsenic (As) Detection

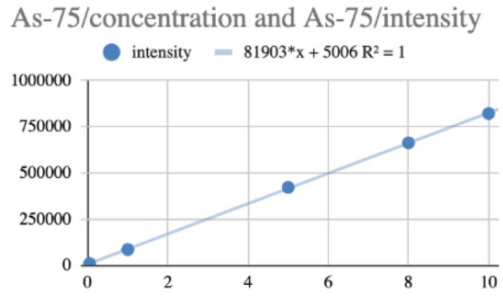


Figure 19: *Arsenic calibration curve*

Petri dish	Crucible	Replicate	Dilution	Intensity	Conc. (ppb)	Actual conc. (ppb)	Dry Fungal mass (g)	Metal/fungus (ng/g)
A	9	1	5×	42880.0	0.462425	2.31213	0.075	308.28
A	9	2	5×	43086.7	0.464949	2.32474	0.075	309.97
A	42	1	5×	50949.8	0.560954	2.80477	0.088	318.72
A	42	2	5×	50824.7	0.559426	2.79713	0.088	317.86
A	11	1	5×	44315.4	0.479951	2.39975	0.0705	340.39
A	11	2	5×	42889.6	0.462542	2.31271	0.0705	328.04
B	8	1	5×	38067.0	0.403660	2.01830	0.074	272.74
B	8	2	5×	37728.0	0.399521	1.99761	0.074	269.95
B	1	1	5×	27838.6	0.278776	1.39388	0.075	185.85
B	1	2	5×	42880.0	0.283352	1.41676	0.075	188.90
B	P	1	5×	43086.7	0.464608	2.32304	0.069	336.67
B	P	2	5×	50949.8	0.495381	2.47691	0.069	358.97

Table 8: *Arsenic concentration, where Conc. is the amount of As detected in each filter sample after 5× dilution, Actual conc. corrects for the dilution factor, Dry Fungal mass is the amount of dry fungus sample in each crucible, and Metal/Fungus uses the mass of dried fungus on that filter so that values can be directly compared between samples.*

The calibration curve used for As detection is shown in Figure 19, represented by the equation Intensity = 81903[As] + 5006. This curve had an R^2 value of 0.9998. The calculations described for the silver data were repeated with the Arsenic data (Table 8). No data can be Q dropped as outliers. Once dry fungal mass has been used to convert to ng/g, results from both plates were compared by a t-test to confirm that there is no statistically significant difference between the replicates from each plate, meaning all data can be combined and using standard error for the uncertainty (=standard deviation /√n, where n=12 replicates), we report detection of 290 ± 20 ng Arsenic per gram of dried fungus, which indicates that the fungi was able to biosorb Arsenic.

Cadmium (Cd) Detection

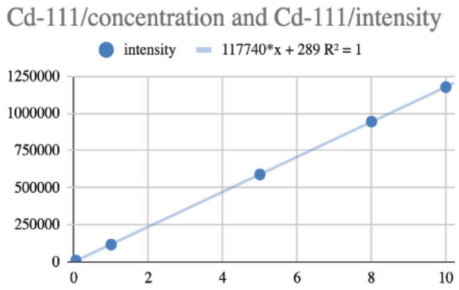


Figure 20: *Cadmium calibration curve*

Petri dish	Crucible	Replicate	Dilution	Intensity	Conc. (ppb)	Actual conc. (ppb)	Dry Fungal mass (g)	Metal/fungus (ng/g)
A	9	1	5×	49806.9	0.420570	2.10285	0.075	280.38
A	9	2	5×	49421.1	0.417293	2.08647	0.075	278.20
A	42	1	5×	50463.7	0.426148	2.13074	0.088	242.13
A	42	2	5×	49421.5	0.417297	2.08648	0.088	237.10
A	11	1	5×	38396.4	0.323657	1.61829	0.0705	229.54
A	11	2	5×	38086.6	0.321026	1.60513	0.0705	227.68
B	8	1	5×	40706.3	0.343276	1.71638	0.074	231.94
B	8	2	5×	41291.0	0.348242	1.74121	0.074	235.30
B	1	1	5×	38011.9	0.320392	1.60196	0.075	213.59
B	1	2	5×	38013.1	0.320402	1.60201	0.075	213.60
B	P	1	5×	44781.5	0.377888	1.88944	0.069	273.83
B	P	2	5×	47214.1	0.398548	1.99274	0.069	288.80

Table 9: *Cadmium concentration, where Conc. is the amount of Cd detected in each filter sample after 5× dilution, Actual conc. corrects for the dilution factor, Dry Fungal mass is the amount of fungus sample in each crucible, and Metal/Fungus uses the mass of dried fungus on that filter so that values can be directly compared between samples.*

The calibration curve used for Cd detection is shown in Figure 20, represented by the equation Intensity = 117740[Cd] + 289. This curve had an R^2 value of 0.99998. Repeating the previous calculations with the Cadmium data (Table 9). No data can be Q-dropped as outliers. We detected 246 ± 8 ng Cadmium per gram of dried fungus which means that the fungi's ability to biosorb Cd is similar to that of As.

Chromium (Cr) Detection

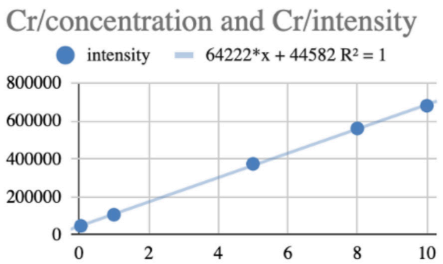


Figure 21: *Chromium calibration curve*

Petri dish	Crucible	Replicate	Dilution	Intensity	Conc. (ppb)	Actual conc. (ppb)	Dry Fungal mass (g)	Metal/fungus (ng/g)
A	9	1	5×	504397	7.15978	35.7989	0.075	4773
A	9	2	5×	512470	7.28549	36.4275	0.075	4857
A	42	1	5×	683371	9.94657	49.7329	0.088	5651
A	42	2	5×	709552	10.3542	51.7712	0.088	5883
A	11	1	5×	323786	4.34748	21.7374	0.0705	3083
A	11	2	5×	305101	4.05654	20.2827	0.0705	2877
B	8	1	5×	499091	7.07715	35.3858	0.074	4782
B	8	2	5×	502162	7.12497	35.6248	0.074	4814
B	1	1	5×	471787	6.65201	33.2600	0.075	4435
B	1	2	5×	475871	6.71559	33.5780	0.075	4477
B	P	1	5×	450032	6.31325	31.5663	0.069	4575
B	P	2	5×	505986	7.18452	35.9226	0.069	5206

Table 10: *Chromium concentration, where Conc. is the amount of Cr detected in each filter sample after 5× dilution, Actual conc. corrects for the dilution factor, Dry Fungal mass is the amount of fungus sample in each crucible, and Metal/Fungus uses the mass of dried fungus on that filter so that values can be directly compared between samples.*

The calibration curve used for Cr detection is shown in Figure 21, represented by the equation Intensity = 64222[Cr] + 44582. This curve had an R^2 value of 0.9996. Repeating the previous calculations with the Chromium data (Table 10). No data can be Q-dropped as outliers. We detected 4.6 ± 0.3 µg/g of chromium. This species of fungi has shown over an order of magnitude higher biosorption of Cr as compared to other metals measured so far.

Copper (Cu) Detection

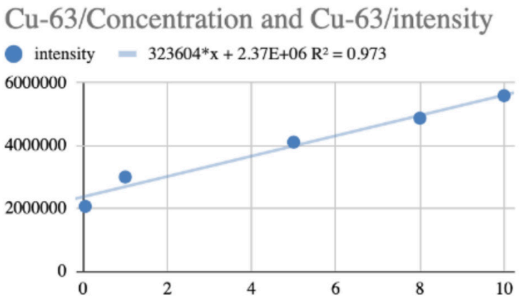


Figure 22: *Copper calibration curve*

Petri dish	Crucible	Replicate	Dilution	Intensity	Conc. (ppb)	Actual conc. (ppb)	Dry Fungal mass (g)	Metal/fungus (ng/g)
A	9	1	100×	2167250	-0.62654	-62.6537	0.075	ND
A	9	2	100×	1377840	-3.06597	-306.597	0.075	ND
A	42	1	100×	1366360	-3.10143	-310.143	0.088	ND
A	42	2	100×	1361590	-3.11620	-311.620	0.088	ND
A	11	1	100×	2040750	-1.01745	-101.745	0.0705	ND
A	11	2	100×	1842700	-1.62947	-162.947	0.0705	ND
B	8	1	100×	1906060	-1.43365	-143.365	0.074	ND
B	8	2	100×	1256140	-3.44206	-344.206	0.074	ND
B	1	1	100×	437269000	1343.92	134392.5	0.075	Q-dropped
B	1	2	100×	2216260	-0.47508	-47.5076	0.075	ND
B	P	1	100×	4016480	5.08795	508.795	0.069	73738.473738.4
B	P	2	100×	1524660	-2.61228	-261.228	0.069	ND

Table 11: *Copper concentration, where Conc. is the amount of Cu detected in each filter sample after 100× dilution, Actual conc. corrects for the dilution factor, Dry Fungal mass. corrects for the amount of fungus sample in each crucible, and Metal/Fungus uses the mass of dried fungus on that filter so that values can be directly compared between samples.*

The calibration curve used for Cu detection is shown in Figure 22, represented by the equation Intensity = 323604[Cu] + 2.37*106. This curve had an R^2 value of 0.973. Repeating the previous calculations with the Copper data (Table 11). The majority of readings below the limits of detection. Only one replicate each of filters B1 and BP saw copper signal, one of which was abnormally high in intensity (B1-1). The B1-1 data point can be Q-dropped with over 95% confidence. We will see that all B1-1 filter samples that underwent 100× dilution have abnormally high readings, which leads us to suspect that there might have been human error during the making of this particular dilution replication. That leaves a single Cu reading of 74 µg/g. Given that all other samples were nondetects, it is hard to put much faith in this reading. However, since fungi were scraped onto each filter by moving towards the center of the petri dish gradually from the outer edges, this detection might have been from fungal spores in a specific area of the plate, leading to the question of which part of a fungal culture can biosorb more metal ions.

Lead (Pb) Detection

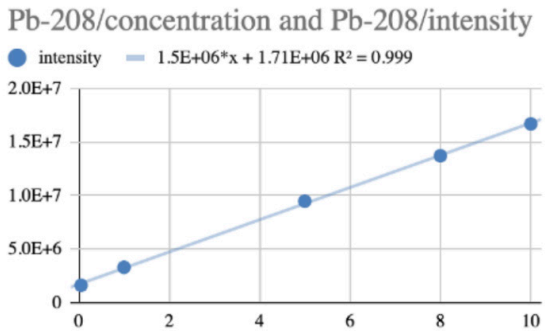


Figure 23: *Lead calibration curve*

Petri dish	Crucible	Replicate	Dilution	Intensity	Conc. (ppb)	Actual conc. (ppb)	Dry Fungal mass (g)	Metal/fungus (ng/g)
A	9	1	100×	1569950	-0.093364	-9.33639	0.075	ND
A	9	2	100×	1501970	-0.138684	-13.8685	0.075	ND
A	42	1	100×	2159600	0.299730	29.9730	0.088	3406.02
A	42	2	100×	2155250	0.296834	29.6834	0.088	3373.11
A	11	1	100×	2398950	0.459297	45.9297	0.0705	6514.86
A	11	2	100×	1991550	0.187697	18.7697	0.0705	2662.37
B	8	1	100×	1567170	-0.095223	-9.52227	0.074	ND
B	8	2	100×	1586180	-0.082549	-8.25493	0.074	ND
B	1	1	100×	54906400	35.4642	3546.42	0.075	Q-dropped
B	1	2	100×	1001460	-0.472357	-47.2357	0.075	ND
B	P	1	100×	1118130	-0.394582	-39.4582	0.069	ND
B	P	2	100×	1119590	-0.393604	-39.3604	0.069	ND

Table 12: *Lead concentration, where Conc. is the amount of Pb detected in each filter sample after 100× dilution, Actual conc corrects for the dilution factor, Dry Fungal mass corrects for the amount of fungus sample in each crucible, and Metal/Fungus uses the mass of dried fungus on a filter so that values can be directly compared between samples.*

The calibration curve used for Pb detection is shown in Figure 23, represented by the equation Intensity = 1.5*106[Pb] + 1.71*106. This curve had an R^2 value of 0.9994. Repeating the previous calculations with the Lead data (Table 12). The majority of readings were below the limits of detection. The B1-1 (100× dilution) data point discussed previously can be Q-dropped with over 95% confidence. That leaves four Pb readings, all from Petri dish A, that yield a detection of 4.0 ± 0.9 µg/g of lead. It is not clear why there was no lead detectable in any of the Petri dish B samples. The ability of this fungus in bioremediating Pb still has to be investigated more due to these uncertainties, but it seems that this fungus has similar high biosorption properties for Pb and Cr.

Zinc (Zn) Detection

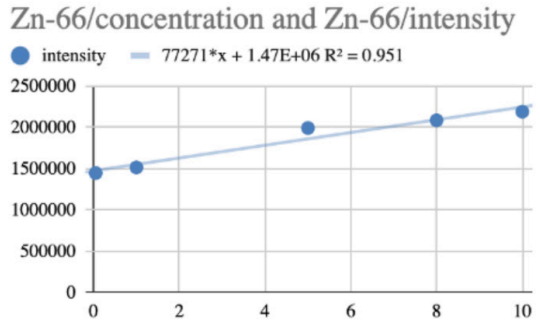


Figure 24: *Zinc calibration curve*

Petri dish	Crucible	Replicate	Dilution	Intensity	Conc. (ppb)	Actual conc. (ppb)	Average conc. (ppb)	Metal/fungus (ng/g)
A	9	1	100×	1943650	6.12970	612.970	688.724	91829.9
A	9	2	100×	2060720	7.64478	764.478		
A	42	1	100×	1999350	6.85063	685.063	737.098	83761.1
A	42	2	100×	2079770	7.89133	789.133		
A	11	1	100×	3520110	26.5314	2653.14	1964.61	278668
A	11	2	100×	2456040	12.7608	1276.08		
B	8	1	100×	1976580	6.55591	655.591	675.589	91295.9
B	8	2	100×	2007490	6.95588	695.588		
B	1	1	100×	45191700	565.824	56582.4	28533.9	3804520
B	1	2	100×	1845140	4.85488	485.488		
B	P	1	100×	1572360	1.32472	132.472	271.664	39371.6
B	P	2	100×	1787470	4.10855	410.855		

Table 13: *Zinc concentration, where Conc. is the amount of Zn detected in each filter sample after 100× dilution, Actual conc. corrects for the dilution factor, Dry Fungal mass corrects for the amount of fungus sample in each crucible, and Metal/Fungus uses the mass of dried fungus on a filter so that values can be directly compared between samples.*

The calibration curve used for Pb detection is shown in Figure 24, represented by the equation Intensity = 77271[Zn] + 1.47*106. This curve had an R^2 value of 0.951. Repeating the previous calculations with the Zinc data (Table 13). The B1-1 (100× dilution) data point discussed previously can be Q-dropped with over 95% confidence. The amount of detected Zinc was 110 ± 30 µg/g. Compared to the other five metals this is the highest amount of heavy metal adsorbed to the surface of this fungi.

Results Overview

Of the various fungi isolated from Waller Creek site samples, only *Penicillium spp,* isolated from Waller Creek site CS was successfully cultured on heavy metal spiked agar. Twelve replicate samples of fungal spores collected from *Penicillium spp,*, cultured on heavy metal spiked agar, were analyzed for heavy metal content using ICPMS (Table 14).

	Number of Replicates	Average (µg metal/ g dried fungus)	Uncertainty* (µg metal/ g dried fungus)
Silver (Ag)	1	0.003	
Arsenic (As)	12	0.29	0.02
Cadmium (Cd)	12	0.246	0.008
Chromium (Cr)	12	4.6	0.3
Copper (Cu)	1	74	
Lead (Pb)	4	4	0.9
Zinc (Zn)	12	110	30

* Uncertainty estimated using standard error

Table 14: *Summary of quantities of heavy metal biosorbed to Penicillium spp, isolated from Waller Creek site CS, cultured on heavy metal spiked agar*

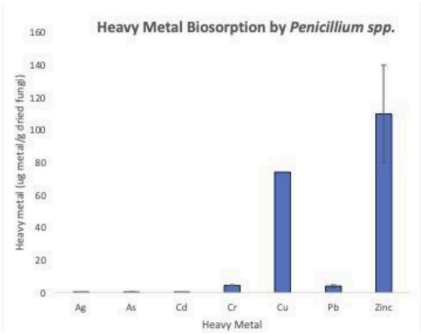


Figure 25: *Summary of quantities of heavy metal biosorbed to Penicillium spp, isolated from Waller Creek site CS, cultured on heavy metal spiked agar*

A plot of this data, using standard error to show uncertainty is shown in Figure 25. The majority of heavy metal data has excellent uncertainty, giving us confidence in these results. We found that *Penicillium spp.* from Waller Creek site CS was able to best biosorb Zn (110 µg Zn/g fungal dry mass), while also performing well with Cr and Pb (4.6 and 4.0 µg/g, respectively) and having detectable levels of As and Cd (0.3 and 0.2 µg/g, respectively). Ag and Cu were only detected in single replicates, and so are not reliable data, although the amount of copper detected in that single replicate was at the high end of the range, comparable to Zn biosorption.

DISCUSSION

Despite limitations, positive results were obtained. *Penicillium spp.* isolated from Waller Creek site CS was able to be cultured on heavy metal spiked agar and was seen to bioabsorb all seven heavy metals investigated. It was able to best biosorb Zn (110 µg Zn/g fungal dry mass),

while also performing well with Cr and Pb (4.6 and 4.0 µg/g, respectively) and having detectable levels of As and Cd (0.3 and 0.2 µg/g, respectively). Ag and Cu were only detected in single replicates, and so are not reliable data. Previous research has found that Penicillium chrysogenum was able to biosorb 96 mg Pb/g of fungal biomass, 21.5 mg Cd/g, 13 mg Zn/g, and 11.7 mg Cu/g, with optimum pH for Cd, Zn, and Cu biosorption at around 7 while that of Pb was around 6.31 The biosorbed metal quantities found here fall well below the amount reported in this previous research.

Additionally, during the incubation process when fungi isolates were grown on PDA spiked with 50 ppb heavy metals standard, other than *Penicillium spp.*, all other fungi species including *Aspergillus spp*. experienced difficulty thriving and growing in the presence of heavy metals. This result was unexpected, because previously, *Aspergillus spp*. like *Aspergillus terreus*, and other common fungal species have been found to be able to tolerate up to 400 ppm of heavy metals.[15] Additionally, *Aspergillus terreus* has been observed to be able to remove substantial amount of heavy metals, particularly Pb (59.67 mg/g)[15], but *Aspergillus niger* and other *Aspergillus spp*. taken from Waller Creek's AC site were not able to even grow in the presence of heavy metals. Possible explanations for these observations include the following issues. As mentioned previously, breaks in time during the incubation process might have contributed. Secondly, although most fungi grow in mildly acidic environments,[32] the 5% (v/v) nitric acid used to dilute the heavy metals solution used to spike the plates might have affected the fungal spores negatively, as nitric oxide has been previously found to be able to inactivate *Aspergillus flavus* spores.[33] In this current research, the pH of fungal cultures were also not monitored, other than knowing they were acidic due to the heavy metal standard solution used to spike the PDA. To remedy this, future replications should replace nitric acid solvent with high purity water for dilutions and involve pH monitoring.

The re-culturing technique also might not have been the most effective, because agar cubes were placed on new petri dishes face-down in order to allow for growth, however, the spatula used to cut out these fungal containing agar cubes were first sterilized with the glass bead sterilizer and was still hot when used to cut into the agar. The heat from the spatula might have killed the spores around the edges of the agar cube, thereby slowing down and halting any further growth. To remedy this in future, the spatula should not be used until it has cooled down, and instead of cutting agar cubes, you could instead slightly scrape the surface of each fungal cultures without needing to pick up any agar. Then, a small amount of DI water can be added to the surface of the plate to create spore-infused water that can be used to inoculate PDA plates.[34]

Other limitations of the study include bacterial contamination and incubation temperature. Although the optimum incubation temperature for fungi falls between 25 – 30˚C, fungi cultures were left to incubate at room temperature ~ 22˚C, which is a bit lower than the ideal temperature range for growth. Additionally, in earlier plating processes, sample solutions were placed on petri dishes in 5 or more spots with only around 1 - 1.5 cm of space between them, which proved to have not been enough room and therefore might have stifled some growth of less persistent species.

For the ICPMS procedure to quantify the amount of heavy metal biosorbed to fungi, fungi had to be scraped off each agar plate onto filters. Although most of the fungal spores were located on the surface or each agar plate, there were some hyphae that were embedded within or had adhered tightly to the agar, therefore in order to avoid accidentally picking up some of the heavy metal-spiked medium and skewing the results, not all parts of the fungi were able to be transferred to the filters. To remediate this problem, an alternative culturing method involving an overlay of a nylon membrane has been developed. This method is superior to others because it allows for the production of large amounts of biomass and easier harvesting of fungal mycelia.[35] Future replications using this method would reduce the possibility of contamination from the metal-spiked media and potentially increase yield. Another alternate approach would be to grow the fungi in spiked liquid media, instead of upon spiked solid agar. This would allow for comparison of the initial concentration of metals in the media before culturing to the final concentrations of metals after the addition of fungal biomass, assuming that the missing

heavy metal has all been biosorbed. This would lead to a different way to report biosorption: the proportion of heavy metal contaminant that is adsorbed by the fungus, rather than the amount adsorbed per mass of fungus. We have listed a number of ways to improve this experiment. Although our data was not at the level of detection of previous work; ultimately, it can still be concluded that *Penicillium spp.* is a strong bioremediator of Zn, Cr, and Pb, while also being a good choice for remediating Cd and As at a lower level as well.

REFERENCES

[1] Kuddus, M.A., Tynan, E. & McBryde, E. (2020). Urbanization: a problem for the rich and the poor? Public Health Rev, 41, 1. doi: 10.1186/s40985-019-0116-0

[2] Paul, M., & Meyer, J. (2001). Streams in urban landscape. Annual Review of Ecology and Systematics, 32, 333-365. doi:10.1146/annurev.ecolsys.32.081501.114040

[3] Sarker, B., Keya, K., Mahir, F., Nahiun, K., Shahida, S., & Khan, R. (2021). Surface and ground water pollution: Causes and effects of urbanization and industrialization in South Asia. Scientific Review, 7(3), 32-41. doi:10.32861/sr.73.32.41

[4] Nahiun, K., Sarker, B., Keya, K., Mahir, F., Shahida, S., & Khan, R. (2021). A review on the methods of industrial wastewater treatment. Scientific Review, 7(3), 20-31. doi: 10.32861/sr.73.20.31

[5] Ali, H., Khan, E.,& Ilahi, I. (2019). Environmental chemistry and ecotoxicology of hazardous heavy metals: Environmental persistence, toxicity, and bioaccumulation. Hindawi Journal of Chemistry, 2019, 1-14. doi: 10.1155/2019/6730305

[6] Muhammad S., Khan B., & Khan H. (2011). Investigating the levels of selected heavy metals in surface water of Shah Alam River (a tributary of River Kabul, Khyber Pakhtunkhwa). Journal of Himalayan Earth Sciences, 44(2), 71–79.

[7] Environmental Protection Agency. (1995). National Recommended Water Quality Criteria. U.S. Environmental Protection Agency. https://www.epa.gov/wqc/national-recommended water-quality-criteria-aquatic-life-criteria-table

[8] Humenik, F. J., & Hanna, G. P. (1971). Algal-bacterial symbiosis for removal and conservation of wastewater nutrients. Journal (Water Pollution Control Federation), 43(4), 580–594.

[9] Wasi, S., Tabrez, S., & Ahmad, M. (2013). Use of Pseudomonas spp. for the bioremediation of environmental pollutants: A review. Environ Monit Assess, 185, 8147–8155. doi: 10.1007/s10661-013-3163-x

[10] de Wet, M., & Brink, H. (2021). Lead biosorption characterisation of Aspergillus piperis. Sustainability, 13(23), 13169. doi: 10.3390/su132313169

[11] Nies, D.H. (2003). Efflux-mediated heavy metal resistance in prokaryotes. FEMS Microbiol. Rev., 27, 313–339.

[12] Losa, G., & Bindschedler, S. (2018). Enhanced tolerance to Cadmium in bacterial-fungal co cultures as a etrategy for metal biorecovery from e-waste. Minerals, 8(4), 121. doi: 10.3390/min8040121

[13] Mohammadian Fazli, M., Soleimani, N., Mehrasbi, M., Darabian, S., Mohammadi, J., & Ramazani, A. (2015). Highly cadmium tolerant fungi: Their tolerance and removal potential. J Environ Health Sci Eng, 13, 19. doi: 10.1186/s40201-015-0176-0

[14] Dhankhar, R., & Hooda, A. (2010). Fungal biosorption - an alternative to meet the challenges of heavy metal pollution in aqueous solutions. Environmental Technology, 32(5), 467-491. doi:10.1080/09593330.2011.572922

[15] Joshi, P.K., Swarup, A., Maheshwari, S., Kumar, R., & Singh, N. (2011). Bioremediation of heavy metals in liquid media through fungi isolated from contaminated sources. Indian J Microbiol, 51(4), 482-7. doi: 10.1007/s12088-011-0110-9

[16] Manguilimotan, L.C., & Bitacura, J.G. (2018). Biosorption of cadmium by filamentous fungi isolated from coastal water and sediments. J Toxicol., 2018, 7170510. doi: 10.1155/2018/7170510

[17] Grabinska-Loniewska, A. (2007). Occurrence of fungi in water distribution system. Polish Journal of Environmental Studies, 16(4), 539-547.

[18] iNaturalist. Available from https://www.inaturalist.org. Accessed 6 April 2023.

[19] Cladosporium cladosporioides. (n.d.) Retrieved April 6, 2023 from https://www.inaturalist.org/ taxa/350347-Cladosporium-cladosporioides.

[20] Kung'u, J. (n.d.) Mold Pictures. Retrieved April 6, 2023 from https://www.drjacksonkungu.com/resources/mold-pictures/nggallery

[21] Schuster, A., & Schmoll, M. (2010). Biology and biotechnology of Trichoderma. Appl Microbiol Biotechnol, 87(3), 787-99. doi: 10.1007/s00253-010-2632-1

[22] Williams-Woodward, J. (2001). Simplified Fungi Identification Key. Special Bulletin 37, The University of Georgia, Retrieved 6 April 2023 from https://hdl.handle.net/10724/35019

[23] Visagie, C., Houbraken, J., Frisvad, J., Hong, S.-B., Klaassen, C., Perrone, G., Seifert, K., Varga, J., Yaguchi, T., & Samson, R. (2014). Identification and nomenclature of the genus Penicillium. Studies in Mycology, 78, 343-371. doi: 10.1016/j.simyco.2014.09.001

[24] Ogunleye, A., & Olaiya, G. (2015). Isolation, identification and mycotoxin production of some mycoflora of dried stockfish (Gadus morhua). Academic Journal of Science, 4, 345-363.

[25] Moslem, M., Mashraqi, A., Abd-Elsalam, K., Bahkali, A., & Elnagaer, M.A. (2010). Molecular detection of ochratoxigenic Aspergillus species isolated from coffee beans in Saudi Arabia. Genetics and molecular research, 9, 2292-9. doi: 10.4238/vol9-4gmr943

[26] Vallejo-Cardona, A.A., Martínez-Palou, R., Chávez-Gómez, B., García-Caloca, G., Guerra Camacho, J., Ceron-Camacho, R., Reyes-Avila, J., Karamath, J.R., & Aburto, J. (2017). Demulsification of crude oil-in-water emulsions by means of fungal spores. PLOS ONE, 12(2), e0170985. doi: 10.1371/journal.pone.0170985

[27] Sun, H., Shao, C., Jin, Q., Li, M., Zhang, Z., Liang, H., Lei, H., Qian, J. & Zhang, Y. (2022). Effects of cadmium contamination on bacterial and fungal communities in Panax ginseng growing soil. BMC Microbiol, 22, 77. doi: 10.1186/s12866-022-02488-z

[28] Thermo Fisher. Inductively Coupled Plasma Mass Spectrometry (ICP-MS) Information. (n.d.) Retrieved April 27, 2023 from https://www.thermofisher.com/us/en/home/ industrial/ spectroscopy-elemental-isotope-analysis/spectroscopy-elemental-isotope-analysis-learning center/trace-elemental-analysis-tea-information/inductively-coupled-plasma-mass spectrometry-icp-ms-information.html

[29] Wieser, M.E., & Brand, W.A. (2017). Isotope ratio studies using mass spectrometry, In J.C. Lindon, G.E. Tranter, & D.W. Koppenaal (Eds.), Encyclopedia of Spectroscopy and Spectrometry (3rd ed.) (pp. 488-500), Oxford, UK: Academic Press. doi: 10.1016/B978-0-12- 409547-2.05243-4

[30] Wilschefski, S.C., & Baxter, M.R. (2019). Inductively coupled plasma mass spectrometry: Introduction to analytical aspects. Clin Biochem Rev, 40(3), 115-133. doi: 10.33176/AACB-19-00024

[31] Pirszel, J., & Pawlik-Skowroska, B. (2001). Heavy metal removal by the waste biomass of Penicillium chrysogenum. Water Qual. Res. J, 36(4), 793-803. doi: 10.2166/wqrj.2001.042

[32] Vylkova, S. (2017). Environmental pH modulation by pathogenic fungi as a strategy to conquer the host. PLoS Pathog, 13(2), e1006149. doi: 10.1371/journal.ppat.1006149

[33] Liu, Y., Oh, S., & Jurick, W. (2019). Response of Aspergillus flavus spores to nitric oxide fumigations in atmospheres with different oxygen concentrations. Journal of Stored Products Research, 83(Sept 2019), 78-83. doi: 10.1016/j.jspr.2019.06.001

[34] de Wet, M.M., & Brink, H.G. (2021). Chapter 18 - Fungi in the bioremediation of toxic effluents, In V.K. Sharma, M.P. Shah, S. Parmar, & A. Kumar (Eds.), Fungi Bio-Prospects in Sustainable Agriculture, Environment and Nano-technology (Vol. 2) (pp. 407-431), Oxford, UK: Academic Press. doi: 10.1016/B978-0-12-821925-6.00018-6

[35] Schumann, U., Smith, N.A., Wang, M.B. (2013). A fast and efficient method for preparation of high-quality RNA from fungal mycelia. BMC Res Notes, 6, 71. doi: 10.1186/1756-0500-6-71

Quantifying Insect Herbivory Across Plant Diversity Gradients

Mandy Tran
The University of Texas at Austin

ABSTRACT

Conflicting ecological hypotheses exist on whether increasing plant species richness increases or decreases insect herbivory. However, there is a lack of research into how insect herbivory may be impacted by another metric of diversity: phylogenetic diversity, a measure of how closely related the species in a community are to each other. This study investigates whether insect herbivory differs across plant species richness and phylogenetic diversity and if these differences are affected across plant density levels within a biodiversity-ecosystem functioning experiment in Austin, Texas. Individuals of five focal species within plots of varying plant diversity and density values were sampled for leaf herbivory. Then, potential relationships between plant diversity, plant density, and herbivory damage were found using linear mixed-effect and regression models. Findings indicate that plant diversity has a variable effect on insect herbivory but most strongly support a negative correlation between plant phylogenetic diversity and insect herbivory. Additionally, conspecific percent cover exhibits a generally positive correlation with insect herbivory, which is consistent with the Janzen-Connell hypothesis, where individuals in areas of high conspecific density are more likely to be targeted by specialist herbivores. These results suggest that plant diversity has a complex effect on damage by insect herbivores of functionally distinct plant species, which differences in plant density levels may further complicate.

INTRODUCTION

One of the many ways climate change threatens biodiversity is through increasing the frequency and intensity of extreme conditions (Bellard et al., 2012). Stressors like drought can decrease species richness by driving plant species to local extinction, slowing their recolonization rates, and shifting their range distributions (Tilman & El Haddi, 1992; Bellard et al., 2012). Changes in vegetation, in turn, may disrupt trophic interactions, such as between plants and insect herbivores (Bellard et al., 2012), thus setting off bottom-up extinction cascades.

Since biodiversity is positively correlated with a wide range of ecosystem functions and services, ecologists must quantify the effects of its loss in a realistic manner (Balvanera et al., 2006; Zavaleta et al., 2010). For instance, species loss tends to occur in closely related groups (Willis et al., 2008), so studying plant-insect interactions across a gradient of species relatedness may yield relevant findings that can be used to inform conservation policies. Given that models project plant extinctions under climate change are more likely to trigger animal coextinctions than vice versa (Schleuning et al., 2016), investigating how changes in plant diversity affect these interactions is fundamental.

One area of investigation within this topic is the effect of insect herbivory on ecosystem functioning and vice versa across plant diversity levels. While past studies have found that plant diversity has as significant of an impact on ecosystem functioning as herbivory does (Tilman et al., 2012), the interactions between plant diversity, productivity, and herbivory have yet to be fully explored. Previous biodiversity research has found a positive correlation between diversity and productivity (Tilman et al., 2001; Balvanera et al., 2006), but the exact mechanisms behind what species diversity variables affect what ecosystem functions and how are unclear. Regarding the relationship between plant diversity and

herbivory, past studies have yielded conflicting results over whether insect herbivory increases or decreases across species richness (Dinnage, 2013; Loranger et al., 2013; Root, 1973). Notably, species richness is often used as the metric of diversity within experiments, but it may be an oversimplification that fails to consider the effects of the evolutionary relationships within a community on ecosystem resilience and resistance (Bellard et al., 2012; Tucker & Cadotte, 2013).

Instead, one hypothesis is that productivity is positively correlated with phylogenetic diversity—a measure of how closely related the species in a community are to each other—because plots of distant relatives exhibit more complementarity than plots of monocultures or close relatives due to reduced niche overlap (Cadotte, 2013). These findings indicate that a deeper understanding of the relationship between biodiversity and productivity may be found by studying plant communities of varying levels of both species richness and phylogenetic diversity. The value of phylogenetic diversity has been demonstrated by Dinnage (2013), who found that herbivory was highest in plots that were high in species richness but low in phylogenetic diversity, which suggests that insects are phylogenetically specialized to feed on close plant relatives. Although this trend was found under an observational study of an old field habitat (Dinnage, 2013), it has yet to be found in an experiment that explicitly manipulates plant diversity levels. Such an experiment would strengthen the evidence indicating a predictable relationship between plant diversity and insect herbivory.

To address this gap, this study investigates insect herbivory damage changes along plant species richness and phylogenetic diversity gradients using an experiment. Hypotheses are based on two assumptions: insect herbivores are phylogenetically specialized to consume plants closely related to each other due to coevolution from long-term trophic interactions (Dinnage, 2013), and phylogenetic diversity is a suitable proxy for the plant functional traits that insect herbivores are targeting (Moreira et al., 2016). Under these assumptions, it is expected that increasing phylogenetic diversity will cause a decrease in herbivory because, according to the model of optimal foraging, insects would exert more time and energy searching for their preferred hosts in areas of high phylogenetic diversity than in areas of low phylogenetic diversity. If true, the results should show that plants in communities of high phylogenetic diversity experience less herbivory damage than those in communities of low phylogenetic diversity.

Furthermore, species richness and phylogenetic diversity are expected to have a negative interaction, causing plants in communities of high species richness and low phylogenetic diversity to experience the most herbivory damage. Again, if insect herbivores are specialized to consume a selection of closely related plants (Dinnage, 2013), then according to the model of optimal foraging, they will face reduced searching time for optimal hosts in plant communities of low phylogenetic diversity. When factoring in species richness, herbivory estimates are expected to be higher in polycultures of high species richness and low phylogenetic diversity than in monocultures since herbivores can more easily access a broader range of nutritional resources in the former (Dinnage, 2013).

Additionally, when exploring how plant community characteristics affect insect herbivory, plant density must also be considered as a variable due to the Janzen-Connell hypothesis. According to the hypothesis, plant individuals in areas of high conspecific density are likely to face increased herbivory by specialist herbivores (Janzen, 1970; Connell, 1971). As to how it relates to this experiment, communities with low species richness may be more attractive to specialist herbivores if they exhibit high conspecific percent cover. Thus, contrary to the previous hypothesis, if communities of low species richness experience the highest herbivory damage, then plant density may be a stronger predictor for herbivory than phylogenetic diversity. Following this logic, communities of low total percent cover, or the percentage of a defined area that is covered by plants regardless of species, would be expected to experience low herbivory damage since it would be more time-intensive for herbivores to search for sparsely distributed individuals.

Hence, this study aims to find whether species richness, phylogenetic diversity, and plant density influence insect herbivory. Ultimately, the results of this study may contribute to efforts toward accurately predicting how biodiversity loss, specifically phylogenetic diversity loss in plants, affects ecosystem functioning and trophic

interactions.

METHODS

Experimental Setup

This study was conducted at a pre-existing biodiversity-ecosystem functioning experiment at the Brackenridge Field Laboratory in Austin, Texas. The experiment aims to study the effects of phylogenetically structured biodiversity loss on ecosystem functioning in a grassland. The experiment consists of 2m x 2m plots of one, two, four, six, and twelve native local Texan species. The phylogenetic diversity of the total pool of twelve species was calculated based on the distances between the species' nodes on the phylogenetic tree (Figure 1). The plots are seeded to form gradients of species richness and phylogenetic diversity (Figure 2). As species richness increases, the proportion of seeds sowed from each species is reduced, so the communities are controlled for abundance. Consequently, the monocultures have the minimum values for both diversity metrics, the twelve species plots have maximum species richness, and the two- to six-species polycultures have low, medium, or high phylogenetic diversity values. Altogether, plots of each level of species richness and phylogenetic diversity are replicated three times.

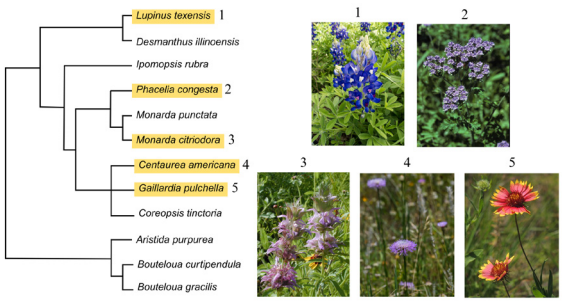


Figure 1: *Phylogenetic tree of the twelve species within the biodiversity-ecosystem functioning experiment with photos of the five focal species (https://www.wildflower.org/).*

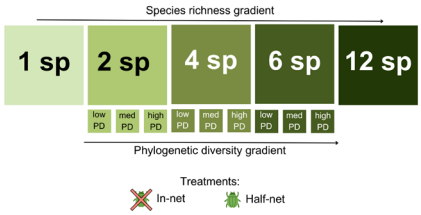


Figure 2: *Overview of how the plots are organized by plant diversity and insect treatments.*

Furthermore, the plots have been designed with aboveground insect reduction treatments so that 25% of the area within the plots is wholly covered in nets and 50% of the area is not; the remaining 25% of the area is covered in half-nets that allow for insect exposure to account for any confounding variables that may arise from net presence such as differences in light (Figure 3). It is of note that while these nets reduce flying insects, they do not necessarily reduce crawling or burrowing ones. Although the experiment also contains watering treatments, these will not be used within this study due to time constraints.



Figure 3: *Example of a plot with a 25% full net, 25% half net, and 50% no net cover.*

The five species out of the species pool that will be used for this study are *Lupinus texensis, Centaurea americana, Gaillardia pulchella, Phacelia congesta, and Monarda citriodora* (see Figure 1). These five species were chosen because they are functionally distinct from each other (e.g., annual vs. biennial, nitrogen fixer vs. non-fixer) and because different species combinations create varying levels of phylogenetic diversity values.

Data Collection

To study differences in herbivory damage across plant diversity levels, three individuals of each of the five focal species were sampled in the in-net and half-net treatments across the one, four, six, and twelve-species plots that they are present in (two-species plots were excluded from data collection since not all five of the focal species were present within them). These plots represent a gradient of species richness and phylogenetic diversity values, while in-net treatments represent environments with greatly reduced exposure to insect herbivory. Whenever possible, individuals were arbitrarily selected for sampling so that they were not directly adjacent to each other within the plots to mitigate proximity-related effects on herbivory damage (Kim, 2017).

From March 27, 2023, to May 5, 2023, in-field data collection for herbivory damage, plant percent covers, and plant height occurred across sampled individuals. The Herbivory Variability Network's primary protocol (https://herbvar.org/) was used to estimate random leaf sample herbivory damage and whole plant herbivory damage; the former was found by randomly subsampling five leaves from an individual. By collecting herbivory damage estimates on both a finer and coarser scale, a more accurate representation of individuals' overall herbivory damage was assessed. Herbivory damage was approximated through in-field visual estimation since this method allows more data to be collected within a limited time constraint than in-lab digital methods. Measurement error from visual estimation was minimized by recording herbivory damage estimates at a high resolution of a tenth of a percentage (0-100%) and by the weekly calibration of the data collector using the ZAX Herbivory Trainer (Xirocostas et al., 2022). Conspecific and total percent cover within the in-net and half-net treatments were also visually estimated. Additionally, vegetative and reproductive height was measured with meter tape to account for differences in herbivory exposure caused by insect herbivores being attracted to taller plants (Kim, 2017) and by varying germination times.

Statistical Analysis

Individual-level herbivory, the percentage of a plant's total leaf area lost to herbivory, was first calculated for each individual as an additional variable using the data collected in the field. This calculation was done by multiplying an individual's average random leaf sample herbivory damage by the number of its leaves with herbivory damage, then dividing that value by the individual's total number of leaves. Anecdotally, variability in leaf-level herbivory seemed different between the five focal species, so this calculated variable was used within the analyses because it considers variability in leaf herbivory.

To determine whether the in-net treatments effectively reduced insect herbivory, insect herbivory damage between the individuals sampled within the in-net and half-net treatments was compared using two-sample t-tests. Five two-sample t-tests were run separately for each of the five species.

Next, since individuals within the half-net treatments experienced ambient levels of insect exposure, herbivory values from the half-net samples were used to evaluate the relationship between plant diversity and insect herbivory. First, to identify broad trends, the effect of species richness on herbivory across the five focal species was found with a linear mixed-effect model. Given that herbivory varies among plant species (Bröcher et al., 2023), the differences between the species groups were accounted for by setting herbivory as the response variable, species richness as the fixed effect, and species as a random effect. Second, to identify trends for each focal species, the effect of species richness on herbivory within each species was found by running five separate linear regressions. These steps were then repeated, with phylogenetic diversity as the fixed effect, to find the effect of phylogenetic diversity on herbivory across and within the focal species; phylogenetic diversity was quantified as the sum of the distances between the nodes of all the species present within a phylogenetic tree.

Finally, linear regressions were run to determine if conspecific and total percent cover were significant explanatory variables for insect herbivory. All statistical analyses were performed in R 4.3.0.

RESULTS

Differences in Insect Herbivory within the In-Net and Half-Net Treatments

Across the five focal species, *L. texensis* was the only one to exhibit significantly less insect herbivory within the in-net treatments than within the half-net treatments as expected (in-net: M = 0.9798738; half-net: M = 2.8516548; p = 0.0008946), although *C. americana* exhibited a similar trend as well (in-net: M = 0.3859050; half-net: M = 0.6960819; p = 0.07634). However, there was no significant difference in insect herbivory between the two net treatments for *G. pulchella*, *P. congesta*, and *M. citriodora* (*G. pulchella*: p = 0.2554972; *P. congesta*: p = 0.2437; *M. citriodora*: p = 0.4965) (Figure 4).

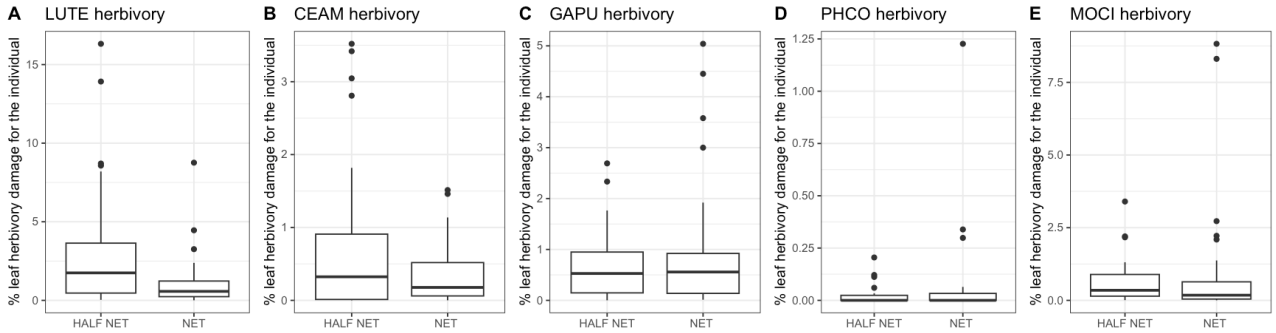


Figure 4: *Insect herbivory within the in-net treatments vs. the half-net treatments across the five focal species. "LUTE" refers to L. texensis, "CEAM" to C. americana, "GAPU" to G. pulchella, "PHCO" to P. congesta, and "MOCI" to M. citriodora.*

Effects of Plant Species Richness on Insect Herbivory

There is no clear trend between plant species richness and insect herbivory. Given species as a random effect, there is a negative, albeit insignificant, relationship between species richness and herbivory across the focal species ($p = 0.149$). When comparing trends between the focal species, while *L. texensis*, *G. pulchella*, and *P. congesta* demonstrate a negative relationship between plant species richness and insect herbivory damage (*L. texensis*: $R^2 = 0.05275$, $p = 0.06346$; *G. pulchella*: $p = 0.3448$; *P. congesta*: $R^2 = 0.04359$, $p = 0.1717$), insect herbivory damage for *C. americana* and *M. citriodora* seem to increase or stay the same, respectively, with plant species richness (*C. americana*: $R^2 = 0.005324$, $p = 0.2797$; *M. citriodora*: $p = 0.6259$). Overall, the correlation between plant species richness and insect herbivory seems weak. (Figure 5).

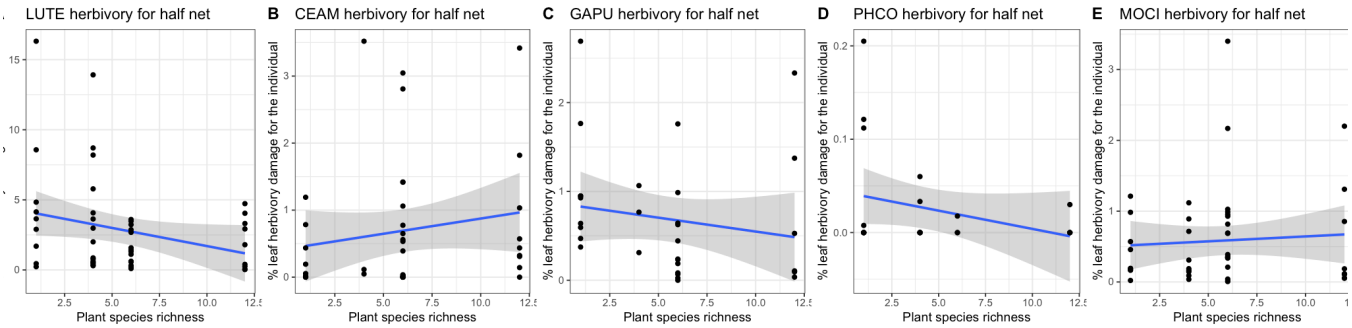
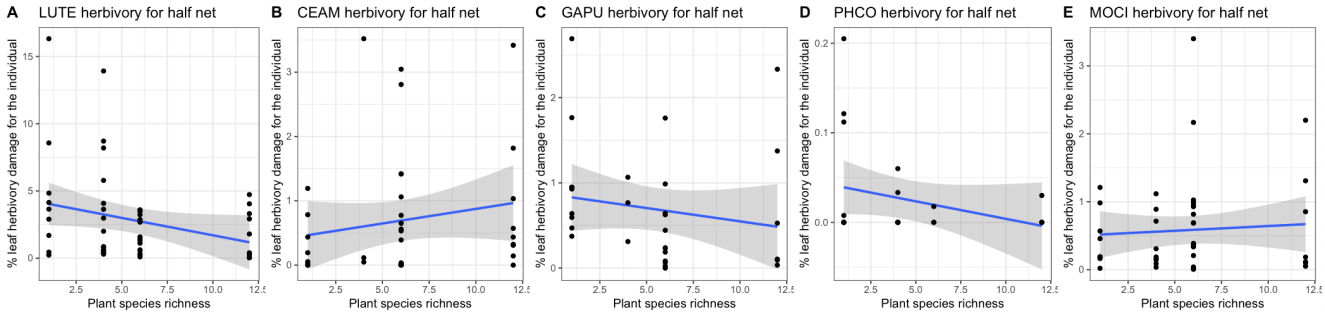


Figure 5: *Insect herbivory within the half-net treatments across the five focal species vs. plant species richness.*

Effects of Plant Phylogenetic Diversity on Insect Herbivory

Similar to the results above, there is no clear trend between plant phylogenetic diversity and insect herbivory. Given species as a random effect, there is a marginally significant negative relationship between phylogenetic diversity and herbivory across the focal species ($p = 0.0565$). When comparing trends between the focal species, *L. texensis* exhibits a significant negative relationship between the plant phylogenetic diversity of the plots it was present in and insect herbivory damage that is also demonstrated to a lesser extent in *G. pulchella* and *P. congesta* (*L. texensis*: $R^2 = 0.1024$, $p = 0.01518$; *G. pulchella*: $R^2 = 0.02883$, $p = 0.1797$; *P. congesta*: $R^2 = 0.07429$, $p = 0.1112$). *C. americana* and *M. citriodora*, on the other hand, demonstrate a positive trend between phylogenetic diversity and insect herbivory (*C. americana*: $p = 0.3328$; *M. citriodora*: $p = 0.4544$). However, the species with negative trends demonstrate a stronger correlation between phylogenetic diversity and insect herbivory than those with positive



trends (Figure 6).

Figure 6: *Insect herbivory within the half-net treatments across the five focal species vs. plant phylogenetic diversity.*

Effects of Conspecific Percent Cover on Insect Herbivory

For most of the focal species, conspecific percent cover seems to have a positive correlation with insect herbivory (Figure 7). For *L. texensis* and *G. pulchella*, increasing conspecific percent cover is significantly correlated with increased insect herbivory damage (*L. texensis*: $R^2 = 0.151$, $p = 0.00369$; *G. pulchella*: $R^2 = 0.1116$, $p = 0.03719$). This pattern is demonstrated to a lesser extent by *P. congesta* and to a nearly negligible extent by *C. americana* (*P. congesta*: $p = 0.3511$; *C. americana*: $p = 0.7969$). Conversely, although very weak, *M. citriodora* is the only species displaying a negative trend between conspecific percent cover and insect herbivory (*M. citriodora*: $p = 0.7029$).

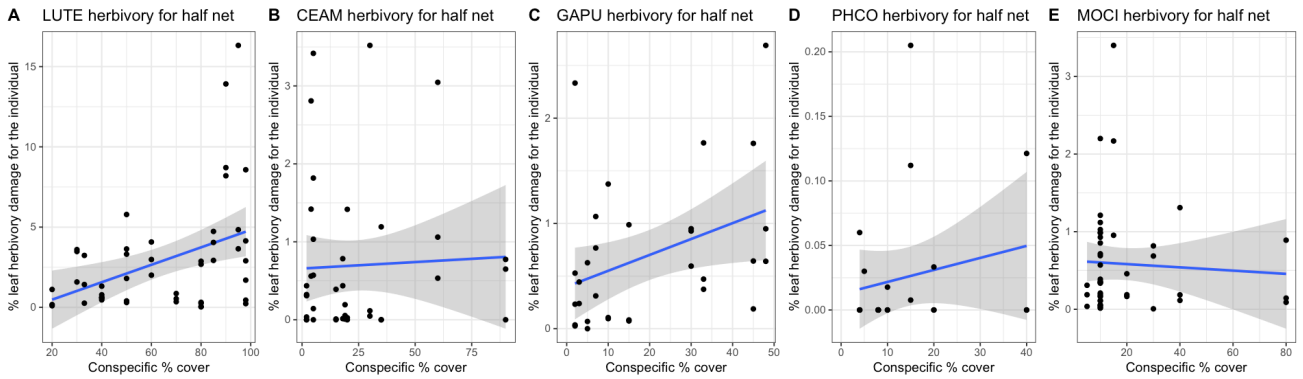


Figure 7: *Insect herbivory within the half-net treatments across the five focal species vs. conspecific percent cover.*

Effects of Total Percent Cover on Insect Herbivory

The trend between total percent cover and insect herbivory seems variable across the focal species (Figure 8). Here, the insect herbivory damage experienced by *L. texensis* increases significantly with total percent cover (*L. texensis*: $R^2 = 0.1098$, $p = 0.01227$). *M. citriodora* and *C. americana* also exhibit positive relationships between total percent cover and insect herbivory, although this is near negligible for the latter (*M. citriodora*: $p = 0.4097$; *C. americana*: $p = 0.781$). A negative relationship between total percent cover and insect herbivory, on the other hand, was found for *G. pulchella*, and to a nearly negligible extent, *P. congesta* (*G. pulchella*: $R^2 = 0.0136$, $p = 0.2441$; *P. congesta*: $p = 0.7928$).

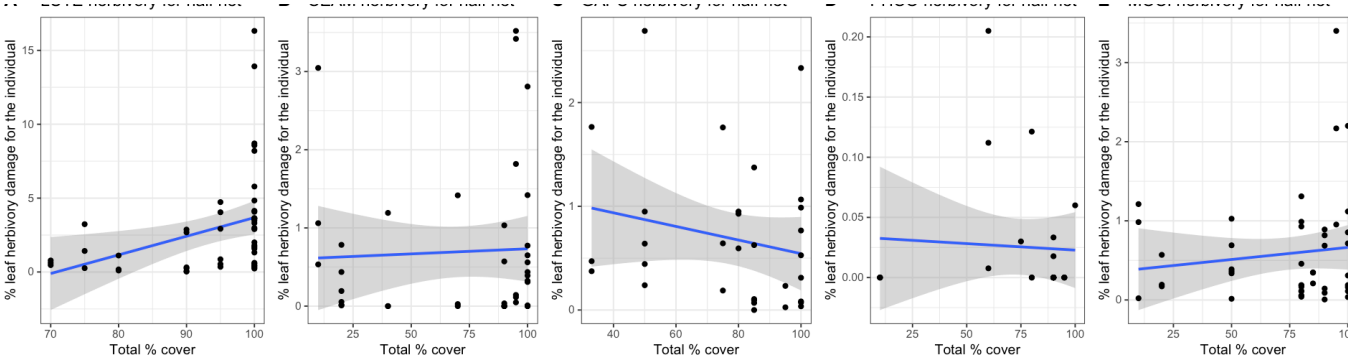


Figure 8: *Insect herbivory within the half-net treatments across the five focal species vs. total percent cover.*

DISCUSSION

This study aimed to determine if and how insect herbivory correlated with species richness, phylogenetic diversity, and plant density. Identifying the relationships between these variables may strengthen the accuracy of a framework that can predict how biodiversity loss will impact ecosystem functioning in real-life environments. Thus, random plant individuals from five focal species within an experimental setup of plots seeded across gradients of plant diversity were sampled for insect herbivory. Overall, this study found that, although the independent variables affecting insect herbivory varied across the five focal species, some broad trends still emerged. Namely, insect herbivory generally displayed a stronger correlation with phylogenetic diversity than with species richness, and negative correlations between insect herbivory and plant diversity were generally stronger than positive correlations. Additionally, analyses indicated that insect herbivory generally increased with conspecific percent cover but that this trend did not necessarily hold with total percent cover.

When insect herbivory was compared between the net treatments, it was found that *L. texensis* was the only focal species to exhibit significantly less herbivory damage within the in-net than within the half-net treatments. While *C. americana* exhibited a marginally significant difference between the net treatments, this was not the case for the other three focal species. Since the purpose of the net treatments is to modify the insect community without complete exclusion, it is possible that these differences in herbivory damage were due to the focal species being targeted by different proportions of above-ground and below-ground insects. Although below-ground herbivory damage was not measured as part of this study, past research has found that root herbivory may reduce a plant's nutritional quality and thus affect leaf herbivory (Soler et al., 2005). Hence, it is possible that in-net *G. pulchella*, *P. congesta*, and *M. citriodora* individuals were targeted by a higher proportion of root herbivores, which triggered increased leaf herbivory as above-ground insects needed to consume more leaf area to receive sufficient nutrition. Alternatively, it is possible that in-net *L. texensis* and *C. americana* individuals were targeted by a higher proportion of root herbivores, which triggered decreased leaf herbivory as insects preferred to target host plants that yielded more nutrition. The relationship between root herbivory and leaf herbivory is further complicated since root herbivory's effect on an individual's above-ground growth may be mediated by its conspecific and heterospecific density (Muller-Scharer, 1991). Investigating differences in above- and below-ground herbivory and how they interact with plant diversity and density may reveal the rationale behind trends regarding in-net leaf herbivory damage.

When insect herbivory in the half-net treatments was compared across gradients of species richness and phylogenetic diversity, plant diversity seemed to have an inconsistent relationship with insect herbivory across the five focal species. However, negative correlations between the variables, particularly between phylogenetic diversity and insect herbivory, were stronger than positive correlations. Previous studies have yielded conflicting findings regarding how species richness impacts insect herbivory, resulting in a lack of consensus on whether herbivorous generalists are more attracted to communities of high

species richness or if herbivorous specialists are more attracted to communities of low species richness (Dinnage, 2013). Thus, species richness was expected to have a weak negative correlation with insect herbivory. This expectation was supported by the results, which found that, across the focal species, species richness had a weak negative effect on herbivory when accounting for variations in herbivory across species. The trends found between each species were also weak. Even so, *L. texensis* displayed a near-significant negative relationship between species richness and insect herbivory. This result supports the resource concentration hypothesis, which states that increasing species richness while keeping plant density constant reduces the chances of a specialist herbivore finding and consuming their preferred hosts (Moreira et al., 2016), which may result in reduced herbivory damage for these hosts.

Phylogenetic diversity followed similar trends to species richness in explaining insect herbivory across the focal species. However, in this case, phylogenetic diversity had a marginally significant negative effect on herbivory when accounting for variations in herbivory across species. Furthermore, the three species that exhibited weak, negative relationships between phylogenetic diversity and insect herbivory still demonstrated stronger relationships than the two species that exhibited positive ones. This observation is further substantiated by *L. texensis*, the only species with a significant correlation between the variables. If insect herbivores are indeed phylogenetically specialized (Dinnage, 2013), it would follow that they would find several viable hosts present in their greatest densities within plots of low phylogenetic diversity. According to the dietary mixing hypothesis, these plots may be preferable to forage in as they provide a wide variety of nutritional resources within close proximity and, therefore, would experience more insect herbivory damage (Moreira et al., 2016). Hence, the negative correlations between phylogenetic diversity and insect herbivory support the hypothesis. However, the positive correlations between phylogenetic diversity and insect herbivory that were displayed by *C. americana* and *M. citriodora*, albeit relatively weak, may be evidence of an alternate result of the resource concentration hypothesis where generalist herbivores prefer foraging in diverse plots due to nutritional advantages (Dinnage, 2013).

Regarding plant density, conspecific percent cover had a more consistent relationship with insect herbivory across the five species than total percent cover. Insect herbivory increased with conspecific percent cover for four of the five focal species, and conspecific percent cover explained 15% and 11% of the variation in insect herbivory for *L. texensis* and *G. pulchella*, respectively. This positive trend is consistent with the Janzen-Connell hypothesis, which explains that individuals are more likely to be found and targeted by specialist herbivores if they are adjacent to others of their species (Janzen, 1970; Connell, 1971). Since the plots within this experiment were seeded so that species were roughly equal in abundance, the communities of low species richness and, thus, higher conspecific percent cover per species may have been more vulnerable to insect herbivory by specialists. If so, then specialists may have also targeted adjacent plants if they were phylogenetically close to their original hosts, thus augmenting the effect of phylogenetic diversity on herbivory (Downey et al., 2018).

A trend is less clear for total percent cover, which was positively correlated with insect herbivory for three species, significantly so for *L. texensis*, and negatively correlated with insect herbivory for the other two. Natural enemies shared between plant species may prefer foraging in plots exhibiting higher total percent cover because they contain more food sources in less space, hence leading to a positive correlation between total percent cover and insect herbivory. In this case, the total percent cover would mainly influence the recruitment of generalists and phylogenetically specialized herbivores in plots of low plant diversity. Meanwhile, other factors may cause total percent cover to have a negative effect on insect herbivory. For instance, if total percent cover is positively correlated with the complexity of vegetative structures within a community, and if said complexity is positively correlated with the recruitment of insect predators (Morante-Filho et al., 2016), then insect herbivory damage may be higher in plots of low total percent cover due to a lack of predation to control for herbivore populations. With these various effects in mind, investigating how plant density interacts with other community variables may reveal what indirect factors should be accounted for to accurately estimate plant density's effect on insect herbivory.

Notably, the only species to consistently show significant or marginally significant relationships between plant diversity and plant density on insect herbivory was *L. texensis*. This pattern may occur because nitrogen fixers are more attractive to insect herbivores than non-fixers for their high foliar nitrogen content (Barker et al., 2022). Thus, as the only nitrogen fixer of the five focal species, *L. texensis* may be more sensitive to the effects of plant diversity and plant density on insect herbivory. Studying functionally distinct plant species may provide insight into how different plant traits may make a species more or less vulnerable to changes in community composition that affect insect herbivory (Moreira et al., 2016).
How plant density interacts with plant diversity's effect on plant resource allocation should also be studied. Currently, it is unclear whether competition due to high plant density would pressure individuals to invest in growth over defense, or if increased herbivore recruitment due to high plant density would pressure individuals to invest in defense over growth (Moreira et al., 2016). Additionally, studying insect herbivore traits such as diet breadth and foraging behavior may clarify how insect herbivory differs across plant diversity and whether changes in top-down feedback, like predator abundance across plant diversity, may contribute to differences in herbivory damage (Moreira et al., 2016).

As biodiversity loss ensues at an increasing rate due to climate change (Bellard et al., 2012), it is vital to understand how changes in community compositions will impact interactions across trophic levels. This research sought to understand how insect herbivory is affected across plant diversity gradients and found that the relationships between plant species richness, plant phylogenetic diversity, and other environmental factors explaining differences in herbivory damage, such as plant density, are complex. These findings may inform the development of a model that can accurately predict how plant-insect interactions would change due to plant extinctions, thus allowing for effective conservation practices. By reaching a more comprehensive understanding of the mechanisms behind ecosystem functioning through additional research, ecologists will continue to improve such models and, ultimately, further mitigate biodiversity loss.

LIMITATIONS

This study has potential limitations. First, there is a lack of literature on the insects that target the five focal species used in this experiment. Understanding the above- and below-ground herbivores that target the species may explain why four of the species, excluding *L. texensis*, experienced no significant differences in herbivory in the half-net and in-net treatments. Additionally, the varied relationships between plant diversity and herbivory between each species may be clarified by understanding the dietary breadth of their natural enemies. Future studies may reach novel interpretations on how plant diversity and plant density affect herbivory by conducting a census of the insects within the plots.

Second, the sample size used in this study was limited due to time constraints. Since herbivory data is highly variable, a limited sample size may have obscured trends between plant diversity, plant density, and herbivory. Thus, it is recommended that future studies collect a greater sample size of plant individuals.

ACKNOWLEDGEMENTS

Thank you to Associate Professor Dr. Caroline Farrior and Graduate Student Fellow Damla Cinoğlu, both of the Department of Integrative Biology at the University of Texas at Austin, for your guidance. Your commitment to mentorship cultivated my passion for research. Lastly, thank you to Dr. Amy Wolf and Graduate Research Fellow Sarah Ortiz for the setup of the experiment.

REFERENCES

Balvanera, P., Pfisterer, A. B., Buchmann, N., He, J.-S., Nakashizuka, T., Raffaelli, D., & Schmid, B. (2006). Quantifying the evidence for biodiversity effects on ecosystem functioning and services: Biodiversity and ecosystem functioning/services. Ecology Letters, 9(10), 1146–1156. https://doi.org/10.1111/j.1461-0248.2006.00963.x

Barker, W., Comita, L. S., Wright, S. J., Phillips, O. L., Sedio, B. E., & Batterman, S. A. (2022). Widespread herbivory cost in tropical nitrogen-fixing tree species. Nature, 612(7940), Article 7940. https://doi.org/10.1038/s41586-022-05502-6

Bellard, C., Bertelsmeier, C., Leadley, P., Thuiller, W., & Courchamp, F. (2012). Impacts of climate change on the future of biodiversity: Biodiversity and climate change. Ecology Letters, 15(4), 365–377. https://doi.org/10.1111/j.1461-0248.2011.01736.x

Bröcher, M., Ebeling, A., Hertzog, L., Roscher, C., Weisser, W., & Meyer, S. T. (2023). Effects of plant diversity on species-specific herbivory: Patterns and mechanisms. Oecologia, 201(4), 1053–1066. https://doi.org/10.1007/s00442-023-05361-6

Cadotte, M. W. (2013). Experimental evidence that evolutionarily diverse assemblages result in higher productivity. Proceedings of the National Academy of Sciences, 110(22), 8996–9000. https://doi.org/10.1073/pnas.1301685110

Connell, J. H. (1971). On the role of natural enemies in preventing competitive exclusion in some marine animals and in rain forest trees. Dynamics of Populations, 298–312.

Dinnage, R. (2013). Phylogenetic diversity of plants alters the effect of species richness on invertebrate herbivory. PeerJ, 1, e93. https://doi.org/10.7717/peerj.93

Downey, H., Lewis, O. T., Bonsall, M. B., Fernandez, D. C., & Gripenberg, S. (2018). Insect herbivory on seedlings of rainforest trees: Effects of density and distance of conspecific and heterospecific neighbors. Ecology and Evolution, ece3.4698. https://doi.org/10.1002/ece3.4698

Janzen, D. H. (1970). Herbivores and the Number of Tree Species in Tropical Forests. The American Naturalist, 104(940), 501–528. https://doi.org/10.1086/282687

Kim, T. N. (2017). How plant neighborhood composition influences herbivory: Testing four mechanisms of associational resistance and susceptibility. PLoS ONE, 12(5), e0176499. https://doi.org/10.1371/journal.pone.0176499

Loranger, J., Meyer, S. T., Shipley, B., Kattge, J., Loranger, H., Roscher, C., Wirth, C., & Weisser, W. W. (2013). Predicting invertebrate herbivory from plant traits: Polycultures show strong nonadditive effects. Ecology, 94(7), 1499–1509.

Morante-Filho, J. C., Arroyo-Rodríguez, V., Lohbeck, M., Tscharntke, T., & Faria, D. (2016). Tropical forest loss and its multitrophic effects on insect herbivory. Ecology, 97(12), 3315–3325. https://doi.org/10.1002/ecy.1592

Moreira, X., Abdala-Roberts, L., Rasmann, S., Castagneyrol, B., & Mooney, K. A. (2016). Plant diversity effects on insect herbivores and their natural enemies: Current thinking, recent findings, and future directions. Current Opinion in Insect Science, 14, 1–7. https://doi.org/10.1016/j.cois.2015.10.003

Muller-Scharer, H. (1991). The Impact of Root Herbivory as a Function of Plant Density and Competition: Survival, Growth and Fecundity of Centaurea maculosa in Field Plots. The Journal of Applied Ecology, 28(3), 759. https://doi.org/10.2307/2404206

Root, R. B. (1973). Organization of a Plant-Arthropod Association in Simple and Diverse Habitats: The Fauna of Collards (Brassica Oleracea). Ecological Monographs, 43(1), 95–124. https://doi.org/10.2307/1942161

Schleuning, M., Fründ, J., Schweiger, O., Welk, E., Albrecht, J., Albrecht, M., Beil, M., Benadi, G., Blüthgen, N., Bruelheide, H., Böhning-Gaese, K., Dehling, D. M., Dormann, C. F., Exeler, N., Farwig, N., Harpke, A., Hickler, T., Kratochwil, A., Kuhlmann, M., … Hof, C. (2016). Ecological networks are more sensitive to plant than to animal extinction under climate change. Nature Communications, 7(1), Article 1. https://doi.org/10.1038/ncomms13965

Soler, R., Bezemer, T. M., Van Der Putten, W. H., Vet, L. E. M., & Harvey, J. A. (2005). Root herbivore effects on above-ground herbivore, parasitoid and hyperparasitoid performance via changes in plant quality. Journal of Animal Ecology, 74(6), 1121–1130. https://doi.org/10.1111/j.1365-2656.2005.01006.x

Tilman, D., & El Haddi, A. (1992). Drought and biodiversity in Grasslands. Oecologia, 89(2), 257–264. https://doi.org/10.1007/BF00317226

Tilman, D., Reich, P. B., & Isbell, F. (2012). Biodiversity impacts ecosystem productivity as much as resources, disturbance, or herbivory. Proceedings of the National Academy of Sciences, 109(26), 10394–10397. https://doi.org/10.1073/pnas.1208240109

Tilman, D., Reich, P. B., Knops, J., Wedin, D., Mielke, T., & Lehman, C. (2001). Diversity and Productivity in a Long-Term Grassland Experiment. Science, 294(5543), 843–845. https://doi.org/10.1126/science.1060391

Tucker, C. M., & Cadotte, M. W. (2013). Unifying measures of biodiversity: Understanding when richness and phylogenetic diversity should be congruent. Diversity and Distributions, 19(7), 845–854. https://doi.org/10.1111/ddi.12087

Willis, C. G., Ruhfel, B., Primack, R. B., Miller-Rushing, A. J., & Davis, C. C. (2008). Phylogenetic patterns of species loss in Thoreau's woods are driven by climate change. Proceedings of the National Academy of Sciences, 105(44), 17029–17033. https://doi.org/10.1073/pnas.0806446105

Xirocostas, Z. A., Debono, S. A., Slavich, E., & Moles, A. T. (2022). The ZAX Herbivory Trainer—Free software for training researchers to visually estimate leaf damage. Methods in Ecology and Evolution, 13(3), 596–602. https://doi.org/10.1111/2041-210X.13785

Zavaleta, E. S., Pasari, J. R., Hulvey, K. B., & Tilman, G. D. (2010). Sustaining multiple ecosystem functions in grassland communities requires higher biodiversity. Proceedings of the National Academy of Sciences, 107(4), 1443–1446. https://doi.org/10.1073/pnas.0906829107

Synthetic Approaches to Prepare and Isolate Halogenated Anthracene Derivatives

Benjamin Rogers
The University of Texas at Austin

ABSTRACT

In this laboratory research, 1,8-dichloroanthraquinone from Sigma-Aldrich was used to generate 1,8-diiodoanthraquinone through a single-step halogen-exchange reaction. Experimental yield of the 1,8-diiodoanthraquinone product was improved from 19 % to 45 % by removing water from the reaction vessel. Optimal conditions for the separation of unreacted 1,8-dichloroanthraquinone from 1,8- diiodoanthraquinone product were testedtesting using silica-column chromatography with several different solvent compositions of toluene, dichloromethane (DCM), and hexanes. Experimentally synthesized 1,8- diiodoanthraquinone was sequentially reduced first generating 1,8-diiodoanthrace-9-none, then reduced once again to generate 1,8-diiodoanthracene with a percent yield of 34 %. A set of viable resonance structures of 1,8-diiodoanthraquinone are proposed for the experimentally-observed selective activation of the oxygen site at the 9-position thus making the isolation of 1,8-diiodoanthracene-9-one possible. It was found that 1,8-diiodoanthracene could be successfully brominated by n-bromoorosuccindamide (NBS) generating 10-bromo-1,8-diiodoanthracene. Although the bromination was successful, the percent mass yield was low at only 18%. The synthesis of each product was confirmed with 1H NMR Agilent 400 MHz. This research will be useful for both enhancing existing synthetic reaction paths and for developing novel chemical synthesis pathways. This synthetic

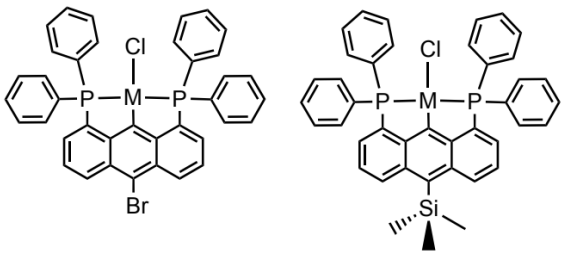
INTRODUCTION

The contributions from the fields of electrical engineering and physics have been instrumental for bringing solar power generation to grid-scale and a chemistry perspective can be applied to develop surfaces that build on these previous achievements to improve solar power generation. Present technologies, such as photovoltaic cells, for converting solar energy to direct current are throttled on average at 21% with the most expensive and efficient systems still at only 40%.[1] Modifying surfaces to change the energy landscape can push these energy efficiencies higher and curtail energy wasted to thermalization or reflection. Here, the advantages of chemical reasoning can be leveraged to develop novel surface modifications using organic functionalizations on inorganic surfaces. To broaden this molecular toolkit, a series of organic chemical synthesis schemes involving 1,8-halogenated anthracene derivatives are explored in order to construct the target molecule [1a]. 1,8-halogenated anthracene derivatives are a class of anthracene structures with halogens covalently bound at the 1 and 8 positions. Critically, these derivatives offer an array of attractive synthetic features such as distinct identifiable proton environments equipped with a backbone that can support larger molecular scaffolds. Halogenated anthracene derivatives are particularly useful as synthetic intermediates in synthesis schemes for performing organic substitutions and surface attachments. The anthracene backbone in 1,8-halogenated anthracene derivatives provides structural stability while possessing discrete reaction sites offering controlled, predictable opportunities for performing synthetic chemistry. The symmetry and inherent planar structure of these species enable the synthesis of organometallic Pincer complexes with square planar coordination geometries.[2] In these configurations, the delocalized electronic structure of the anthracene abuts the electron density of platinum-group metal centers. The

expanded delocalization of the electron density expands the opportunities of molecular interactions with incident solar energies that are currently inaccessible in traditional photovoltaic systems.

Photoelectrochemistry offers a venue to harness abundant solar radiation in semiconductors in order to generate more accessible forms of energy such as driving a direct current. In 2021, Boucher et al. identified distinctive trends in onset potential and differential capacitance demonstrating that the polarizability of surface attachments indeed tunes the photovoltage of the silicon p(111) surfaces.[3]

Ultimately, this project aims to study the effect of polarizability on the band gap of silicon semiconductors by analyzing the surface coupling between surficial organic moieties and bulk silicon. In particular, interest in exploring how an organometallic complex with significant electron density and polarizability affects the electrochemical properties of Si p(111). Figure 1 shows the target molecule for surface attachment on Si p(111). The brominated target molecule prior to surface attachment [1a] is shown with its corresponding surface attachment [1b]. A key feature of the target molecule is the planar backbone structure between the metal coordinating center, anthracene moiety, and phosphine. The planar backbone structure may be optimal for maximizing electronic coupling between the organic-inorganic interface.

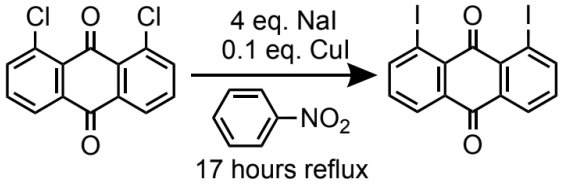


[1a] [1b]

Figure 1: *Target Molecule for surface functionalization of Si p(111) where M = Pt, Ni, or Pd*

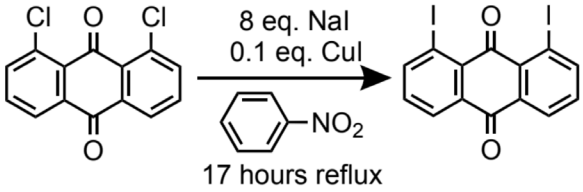
Experimental

I. 1,8-diiodoanthraquinone



Scheme 1: *Iodination Reaction Setup with 4 eq. Sodium Iodide*

In a 50 mL round bottom flask, 2.0818 g of 1,8-dichloroanthraquinone (7.513 mmol) was added with 4.3754 g NaI (29.19 mmol, 4 molar eq.), and 0.1362 g of CuI (0.715 mmol, 0.1 molar eq.) dissolved in 8 mL of nitrobenzene and stirred. The round bottom flask was then placed on a heating mantle connected to an autovariac-transformer. A water-free condenser was affixed to the round-bottom flask. The mixture was refluxed for 17 hours with the autovariac power level set to 40% to achieve a steady, stable reflux. The product material was washed with 50 mL of diethyl ether and extracted into dichloromethane. An aqueous liquid-liquid extraction was performed with excess sodium sulfite to reduce iodine generated as a byproduct. The organic layer was rotary-evaporated resulting in the recovery of 1.3477 g of material. A ^{1}H NMR spectrum showed a 1:1 ratio of product to reactant indicating a 19% yield. ^{1}H NMR (CDCl3): δ_1 = 7.34 (t, 2 H), 8.27 (dd, 2 H), 8.38 (dd, 2 H); Agilent 400 MHz system.

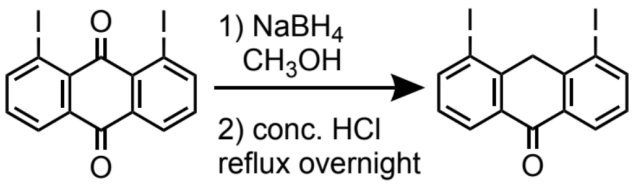


Scheme 2: *Iodination Reaction Setup with 8 eq. Sodium Iodide*

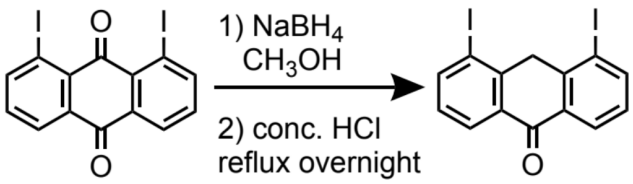
The iodination reaction was performed with a doubled quantity of NaI and a steam distillation to improve the conversion and purity of the reaction. A 50 mL round bottom flask was set up with 2.0227 g of 1,8-dichloroanthraquinone (7.300 mmol), 8.6572 g NaI (57.76 mmol, 8 molar eq.), 0.1372 g of CuI (0.7204 mmol, 0.1

molar eq.), 8 mL nitrobenzene and stirred. A steam distillation was performed on the mixture at 100 °C for 30 minutes in order to remove residual water from the mixture. The round bottom flask was placed on a heating mantle connected to an autovariac transformer and connected to a water free condenser. The autovariac-transformer power level was set at 40%. After 17 hours of reflux the product material was washed with 50 mL of diethyl ether. The product material was extracted into dichloromethane and an aqueous liquid-liquid extraction was performed on the mixture. The organic layer was collected and rotary-evaporated resulting in a mass yield of 1.9353 g. A ^{1}H NMR spectrum showed a 99:1 ratio of product to reactant indicating an overall 45% yield. ^{1}H NMR (CDCl3): δ_1 = 7.33 (t, 2 H), 8.27 (dd, 2 H), 8.38 (dd, 2 H); δ_2 = 7.63 (t, 2 H), 7.78 (dd, 2 H), 8.19 (dd, 2 H) Agilent 400 MHz system.

II. 1,8-diiodoanthracene



Scheme 3: *First Sequential Reduction forming 1,8-diiodoanthracen-9-one*

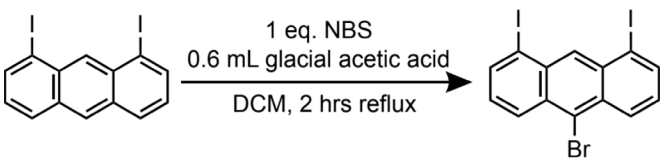


Scheme 4: *Second Sequential Reduction forming 1,8-diiodoanthracene*

In a 100 mL round bottom flask 1.363 g of 1,8-diiodoanthraquinone was dissolved in 26.3 mL of methanol and stirred. At t = 0 minutes, the flask was placed in an ice bath and stirred for five minutes. At t = 5 minutes, 0.3284 g of $NaBH_4$ was added to the reaction flask. At t = 15 minutes, a second addition of 0.3284 g of $NaBH_4$ was added to the reaction mixture. At t = 25 minutes, a third addition of 0.3284 g of $NaBH_4$ was added to reaction mixture. At t = 35 minutes, the round bottom flask was removed from the ice bath and left to stir at room temperature for 3 hours. After the 3 hours of stirring, the mixture was placed on an ice bath and 4.5 mL of 36% – 38% HCl was added dropwise. The round bottom flask was then moved to a heating mantle and refluxed for 17 hours with a water-free condenser. The reaction vessel was removed from reflux and passively cooled to room temperature. The mixture was washed with 50 mL of chilled distilled water and poured over a fritted-glass Büchner funnel with a one-inch thick layer of lightly compressed diatomaceous earth. The material was extracted into 65 mL of dichloromethane. A liquid-liquid extraction was performed on the organic mixture with a saturated Na_2SO_3 aqueous phase in a 250 mL separatory funnel. The organic phase was transferred to a round bottom flask and rotary evaporated.

The product material was then dissolved and stirred in 3 mL of methanol and 21 mL of 2-propanol in a 50 mL round bottom flask. At t = 0 minutes, the flask was placed in an ice bath and stirred for five minutes. At t = 5 minutes, 0.2135 g of $NaBH_4$ was added to the reaction flask. At t = 15 minutes, a second addition of 0.2135 g of $NaBH_4$ was added to the reaction mixture. At t = 25 minutes, a third addition of 0.2135 g of $NaBH_4$ was added to the reaction mixture. At t = 35 minutes, the round bottom flask was removed from the ice bath and left to stir at room temperature for 3 hours. After the 3 hours of stirring, the mixture was placed on an ice-water bath and 4.5 mL of 36% – 38% HCl was added dropwise to the reaction vessel. The round bottom flask was then moved to a heating mantle and refluxed overnight with a water-free condenser. The mixture was then filtered and rotary-evaporated and approximately 0.7135 g of material was recovered. A ^{1}H NMR spectrum showed a 3:2 ratio of product to reactant indicating an overall 34% yield. ^{1}H NMR ($CDCl_3$): δH = 7.184 (t, 2 H); 8.000 (dd, 2 H); 8.139 (dd, 2 H); 8.305 (s, 1 H); 8.939 (s, 1 H); Agilent 400 MHz system.

III. 10-bromo-1,8-diiodoanthracene



Scheme 5: *Bromination of 1,8-diiodoanthracene*

A 50 mL round-bottom flask was prepared with 0.990 g of 1,8-diiodoanthracene, 12 mL of DCM, 0.3831 g of n-bromosuccinimide (2.15 mmol, 1 mol eq.), and 0.6 mL of glacial acetic acid. The mixture was refluxed in the dark at 40 °C for two hours. After passive cooling to room temperature, excess sodium sulfite was added to the mixture and an aqueous extraction was performed. The organic layer was collected and rotary evaporated, recoveringevaporated recovering 0.3860 g of solid 10-bromo-1,8-diiodoanthracene. An ^{1}H NMR spectrum showed approximately a 1:1 ratio of product to reactant indicating an 18% yield. ^{1}H NMR (CDCl3): δH = 7.302 (t, 2H); 8.139 (d, 2H); 8.543 (d, 2H); 9.099 (s, 1H); Agilent 400 MHz system.

DISCUSSION

The first step to construct the target molecule for surface attachment [1a] was the synthesis of 1,8- diiodoanthra-9,10-quinone [2b] from 1,8-dichloroanthra-9,10-quinone [2a]. Since the iodination was the first step in the overall synthesis scheme, optimization of the procedure for the highest yield possible was vital so the reaction was attempted under multiple reaction conditions. The conditions of the iodination reaction were previously reported by Lovell et al. demonstrating the utility of the coupled halogen exchange with iodine.[4] Goichi et al. provided additional findings in 2005 that enhanced the yield by highlighting the importance of the steam distillation prior to refluxing the mixture.[5] Additionally, yields were increased by doubling the quantity of excess sodium iodide from 4 molar equivalents to 8 molar equivalents.

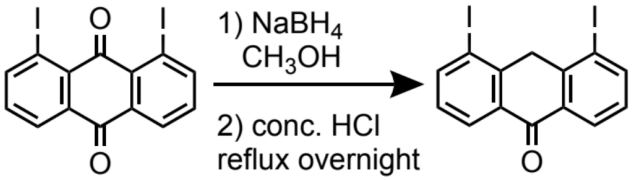


Figure 2: *General Overview of Iodination Substitution Reaction*

Although the reaction successfully produced the desired iodinated quinone, the ^{1}H NMR spectrum revealed that some 1,8-dichloroanthraquinone remained unreacted in most trials. The integrations of the resonances indicated that the material had a 10:4 ratio of 1,8-diiodoanthraquinone to 1,8- dichloroanthraquinone without the steam distillation. However, when a steam distillation was performed prior to refluxing the mixture, the overall ratio of product material was greater than 99% 1,8- diiodoanthraquinone and less than 1% 1,8-dichloroanthraquinone. Furthermore, the improved yield observed under the conditions presented here uses a shorter reaction time (17 hours) compared to those established by Goichi (43 hours), suggesting there may be kinetic influences at play.[6] Overall, the preparation of 1,8-diiodoanthraquinone from commercially available 1,8-dichloroanthraquinone was achieved with a straightforward and reproducible method requiring a shorter reaction time and attaining a higher yield than previously reported.

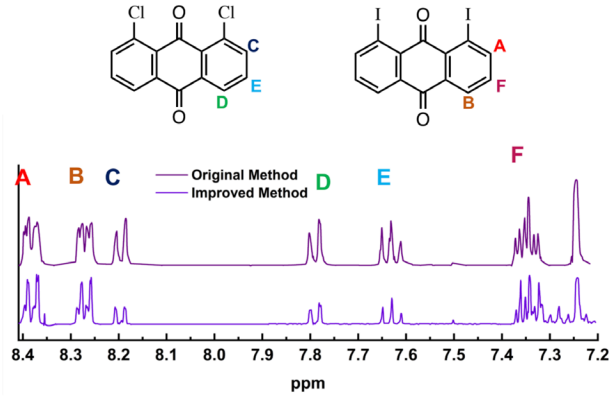


Figure 3*: 1H NMR spectrum of product mixture from the iodination reaction with original and improved methods for comparison, zeroed with TMS reference.*

The improved method with water removed from the reaction vessel shows significantly sharper magnetic shifts and a smaller reactant signal relative to the product. Though the mass yield was improved through the removal of water prior to initiating the iodination reaction, some reactant still remained. In order to maximize purity, additional workup steps were tested, however, no column or recrystallization conditions showed successful separation of the 1,8- diiodoanthraquinone and 1,8-dichloroanthraquinone species. Thin-layer chromatography successfully yielded spot separation of material, but scaling to column chromatography resulted in excessive streaking so separation was infeasible. Thin-layer chromatography was performed on the product in several ratios shown in Table 1. Toluene was thought to disrupt intermolecular π–π stacking interactions between

anthranoids, so it was used to spike the solvent and it greatly increased the resolution of the spot separation, thus mitigating the significant streaking previously observed. Volumetric ratios of DCM to hexanes all showed multiple band separations with varying resolution. All showed more than 2 distinct bands, inconsistent with the separation of pure 1,8-diiodoanthraquinone and 1,8-dichloroanthraquinone. The 70:30 DCM to hexanes TLC plate appeared to have the best band separation, so column chromatography was performed with the 70:30:10 solvent blend of DCM to hexanes to toluene. Multiple columns appeared to yield distinct band separations, but ^{1}H NMR spectra consistently indicated that the distinct bands did not represent separation of pure 1,8-diiodoanthraquinone and pure 1,8-dichloroanthraquinone. In fact, the band separation did not appear any purer than the crude material.

Hexanes (mL)	DCM (mL)	Toluene (mL)	Resolution	Separation
9	1	--	Poor	Low
8	2	--	Poor	Low
7	3	--	Poor	Low
5	5	--	Poor	Moderate
3	7	--	Poor	High
2	8	--	Poor	Moderate
1	9	--	Poor	Low
9	1	1	Good	Low
7	3	1	Good	Low
5	5	1	Good	Moderate
3	7	1	Good	High

Table 1: *Comparison of Volumetric Solvent Ratios used in Chromatography.*

Prior to observing the quantitative conversions provided by the steam distillation for the iodination, other reactions were explored to quantitatively convert 1,8-dichloroanthraquinone to 1,8- diiodoanthraquinone. Klapars et al. investigated the halogen exchange conversions of bromobenzene to iodobenzene, utilizing three organic vicinal diamino compounds as catalysts.[7] From Klapars' reported success, a similar reaction was attempted for the chloro-iodo substitution where trans-1,2- diaminocyclohexane was utilized as a catalyst to recreate Klapars' quantitative conversion, in the same molar ratio, at a 2 g scale, under air-free conditions. However, attempts at performing the iodination with 10% molar eq. of the catalyst trans-1,2-diaminocyclohexane in dioxane failed to generate any 1,8- diiodoanthraquinone, verified by ^{1}H NMR.

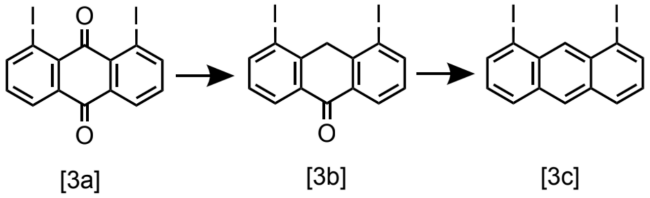


Figure 4: *Overview of Sequential Reductions*

Lovell et al. previously discussed the synthesis of 1,8-diiodoanthracene from 1,8- diiodoanthraquinone.[1] Figure 3 shows the reaction scheme for the sequential reductions of 1,8- diiodoanthraquinone [3a] to 1,8-diiodoanthracene [3c] with an isolable, stable, intermediate: 4,5- diiodoanthracen-9(10H)-one [3b]. The sequential reduction conditions employed a dilution of methanol with 2-propanol in the second reduction because 2-propanol has a more stabilized transition state providing stronger protonating conditions. The stronger protonating conditions are not needed in the first reduction due to the activated carbonyl depicted in Figure 4 participating in resonance.[8] Since 2-propanol can stabilize a transition state in the reduction of the anthrone, the second reduction requires a lower molar ratio of sodium borohydride. An ancillary singlet upstream was observed in each ^{1}H NMR of 1,8- diiodoanthracene that accounted for discrepancies in integrations.

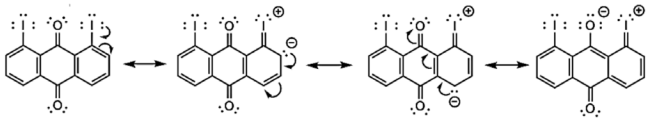


Figure 5: *Contributing Resonance Structures of 1,8-diiodoanthraquinone*

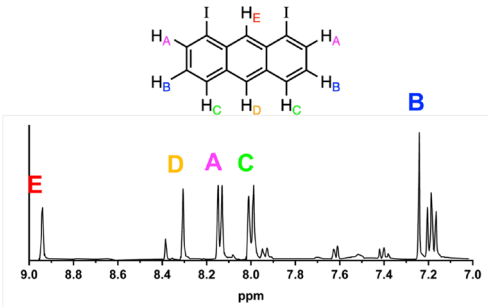


Figure 6: *^{1}H NMR of product mixture from the sequential reduction reactions, zeroed with TMS*

The bromination reaction generated a 34 % yield of 10-bromo-1,8-diiodoanthracene, after accounting for the presence of unreacted starting material with ^{1}H NMR. On the benchtop exposed to light, 10-bromo-1,8-diiodoanthracene changed color from fluorescent yellow to brown. Due to degradation of 10-bromo-1,8-diiodoanthracene under environmental light, the bromination was performed in the dark.

Additionally, TLC spots with 10-bromo-1,8-diiodoanthracene changed color from pale yellow to brown within hours. When the bromination was performed in the dark, yields were found to be less than 5% and the ^{1}H NMR spectra were excessively noisy. The bromination reaction was subsequently attempted with 1 molar equivalency of Br2 instead of NBS and the ^{1}H NMR spectra of the products were notably similar.

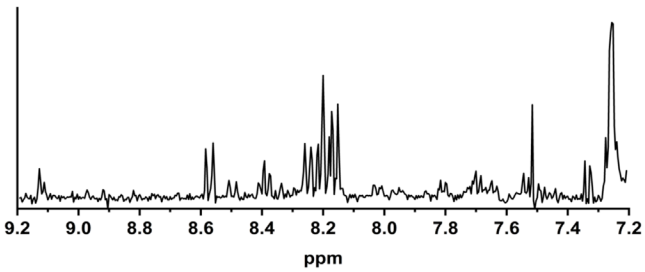


Figure 7: *^{1}HNMR of brominated 1,8-diiodoanthracene, zeroed with TMS reference.*

A solubility test was performed on the brominated 1,8-diiodoanthracene species. Chloroform solubilized the species the best, whereas dichloromethane took approximately double the volume of solvent and toluene required roughly quadruple the volume for each to dissolve 10 mg of 1,8- diiodoanthracene. The results of this solubility test can be useful for preloadingpre-loading the species onto silica to perform column chromatography in the future.

CONCLUSION

We significantly improved the yield of 1,8-diiodoanthraquinone from 1,8-dichloroanthraquinone from 19% to 45% by boiling off residual water via steam distillation prior to refluxing. The steam distillation also enabled the recovery of pure product, alleviating the need to separate unreacted starting material from the product. After performing a DCM wash and aqueous extraction, the presence of 99% pure 1,8-diiodoanthraquinone was confirmed via 1H NMR. Two sequential reductions were performed to synthesize 1,8-diiodoanthracene with an overall 34% yield. Subsequently, 1,8-diiodoanthracene was brominated to produce 10-bromo-1,8-diiodoanthracene with an 18% yield. Brominating at the 10 position is vital to attaching the aforementioned target molecule to the surface of Si p(111) and further opens the door for future organic synthesis by using the bromine as an aromatic director or leaving group. Many additional strategies worth exploring to improve the isolation of 10-bromo-1,8-diiodoanthracene in future synthesis. The next step will be to substitute the iodine groups with biphenylphosphine groups to synthesize (10-bromoanthracene-1,8-diyl) bis(diphenylphosphane) 10-bromo-1,8-diiodoanthracene. Once the ligand scaffold is phosphinated, the metalation of the compound can be performed to generate the target molecule for surface attachment.

ACKNOWLEDGEMENTS

This work would not have been possible without the guidance and wisdom of Dr. Michael J. Rose, Assistant Professor in the Department of Chemistry at the University of Texas at Austin. Thank you to Dr. Rose for the tremendous opportunity to participate in stimulating scientific discourse and to experience chemistry inquiry in a premier research setting. Thank you to Jeremy Brinker for providing me knowledgeable mentorship to experiment with these chemical reactions. This mentorship has equipped me to be an observant and relentless researcher. My work on this project privileged me with tremendous personal and professional development. I am forever grateful for the guidance and opportunities given to me and I cherish them immensely

.

REFERENCES

[1]Center for Sustainable Systems, University of Michigan, 2024 "Photovoltaic Energy Factsheet" (accessed December 6, 2024).

[2]Hu, Jian; Xu, Huan; Nguyen, Ming-Hai; Yip, John H. K. Photooxidation of Platinum-Anthracene Pincer Complex: Formation and Structure of Pt(II)-Anthrone and -Ketal Complexes Inorg. Chem. 2009 48, 9684-9692. https://doi.org/10.1021/ic900479w

[3]Boucher, Dylan G.; Kearney, Kara; Ertekin, Elif.; Rose, Michael J. Tuning p-Si(111) Photovoltage via Molecule|Semiconductor Electronic Coupling. J. Am. Chem. Soc. 2021 143, 2567–2580. https://doi.org/10.1021/jacs.0c12075

[4]Lovell, & Joule, J. A. (1997). Convenient Synthesis of 1,8-Diiodoanthracene and Its Coupling with Thianthrene Boronic Acids. Synthetic Communications, 27(7), 1209–1215. https://doi.org/10.1080/00397919708003358

[5]Goichi, Segawa, K., Suzuki, S., & Toyota, S. (2005). Improved Synthesis of 1,8-Diiodoanthracene and Its Application to the Synthesis of Multiple Phenylethynyl-Substituted Anthracenes. Synthesis (Stuttgart), 2005(13), 2116–2118. https://doi.org/10.1055/s-2005-869999

[6]Goichi, Segawa, K., Suzuki, S., & Toyota, S. (2005). Improved Synthesis of 1,8-Diiodoanthracene and Its Application to the Synthesis of Multiple Phenylethynyl-Substituted Anthracenes. Synthesis (Stuttgart), 2005(13), 2116–2118. https://doi.org/10.1055/s-2005-869999

[7]Klapars, & Buchwald, S. L. (2002). Copper-Catalyzed Halogen Exchange in Aryl Halides: An Aromatic Finkelstein Reaction. Journal of the American Chemical Society, 124(50), 14844–14845. https://doi.org/10.1021/ja028865v

[8]Muramoto, Patel, D. A., Chen, W., Sautet, P., Sykes, E. C. H., & Madix, R. J. (2022). Direct Observation of Solvent–Reaction Intermediate Interactions in Heterogeneously Catalyzed Alcohol Coupling. Journal of the American Chemical Society, 144(38), 17387–17398. https://doi.org/10.1021/jacs.2c02199

Yang, Cui, J., Li, Z., Zhong, K., Jin, L. Y., & Lee, M. (2016). Self-Assembly of n-Shaped Rod–Coil Molecules into Thermoresponsive Nanoassemblies: Construction of Reversible Helical Nanofibers in Aqueous Environment. Macromolecules, 49(16), 5912–5920. https://doi.org/10.1021/acs.macromol.6b01347